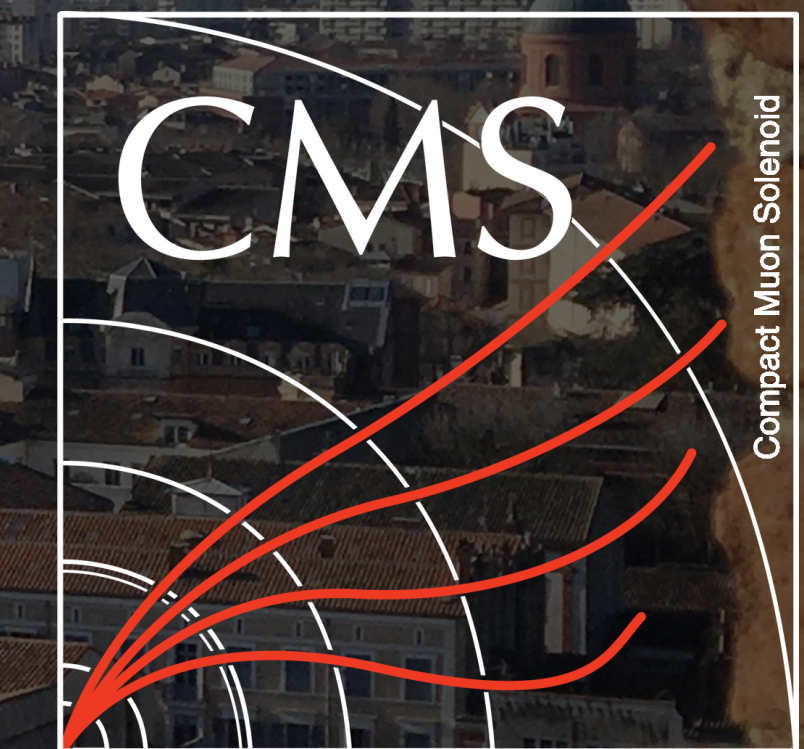


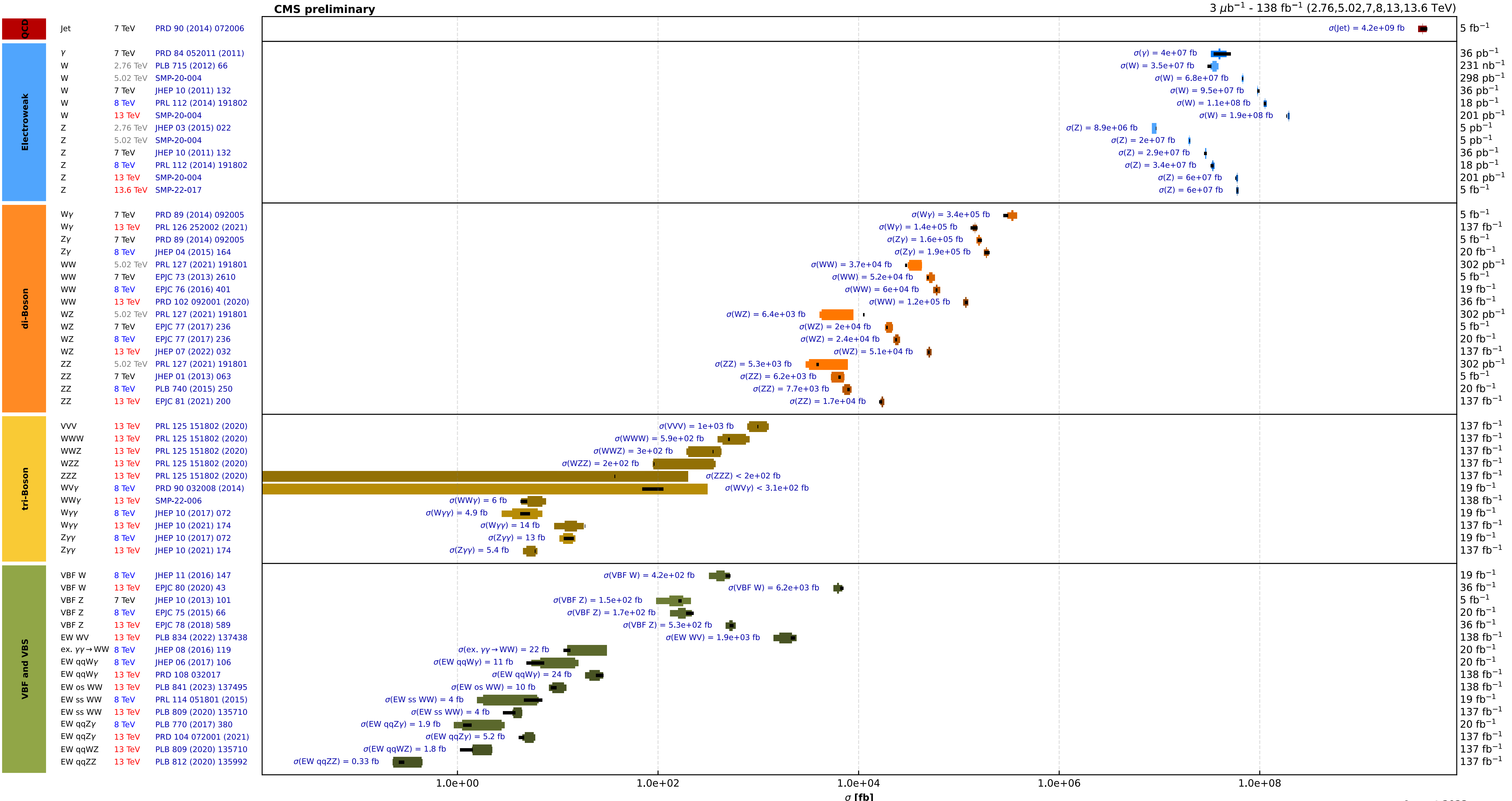
Full Run 2 overview of electro-weak multiboson production in CMS



Saptaparna Bhattacharya
Multiboson Interactions

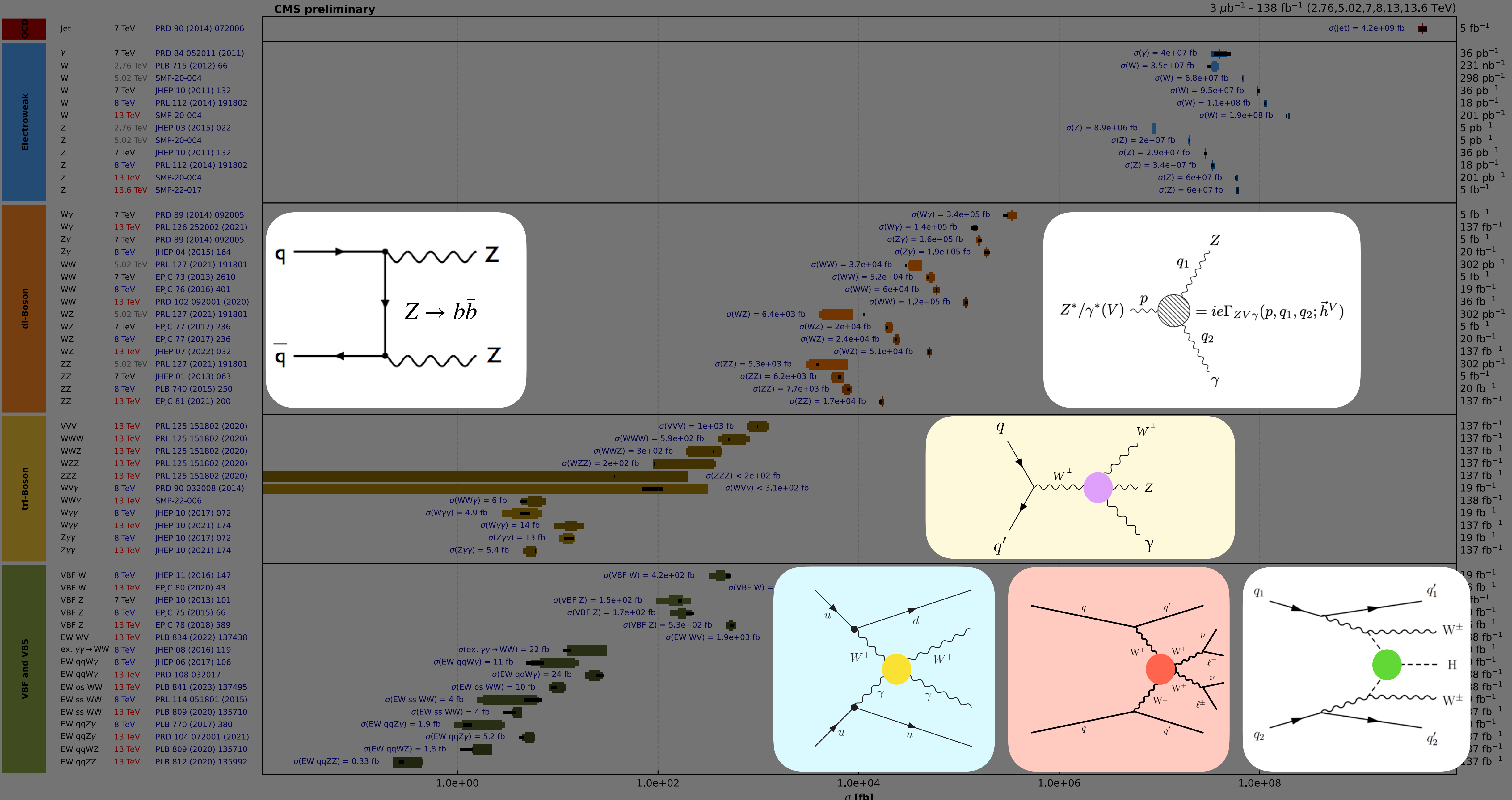
September 25-28th, 2024

Overview of CMS cross section results



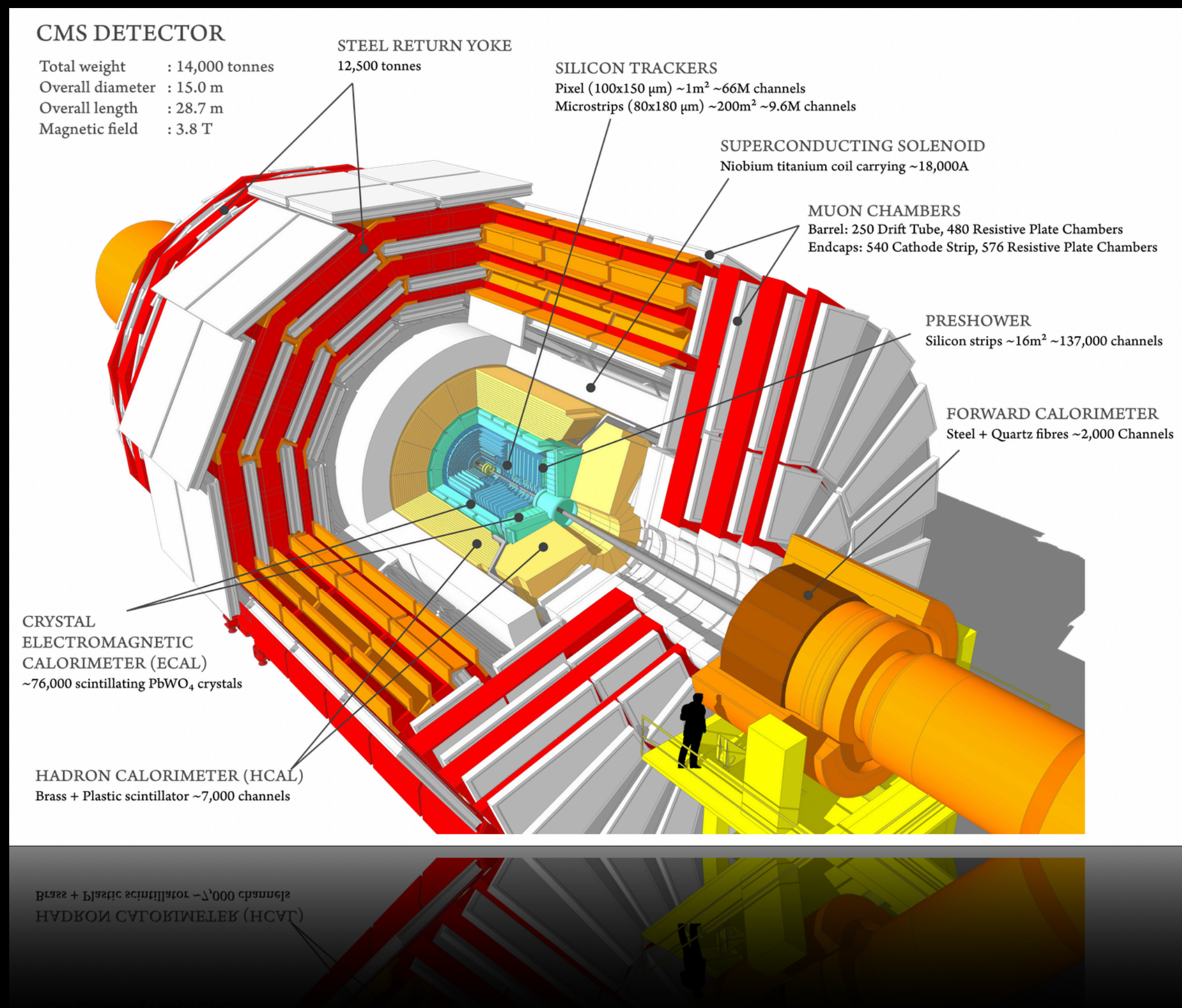
Overview of CMS cross section results

3



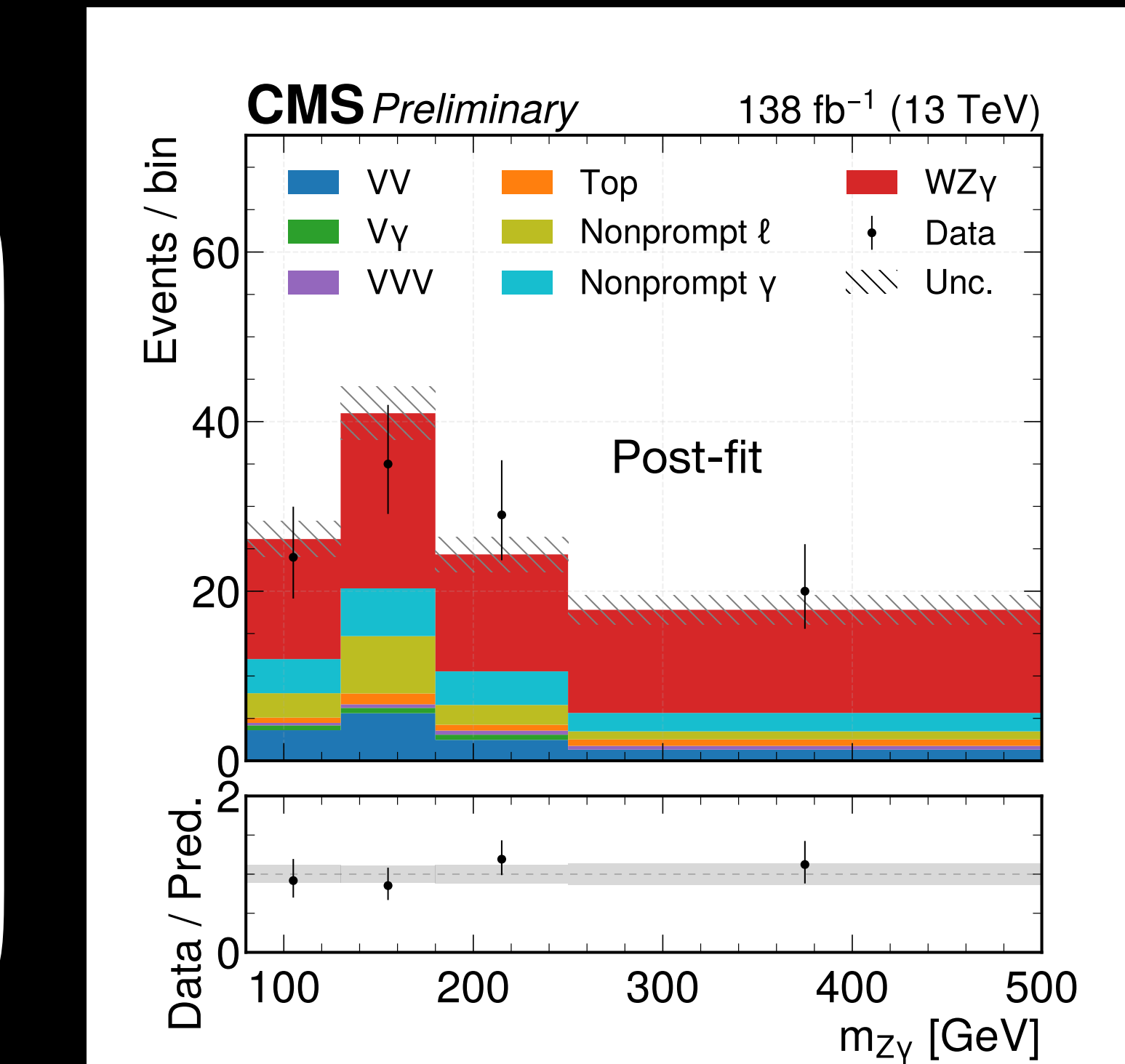
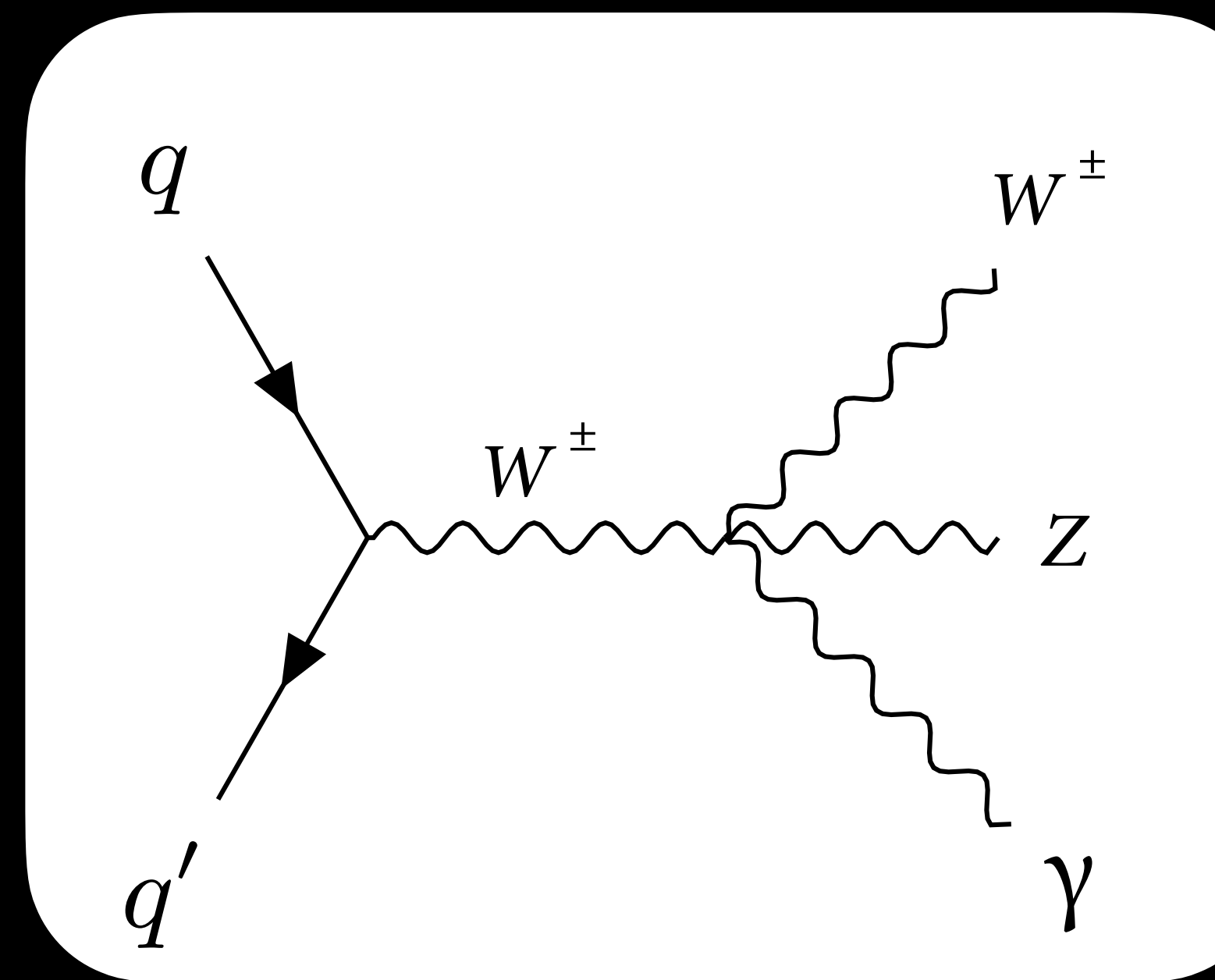
Outline

- Observation of $WZ\gamma$ and $WW\gamma$
 - Exploring the implication of new physics modifying the quartic coupling in the Standard Model – effective field theory (EFT) interpretation
- The $\gamma\gamma \rightarrow \tau\tau$ process and measuring $g_\tau - 2$
- Tagging the protons with the Precision Proton Spectrometer
- Evolution of vector boson scattering (VBS) measurements
 - Same-signed WW with a hadronic τ
 - $W\gamma$ with 2 jets
 - $HHWW$ coupling
 - Future prospects
- Dibosons
 - Neutral couplings and $ZZ/HZ, Z \rightarrow b\bar{b}, H \rightarrow b\bar{b}$



Observation of $WZ\gamma$ production at $\sqrt{s} = 13$ TeV

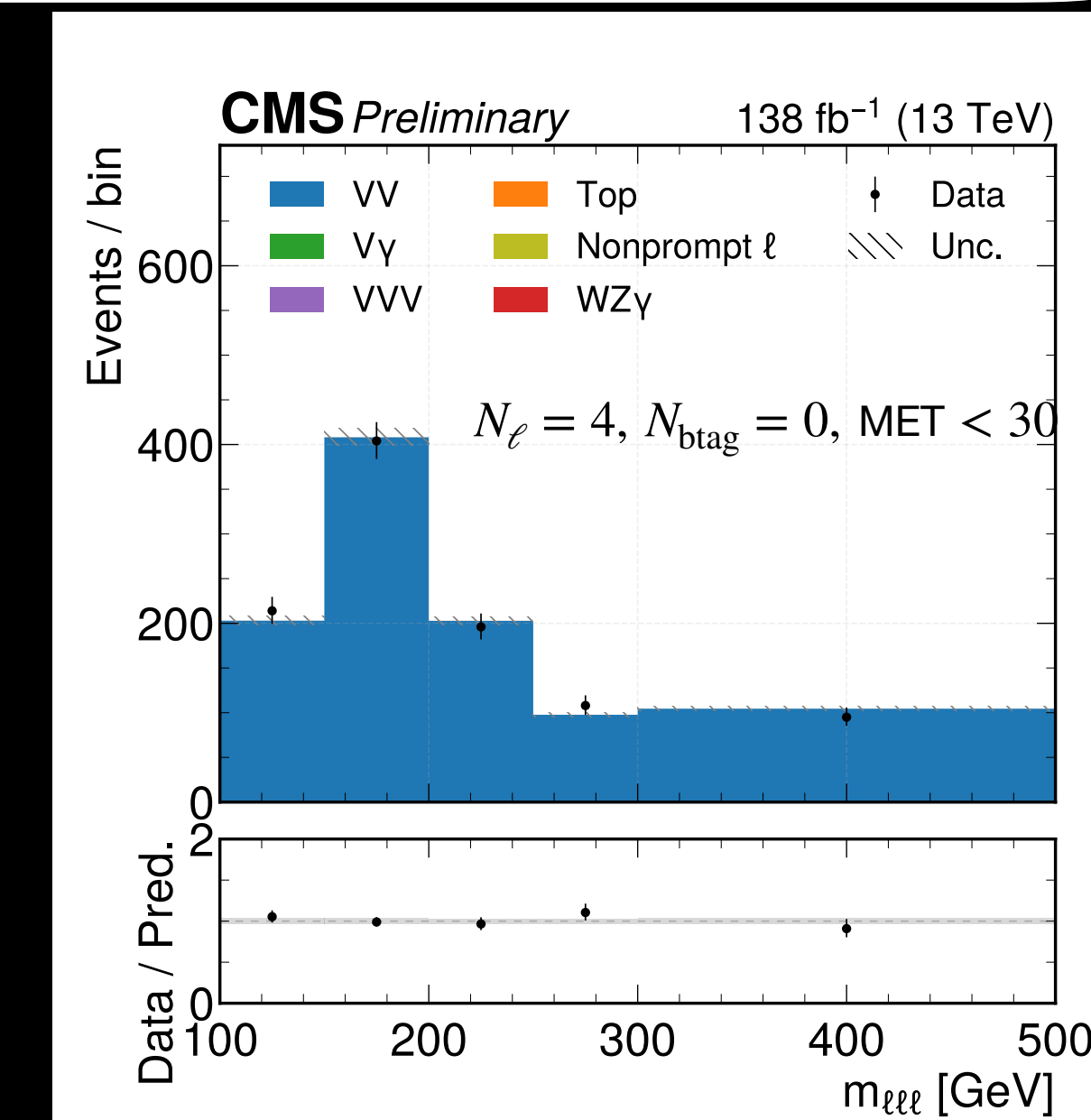
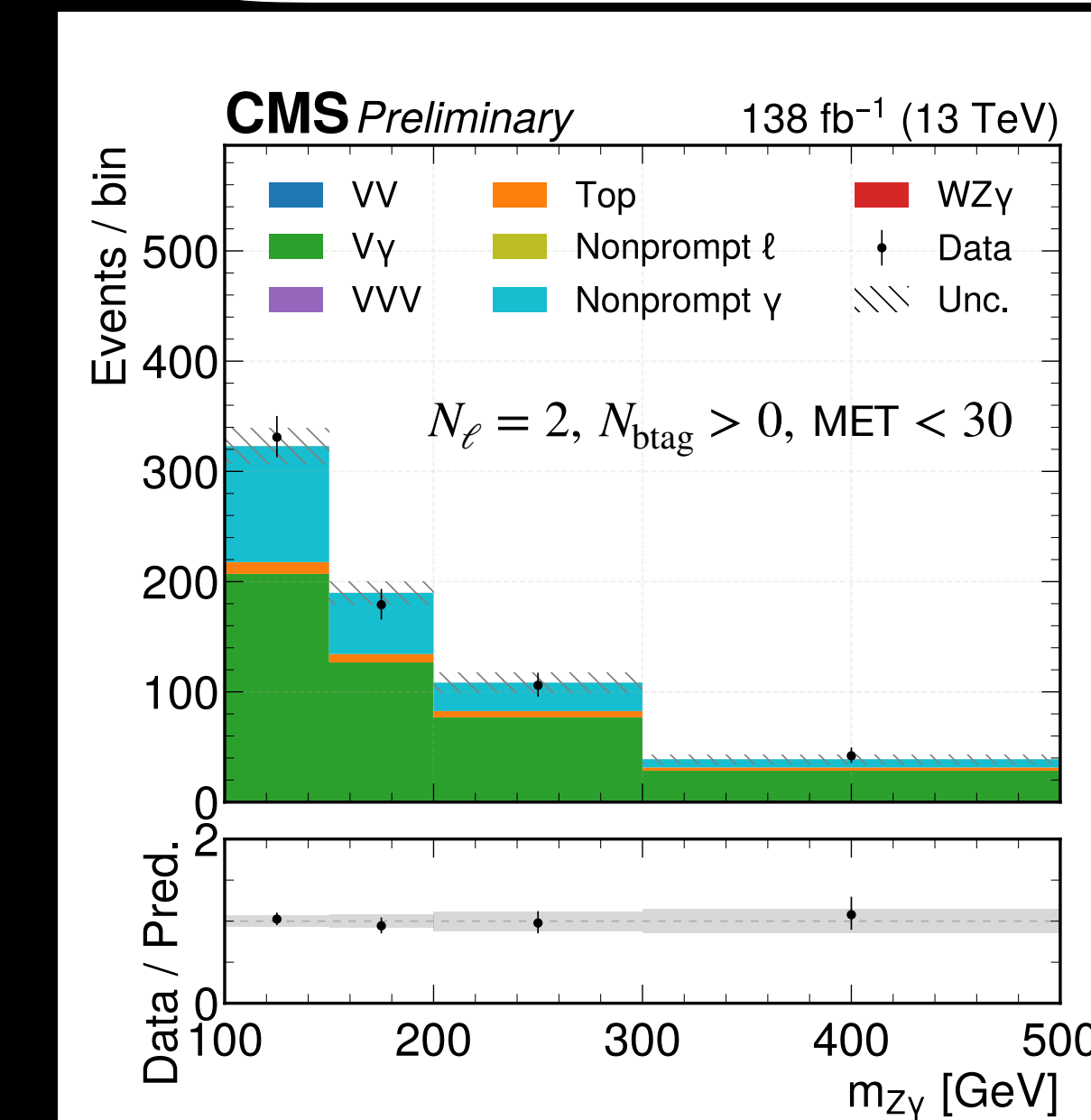
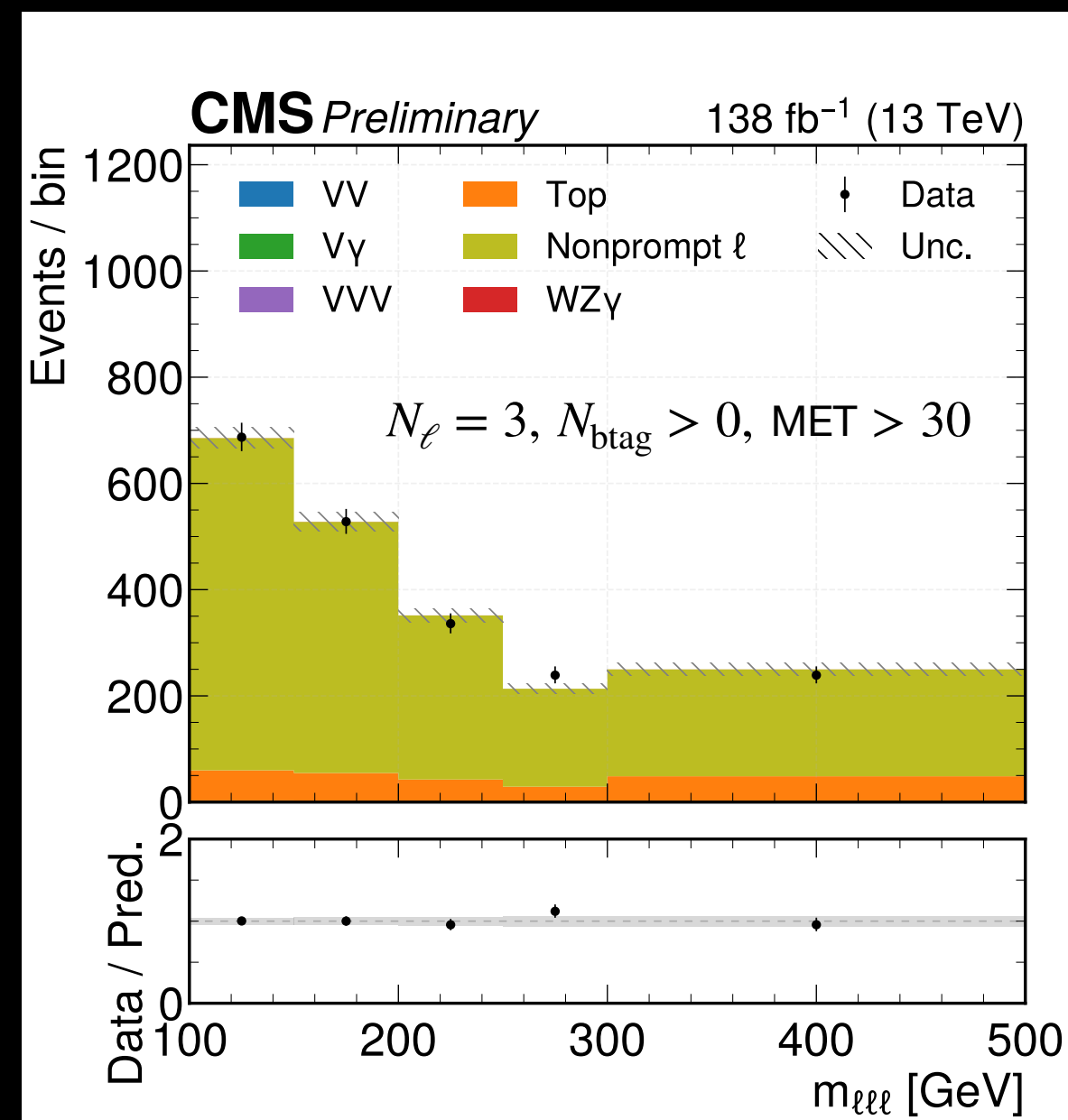
- $WZ\gamma$ process observed (expected) with a significance of 5.4 (3.8) σ
- Final state defined by requiring three charged leptons ($WZ \rightarrow \ell\nu\ell\ell$) and a photon
- Fiducial cross section measured as: 5.48 ± 1.11 fb
- Several new physics scenarios explored including axions-like particles



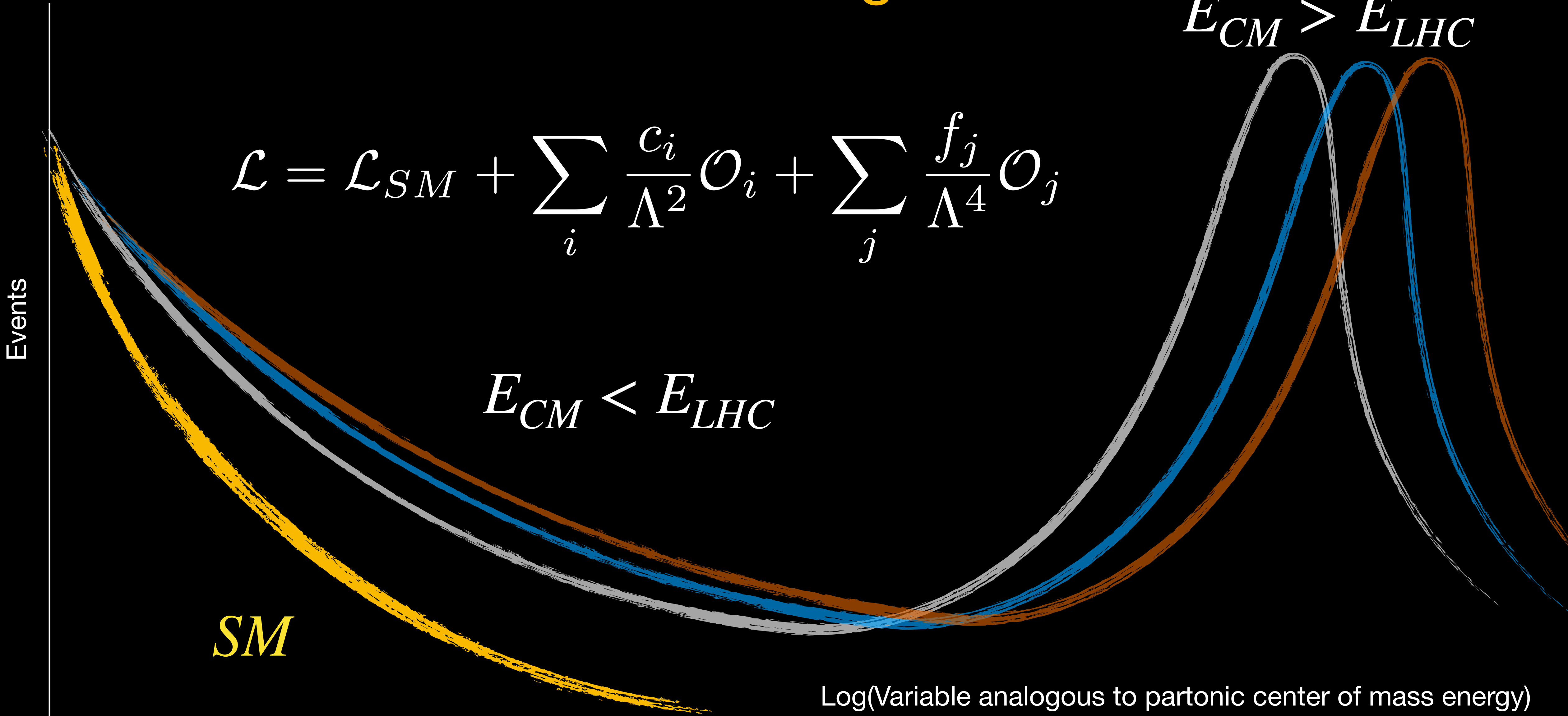
Observation of $WZ\gamma$ production at $\sqrt{s} = 13$ TeV

- Simultaneous fit of signal and background regions
 - Major background sources
 - Non-prompt photon and leptons
 - Prompt ZZ with an ISR photon

Process	SR	Nonprompt ℓ CR	Nonprompt γ CR	ZZ CR
VV	13.0 ± 0.3	1.86 ± 0.12	0.16 ± 0.02	1016 ± 12
VVV	0.69 ± 0.05	0.36 ± 0.11	0.01 ± 0.01	0.10 ± 0.04
$V\gamma$	1.38 ± 0.76	4.66 ± 2.05	438 ± 27	0.01 ± 0.01
Top	3.34 ± 0.55	227 ± 15	27.0 ± 5.9	0.30 ± 0.04
Nonprompt ℓ	12.9 ± 2.8	1792 ± 34	<0.1	<0.1
Nonprompt γ	15.8 ± 2.2	<0.1	195 ± 19	<0.1
WZG signal	60.8 ± 3.5	0.66 ± 0.01	0.20 ± 0.04	0.02 ± 0.01
Total background	48.5 ± 3.7	2027 ± 33	660 ± 21	1016 ± 12
Total prediction	109 ± 5	2027 ± 33	660 ± 21	1016 ± 12
Observed	108	2029	658	1017



New physics at high energies manifesting at low energies



BSM implication of $WZ\gamma$

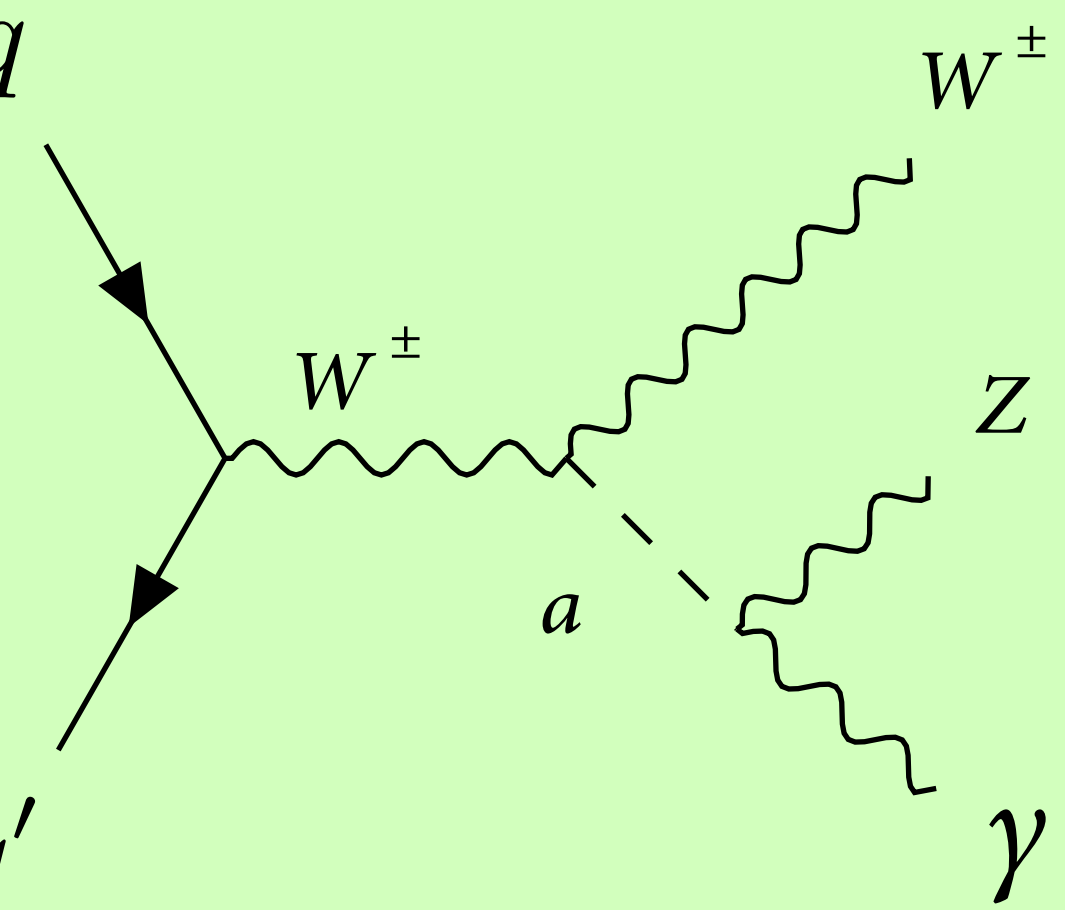
<https://arxiv.org/pdf/2004.05174>

EFT interpretation
of dimension-8
operators featuring
 $SU(2)_L$ and $U(1)_Y$
field strength

Operators	Observed limits [TeV $^{-4}$]	Expected limits [TeV $^{-4}$]	Unitarity bound [TeV]
$F_{T,0}/\Lambda^4$	[-2.60, 2.60]	[-2.52, 2.52]	1.32
$F_{T,1}/\Lambda^4$	[-3.28, 3.24]	[-3.18, 3.14]	1.48
$F_{T,2}/\Lambda^4$	[-7.15, 7.05]	[-6.95, 6.85]	1.35
$F_{T,5}/\Lambda^4$	[-2.54, 2.56]	[-2.46, 2.50]	1.55
$F_{T,6}/\Lambda^4$	[-3.18, 3.22]	[-3.08, 3.14]	1.61
$F_{T,7}/\Lambda^4$	[-6.85, 7.05]	[-6.65, 6.85]	1.71



$$\mathcal{L} = \mathcal{L}_{SM} + \sum_i \frac{c_i}{\Lambda^2} \mathcal{O}_i + \sum_j \frac{f_j}{\Lambda^4} \mathcal{O}_j$$



The $WZ\gamma$ process is also sensitive to mediation by axion-like particles

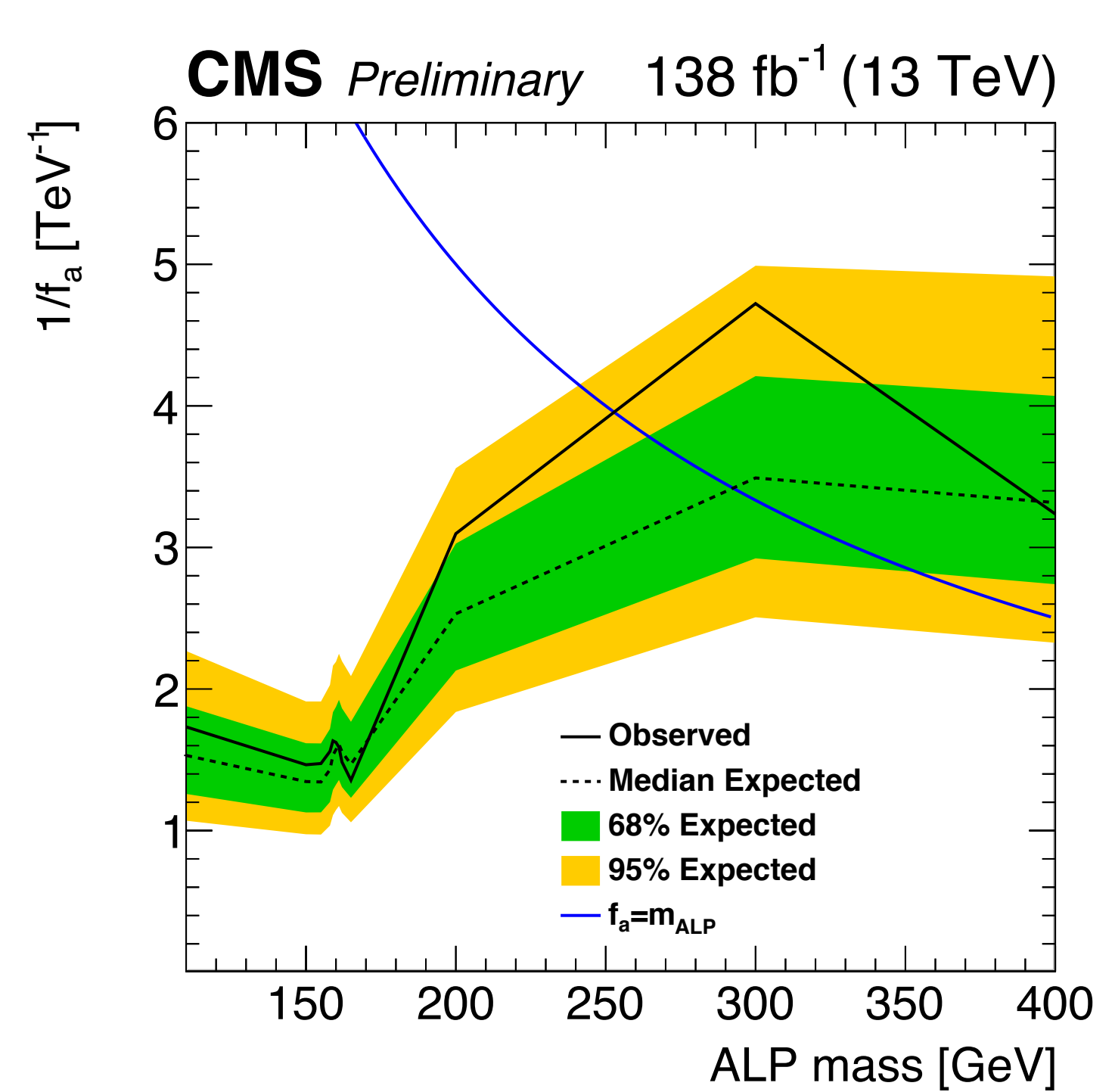
YITP-SB-2020-8

Unitarity Constraints on Anomalous Quartic Couplings

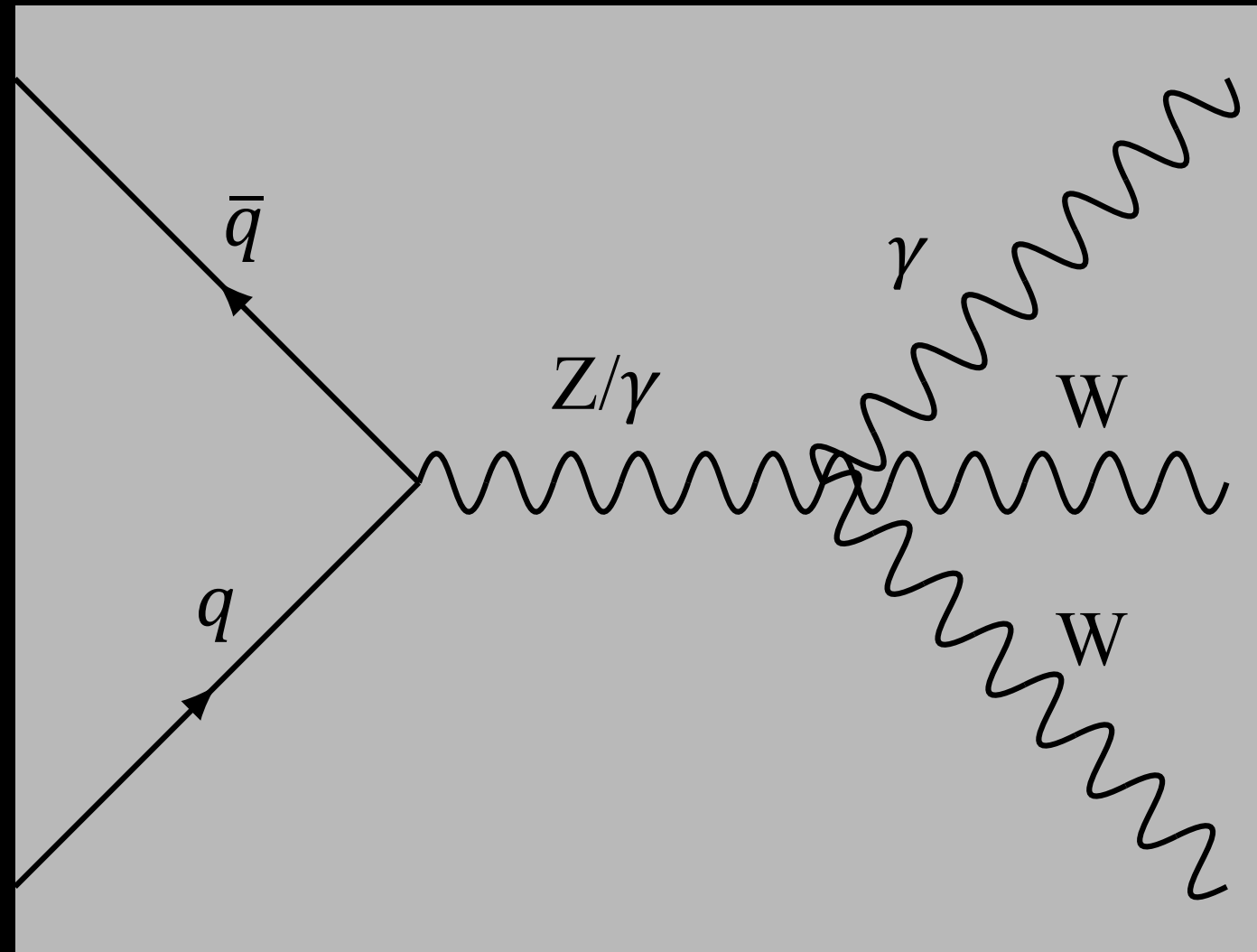
Eduardo da Silva Almeida[✉] and O. J. P. Éboli[✉]
Instituto de Física, Universidade de São Paulo, São Paulo - SP, Brazil.

M. C. Gonzalez-García[✉]
Institutò Català de Recerca i Estudis Avançats (ICREA),
Departament d'Estructura i Constituents de la Matèria,
Universitat de Barcelona, 647 Diagonal, E-08028 Barcelona, Spain and
C.N. Yang Institute for Theoretical Physics, SUNY at Stony Brook, Stony Brook, NY 11794-3840, USA

We obtain the partial-wave unitarity constraints on the lowest-dimension effective operators which generate anomalous quartic gauge couplings but leave the triple gauge couplings unaffected. We consider operator expansions with linear and nonlinear realizations of the electroweak symmetry and explore the multidimensional parameter space of the coefficients of the relevant operators: 20 dimension-eight operators in the linear expansion and 5 $\mathcal{O}(p^4)$ operators in the derivative expansion. We study two-to-two scattering of electroweak gauge bosons and Higgs bosons taking into account all coupled channels and all possible helicity amplitudes for the $J = 0, 1$ partial waves. In general, the bounds degrade by factors of a few when several operator coefficients are considered to be nonvanishing simultaneously. However, this requires considering constraints from both $J = 0$ and $J = 1$ partial waves for some sets of operators.



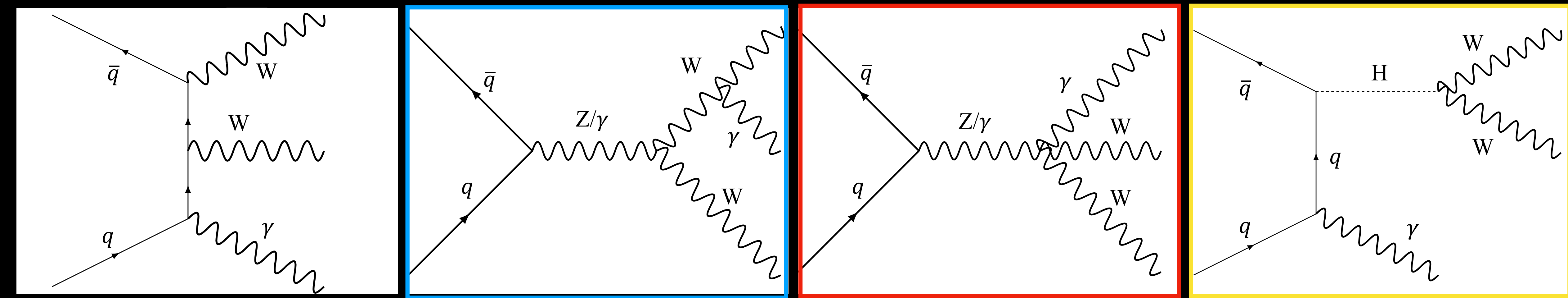
Observation of $WW\gamma$ production at $\sqrt{s} = 13$ TeV



Observation of $WW\gamma$ production at $\sqrt{s} = 13 \text{ TeV}$

- $WW\gamma$ process observed (expected) with a significance of 5.6 (5.1) σ
- Fiducial cross section measured as: 5.9 ± 0.8 (stat.) ± 0.8 (syst.) ± 0.7 (modeling*) fb
- Associated search for H with a photon explored → generated by coupling of the Higgs boson to light quarks

[Phys. Rev. Lett. 132 \(2024\) 121901](#)

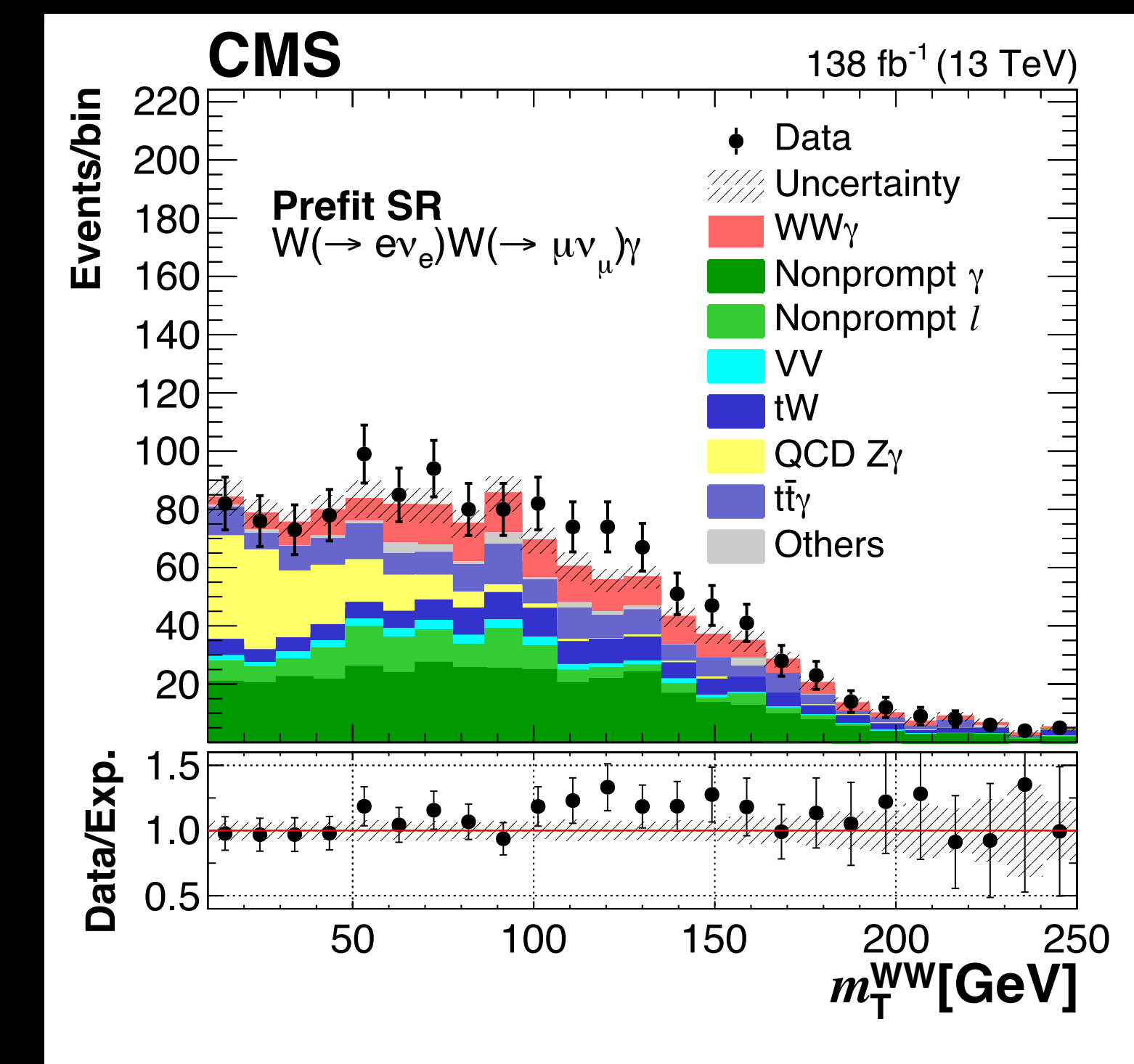
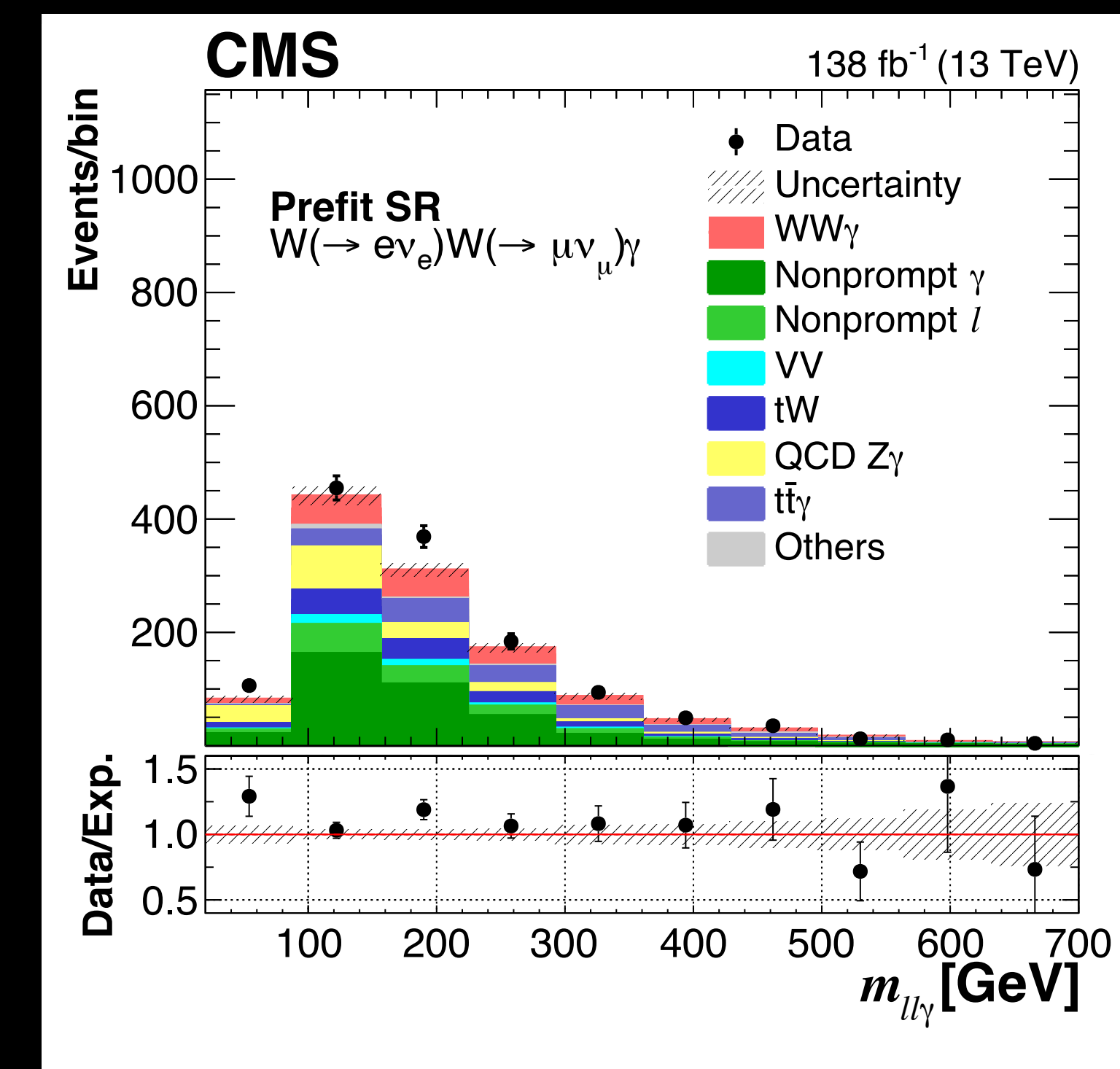


*The theoretical modeling uncertainties include the renormalization and factorization of QCD scales, PDFs, and parton shower modeling

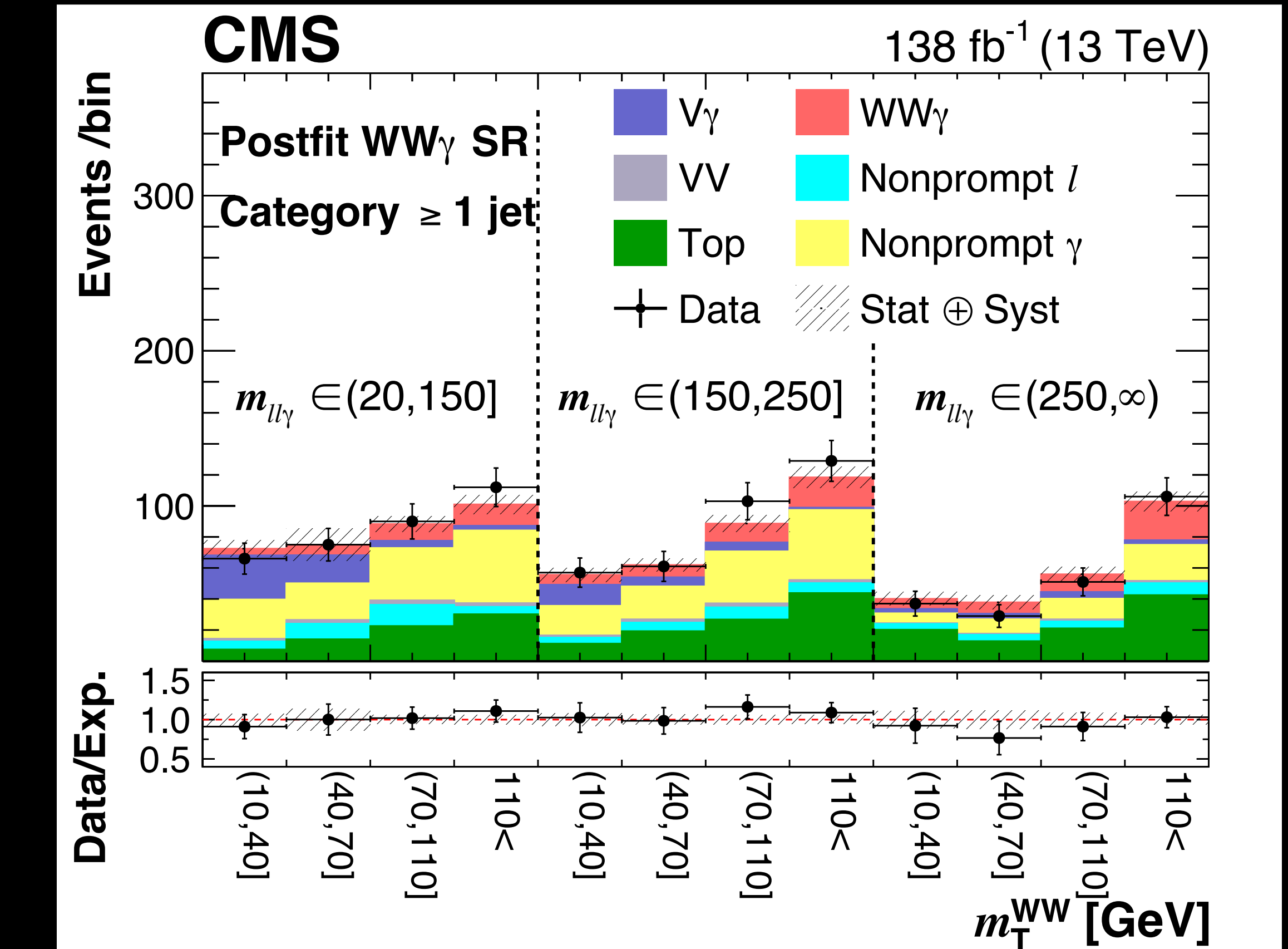
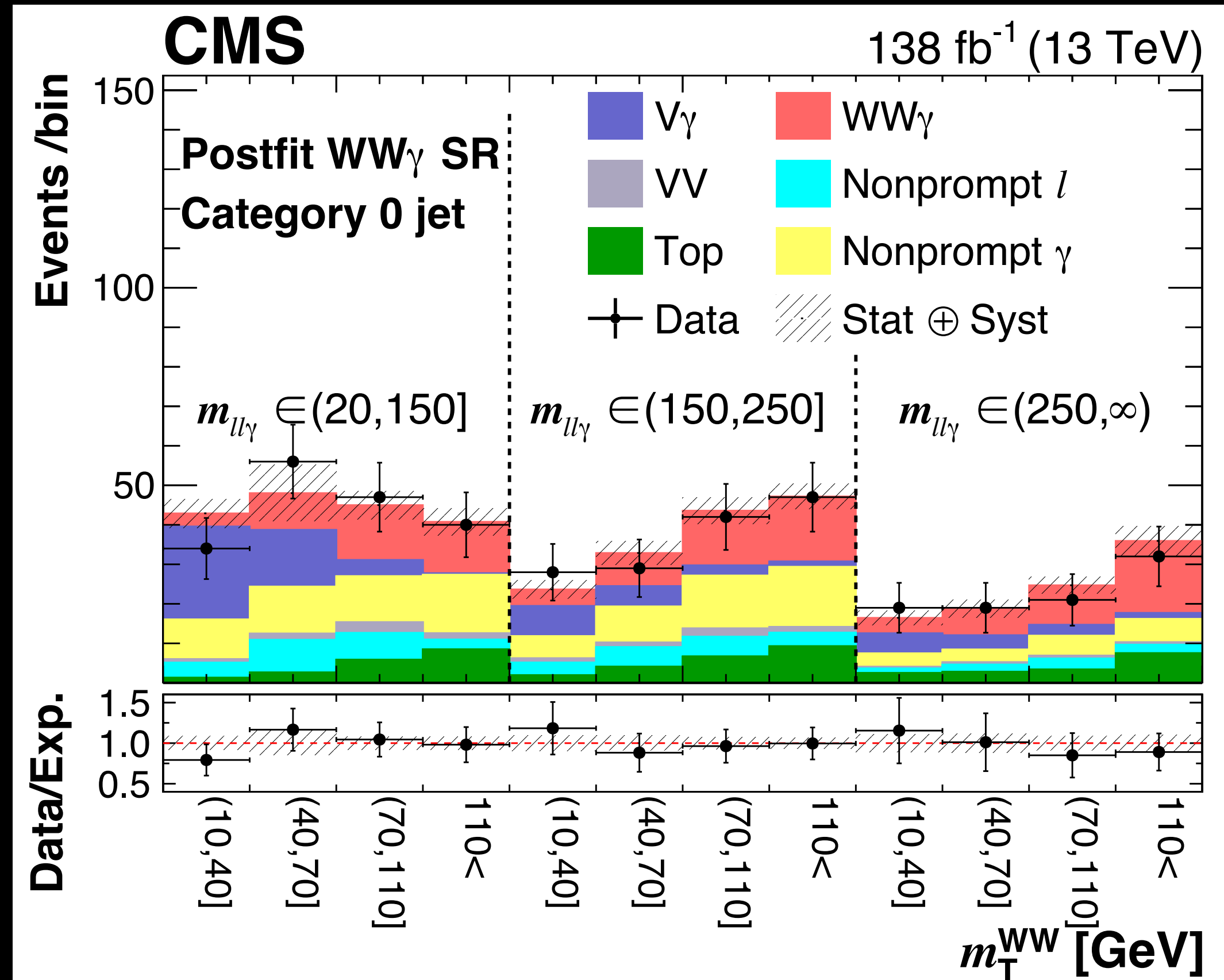
Observation of $WW\gamma$ production at $\sqrt{s} = 13 \text{ TeV}$

- $WW\gamma \rightarrow e^+\nu_e\mu^-\bar{\nu}_\mu\gamma$ or $\mu^+\nu_\mu e^-\bar{\nu}_e\gamma$ final state
- Events with b-jets vetoed
- Additional loose leptons vetoed
- Backgrounds suppressed by
 - $M_{\ell\ell} > 10 \text{ GeV}$
 - $p_T^{\ell\ell} > 15 \text{ GeV}$
 - $m_T^{\text{WW}} > 10 \text{ GeV}$

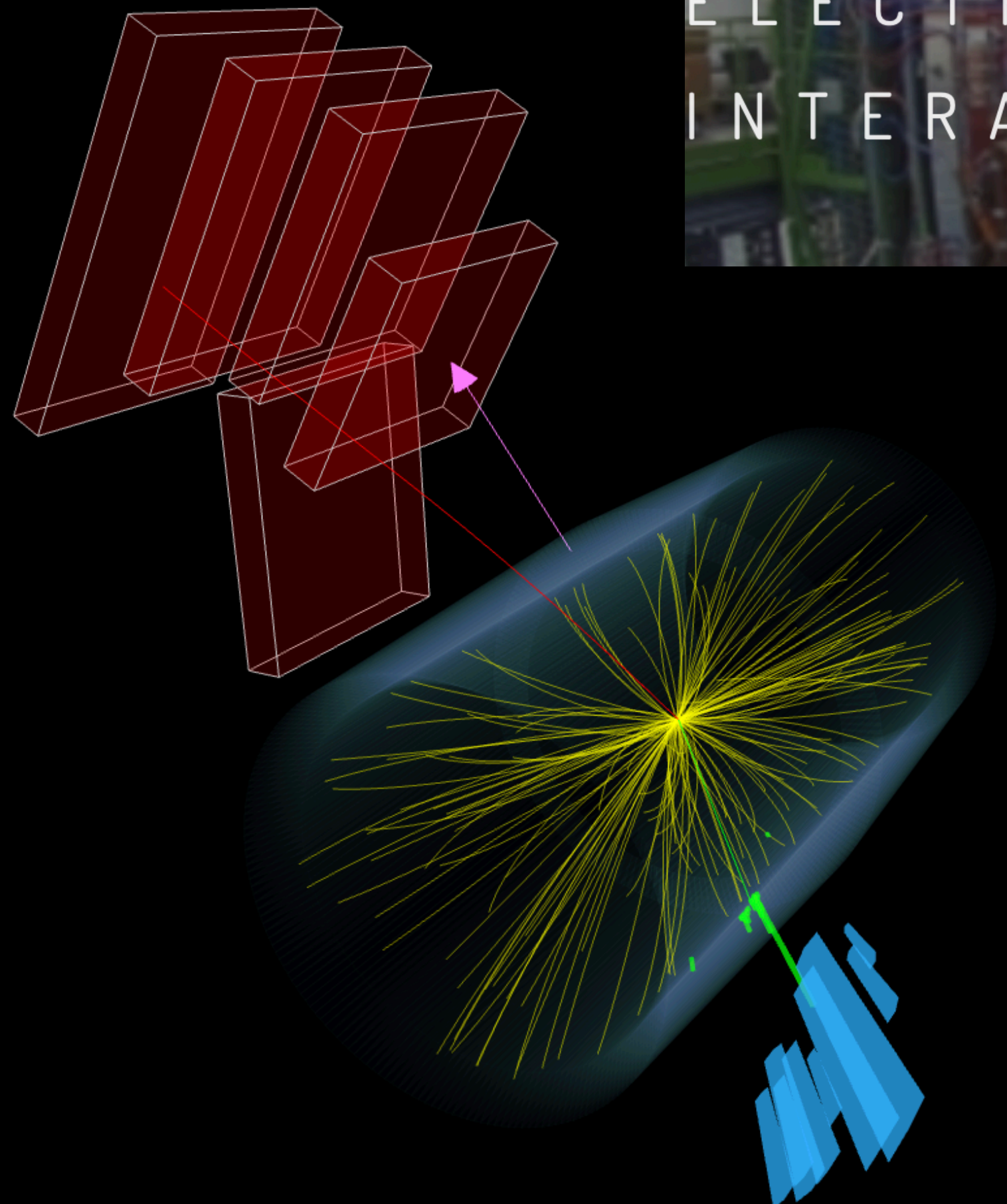
$$m_T^{\text{WW}} = \sqrt{2p_T^{\ell\ell} p_T^{\text{miss}} [1 - \cos \Delta\phi(\vec{p}_T^{\ell\ell}, \vec{p}_T^{\text{miss}})]}$$



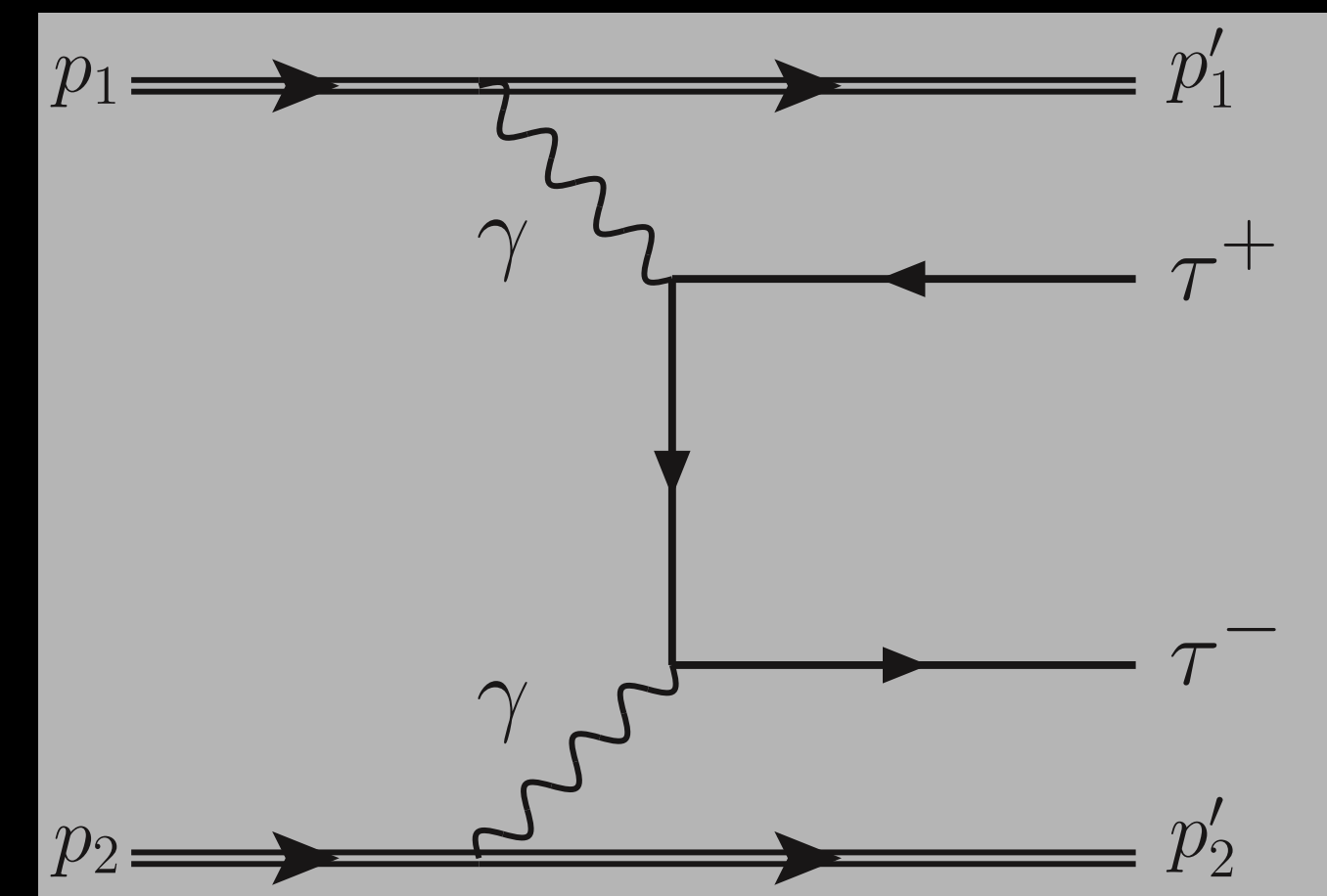
Observation of $WW\gamma$ production at $\sqrt{s} = 13 \text{ TeV}$



- Signal extracted from a binned maximum likelihood fit using two dimensional distributions in m_T^{WW} and $m_{\ell\ell\gamma}$ (product of the Poisson probability mass functions for each bin forms the likelihood function)



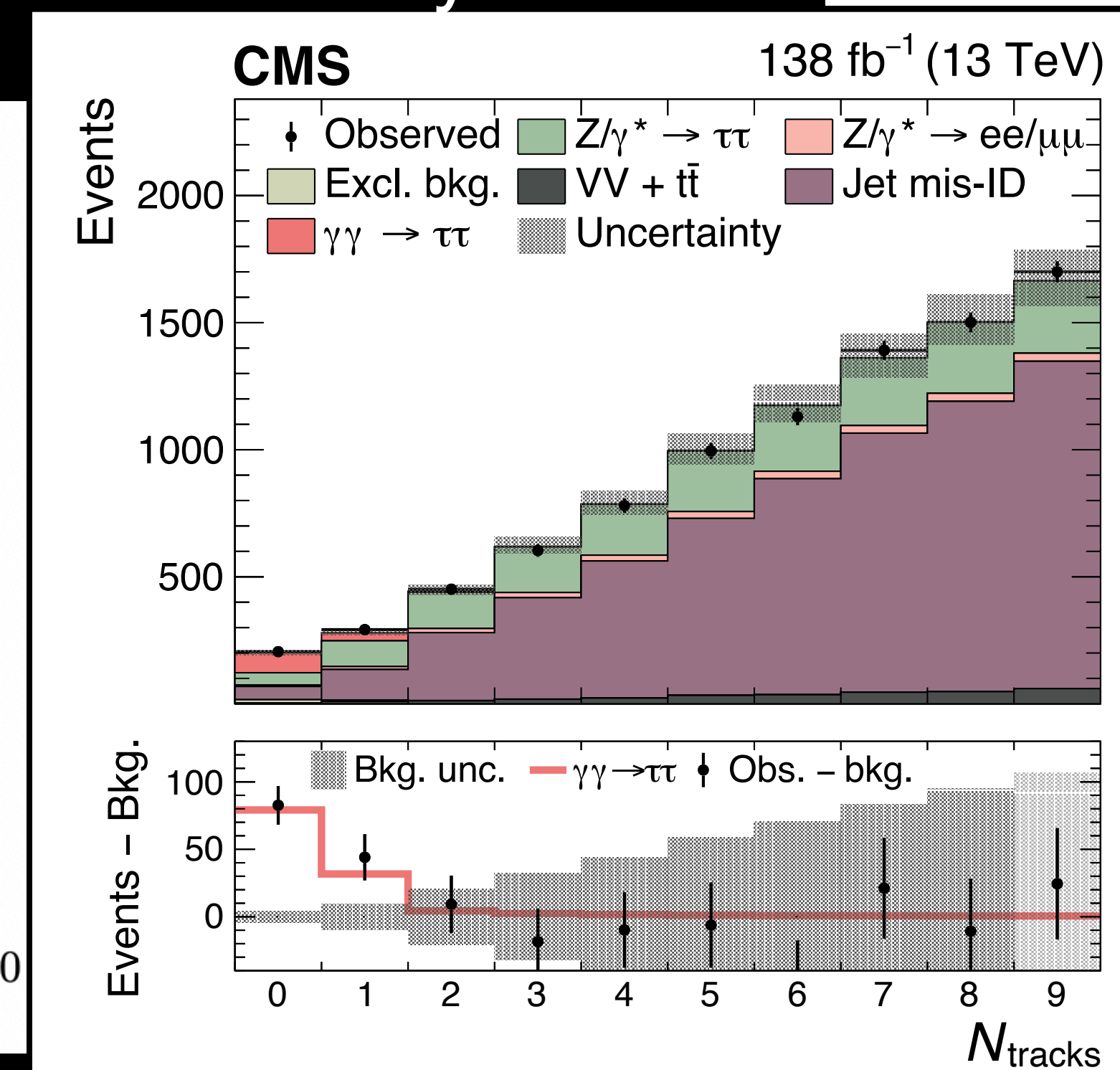
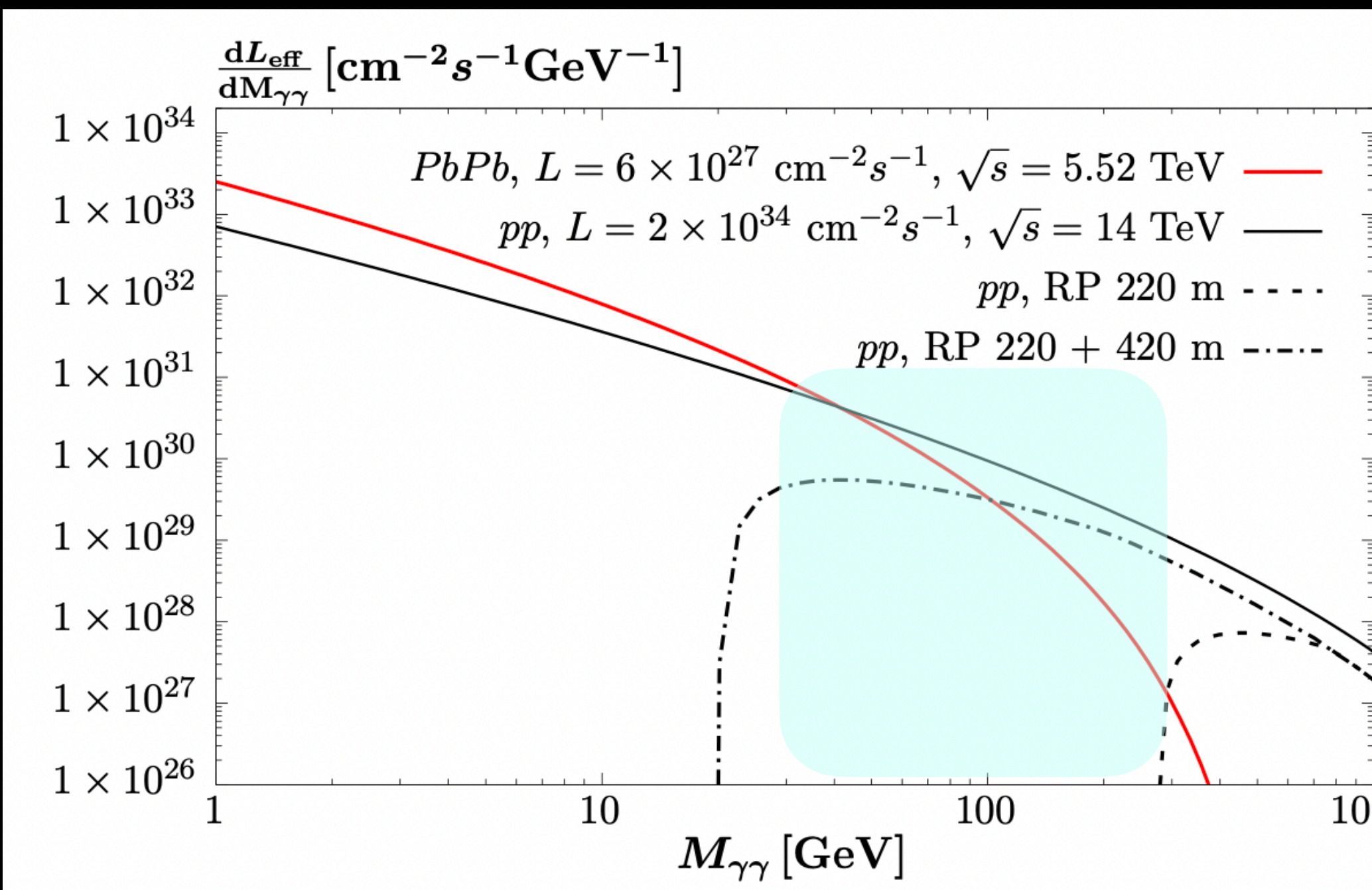
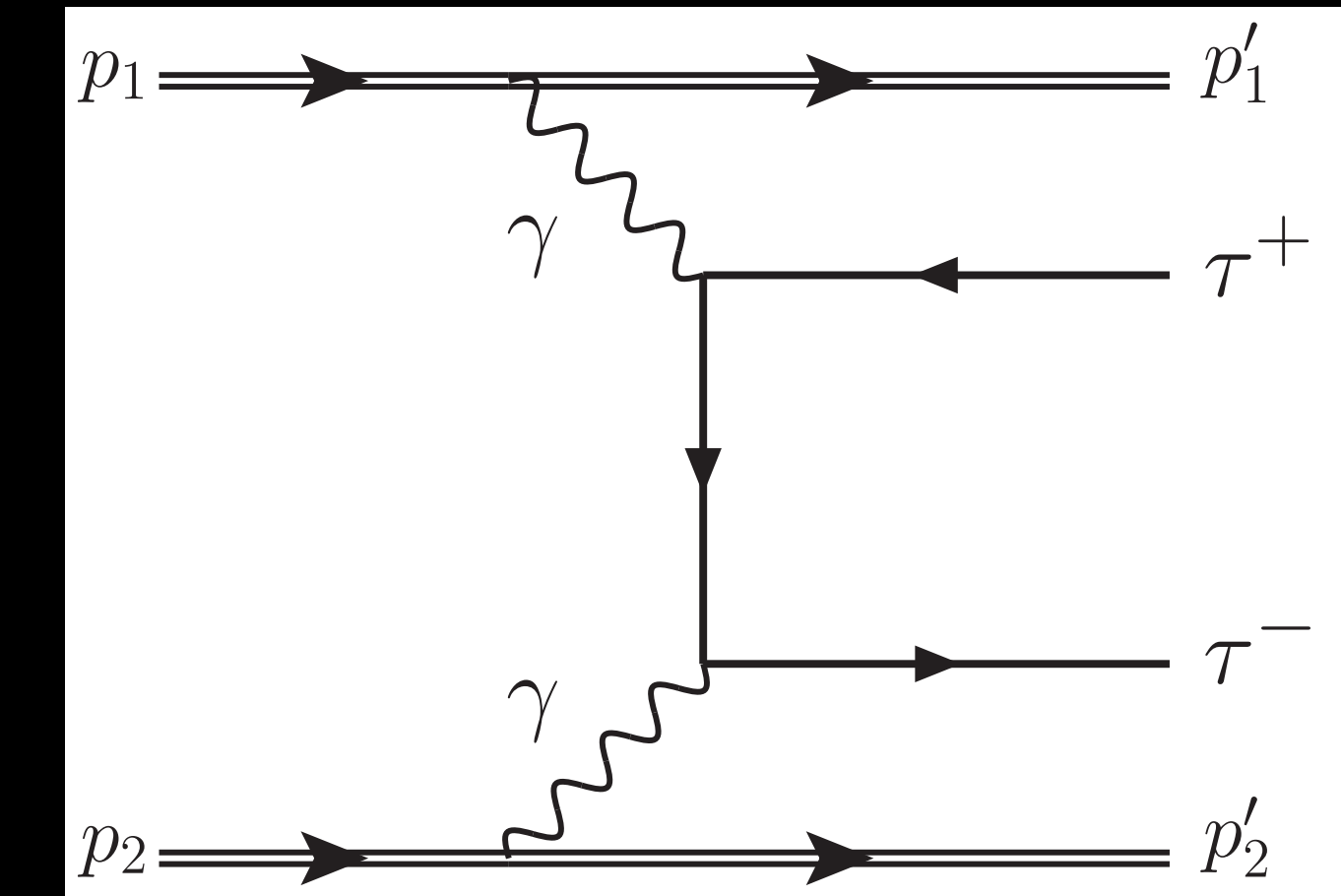
DISCLOSING QUANTUM CORRECTIONS TO ELECTROMAGNETIC INTERACTIONS OF TAU LEPTONS



Candidate $\gamma\gamma \rightarrow \tau\tau$ event measured in proton-proton collisions by CMS. The event is reconstructed as having a leptonic τ decay, $\tau \rightarrow \mu\nu\nu$, with the μ track indicated in red, and a hadronic τ decay, $\tau \rightarrow \pi\pi\pi\nu$, with the 3 charged pions indicated by the yellow tracks and by the energy deposits in the ECAL (green) and HCAL (cyan)

The LHC as a photon collider

- When protons pass each other at relativistic velocities
→ generate intense electromagnetic fields
 - photon-photon collisions occur
- First observation of $\gamma\gamma \rightarrow \tau\tau$ in proton-proton collisions
 - 5.3σ observed, 6.5σ expected
- Non-dissociative protons → low hadronic activity



Elastic signal events characterized by low track multiplicity

Measurement of the g_τ -2

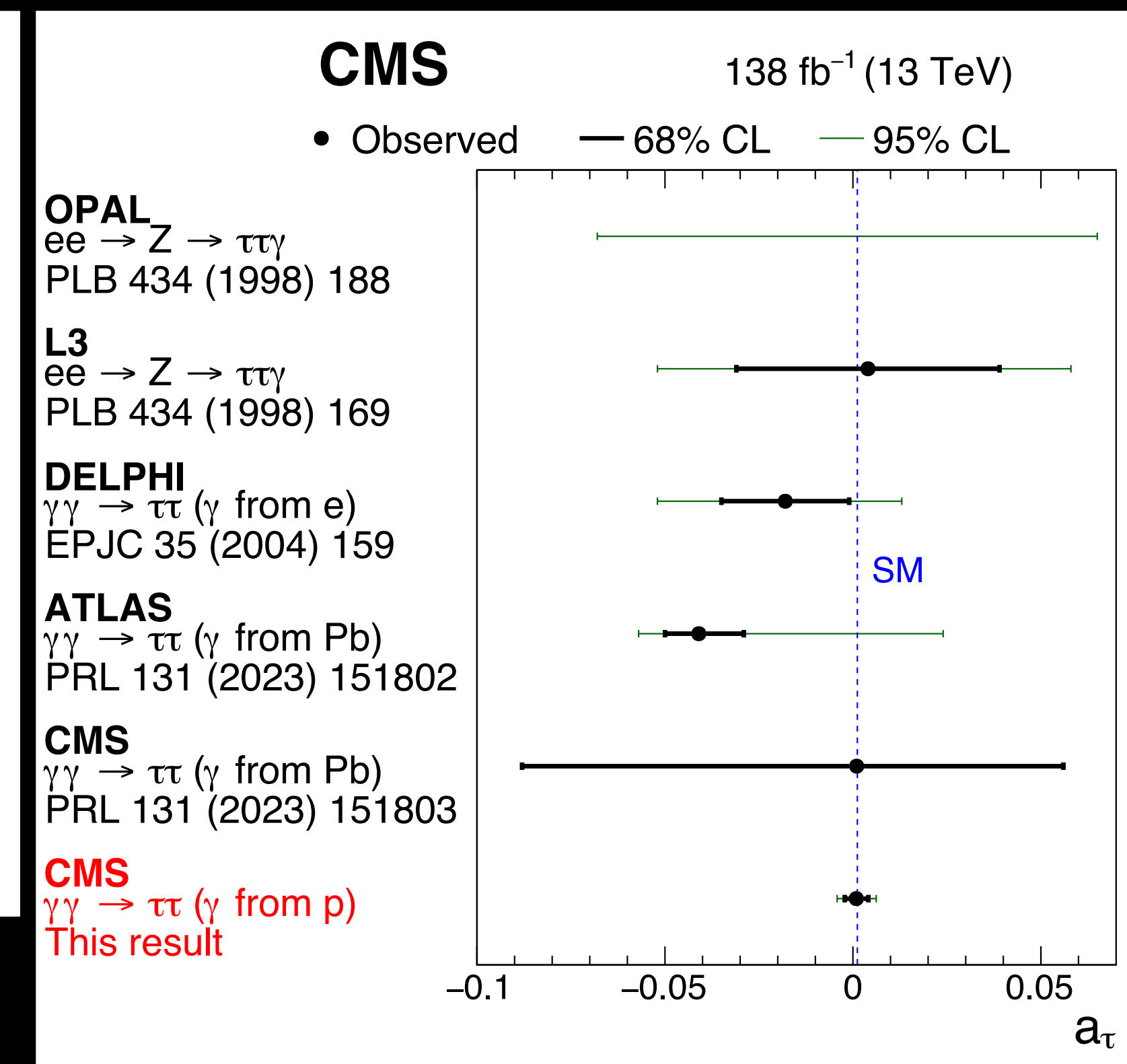
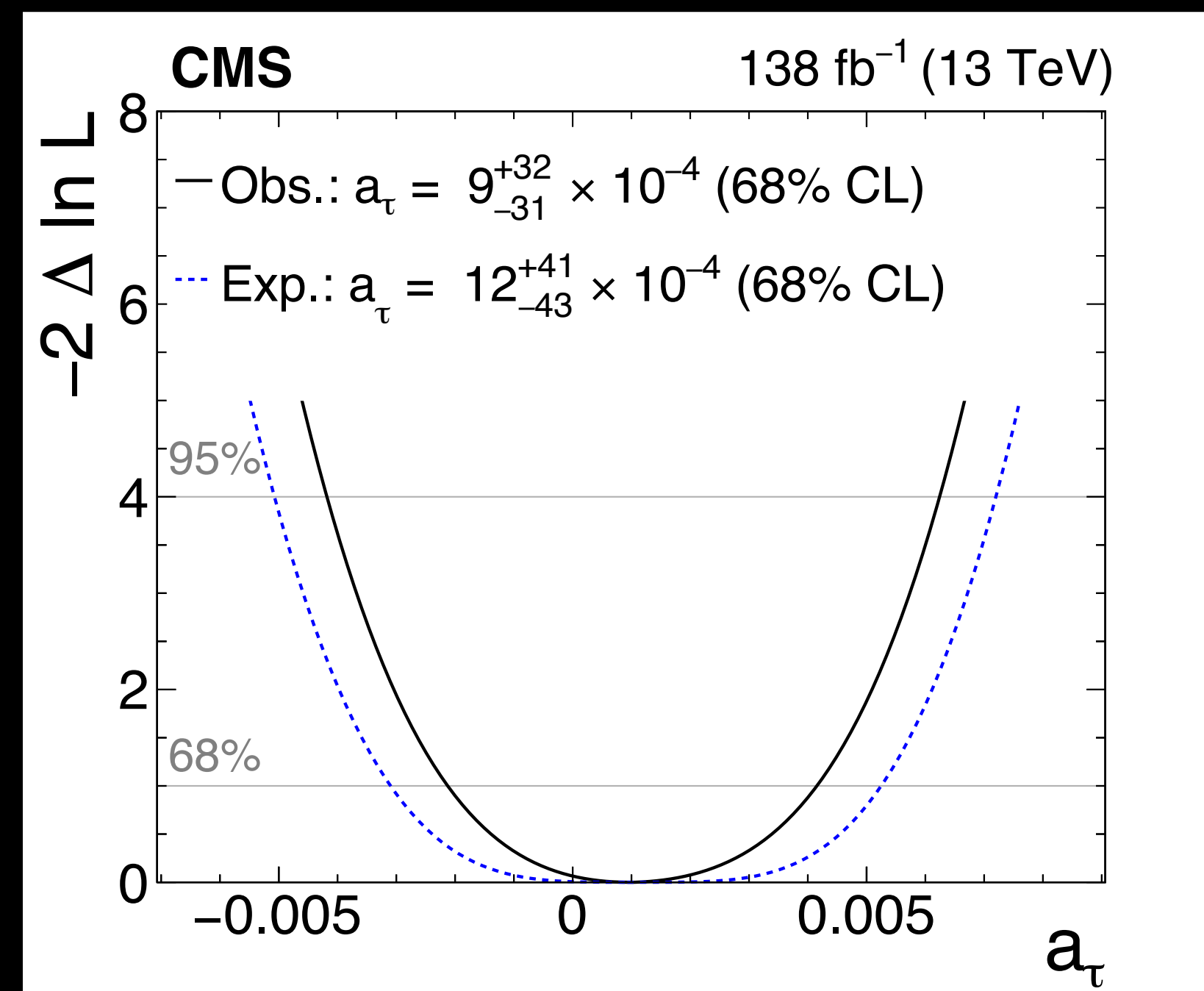
Most general form of the QED vertex:

$$\Gamma^\mu = \gamma^\mu F_1(q^2) + \frac{\sigma^{\mu\nu} q_\nu}{2m} [iF_2(q^2) + F_3(q^2)\gamma_5]$$

$$F_2(0) = a_\ell \equiv (g_\ell - 2)/2$$

$$F_3(0) = -\frac{2m}{e} d_\ell$$

g_ℓ (gyromagnetic ratio) → relates the magnetic moment to the spin of the lepton

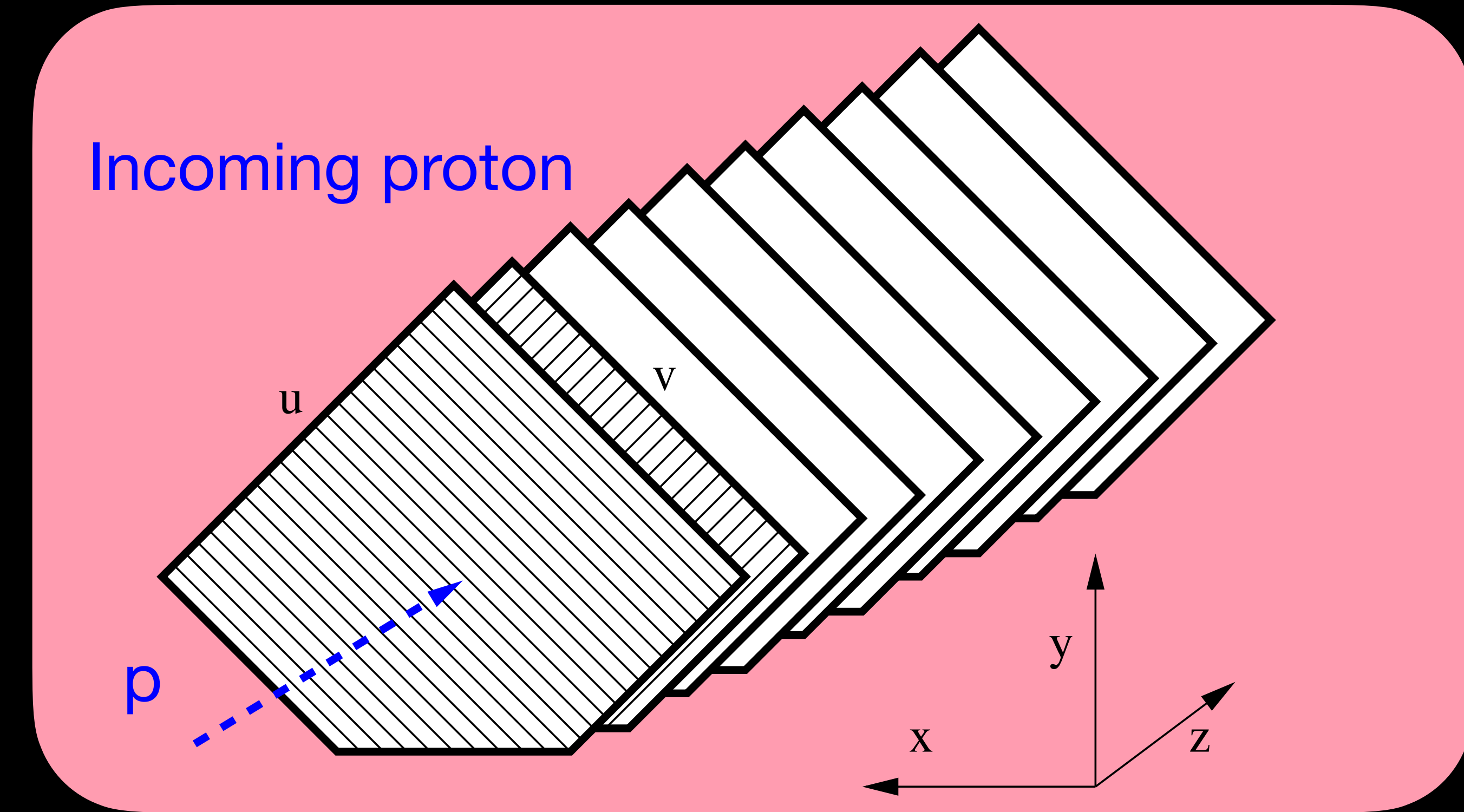


Schwinger term:

$$a_\ell = \frac{\alpha}{2\pi} \simeq 0.00116$$

- Extremely sensitive analysis
- Limits set to ~3 X Schwinger term

Milestone in collider physics!



The TOTEM Roman pot detectors

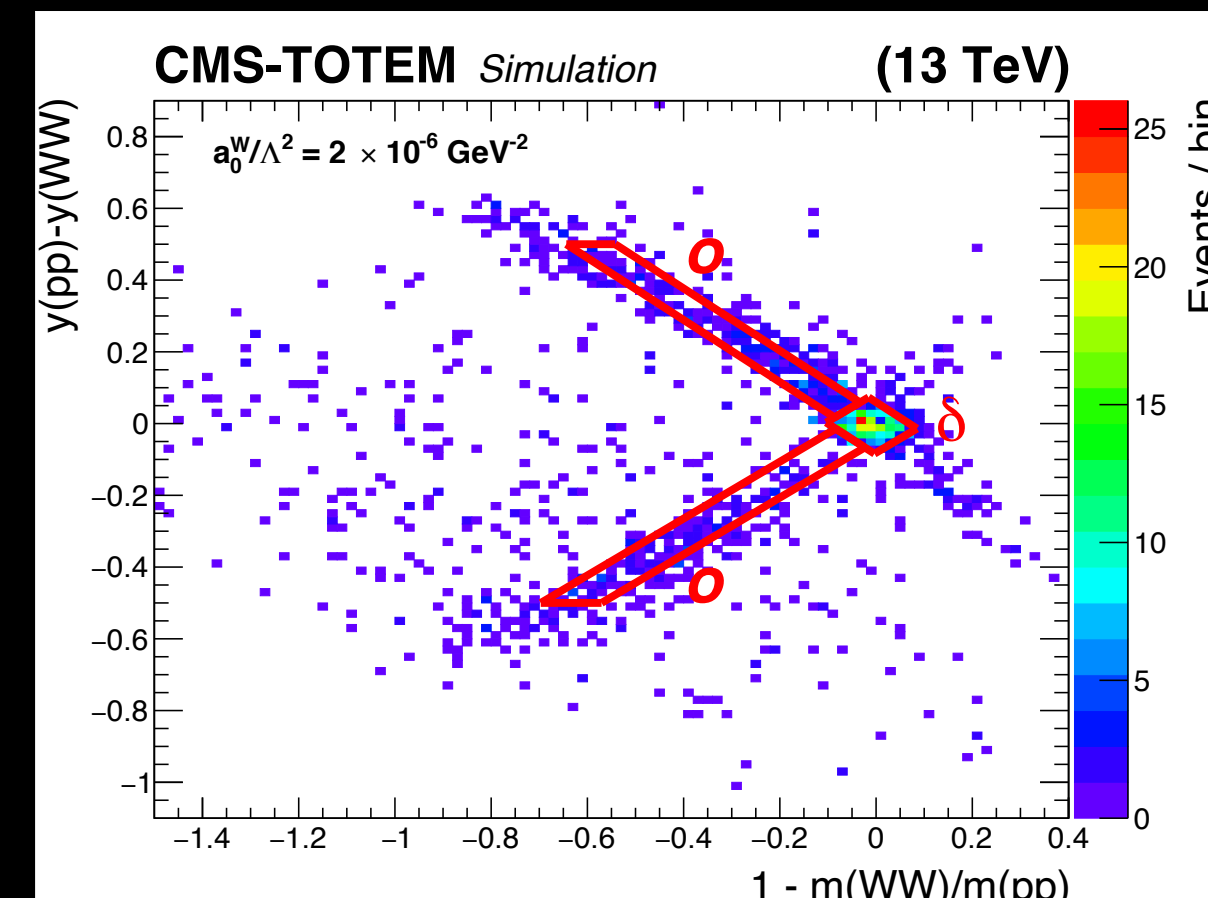
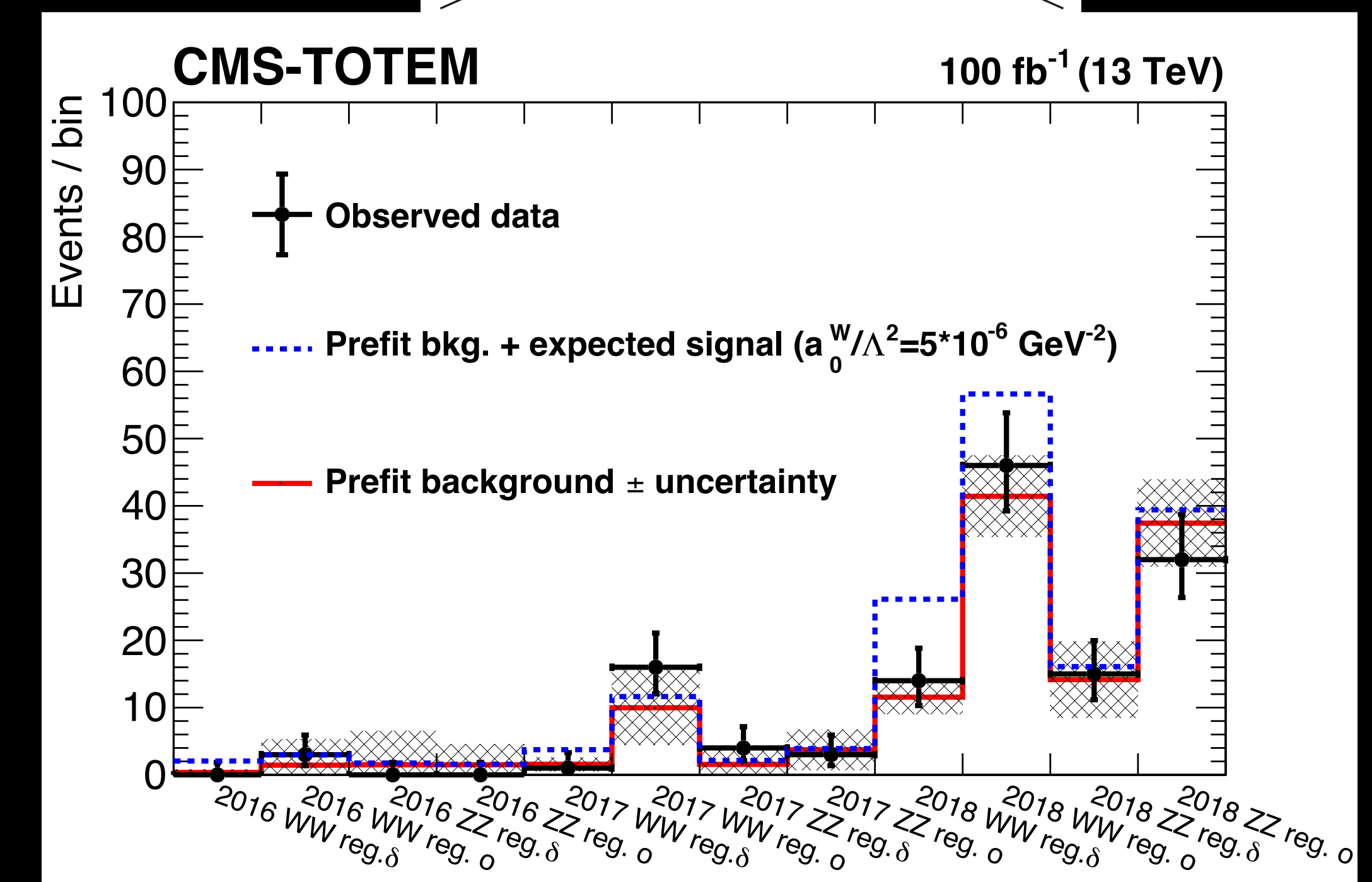
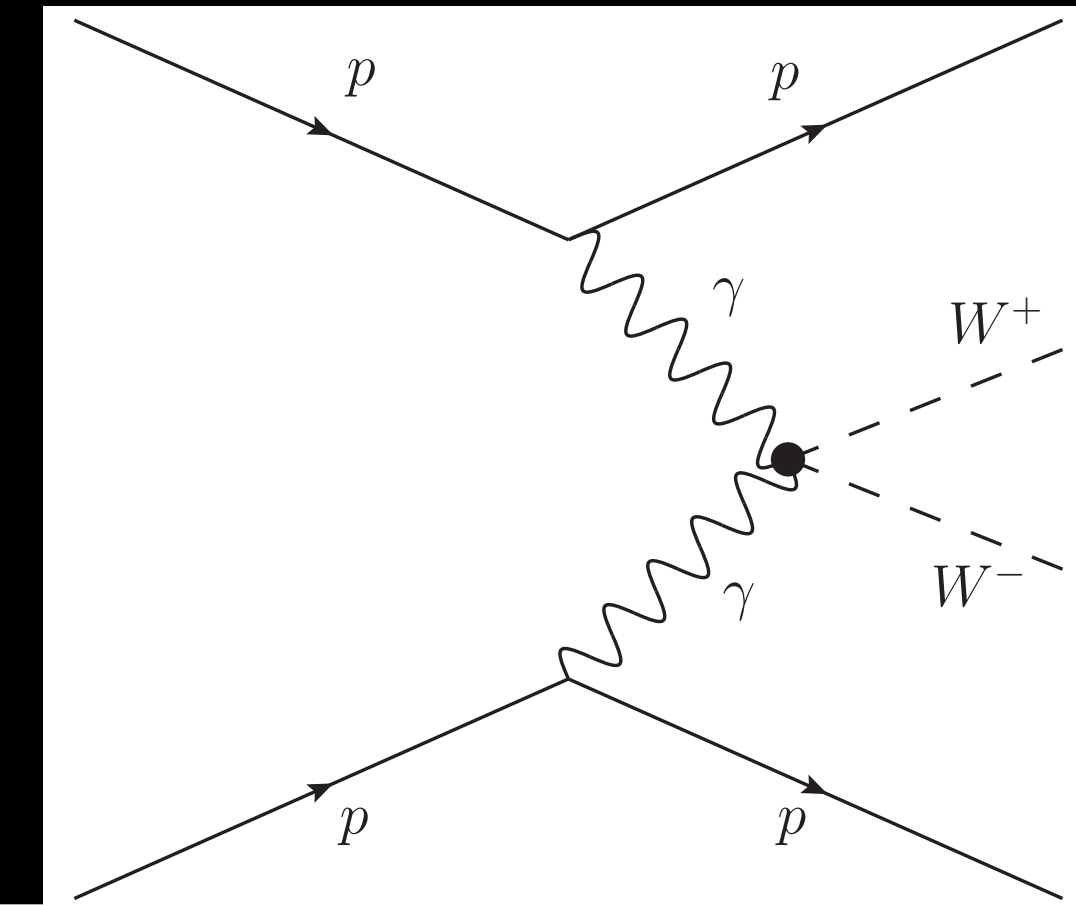
- reconstruct transverse momentum of scattered protons
- estimate the transverse location of the primary interaction

New studies on high- β^* period in 2018 expected to enable several physics analyses

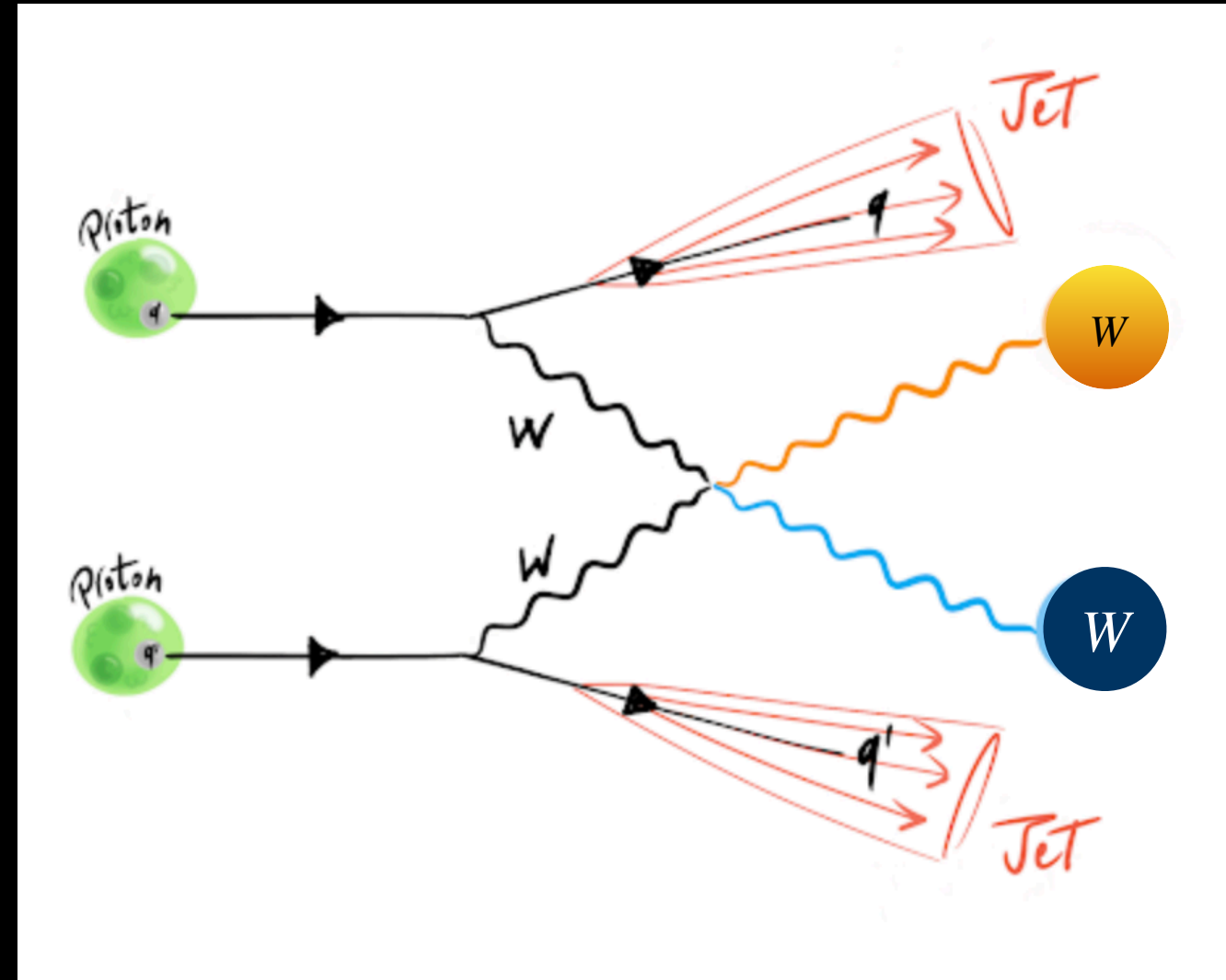
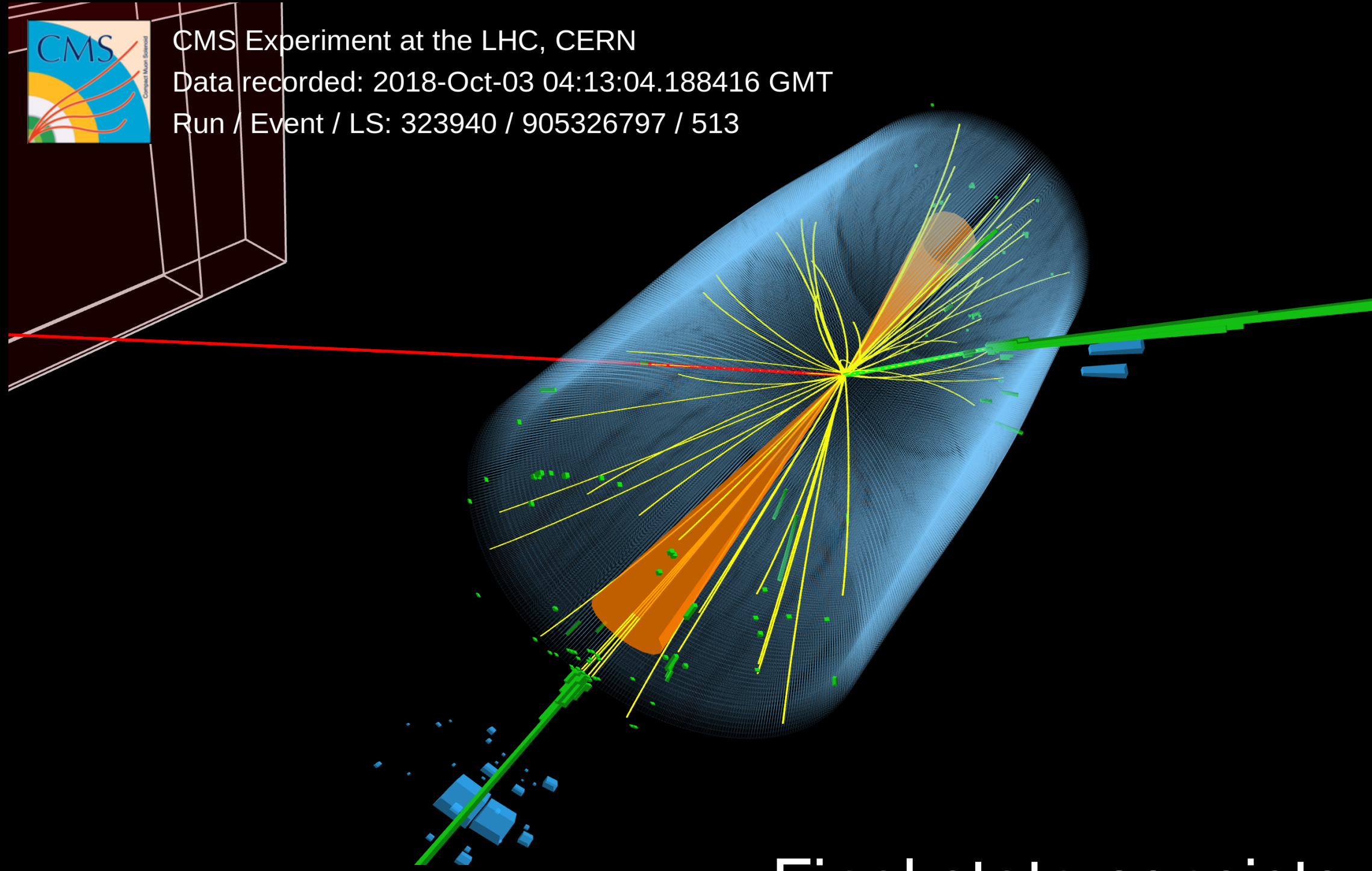


Search for exclusive $\gamma\gamma \rightarrow WW$ and $\gamma\gamma \rightarrow ZZ$ production in final states with jets and forward protons

- Both protons tagged by the precision proton spectrometer (PPS)
- The $\gamma\gamma \rightarrow WW$ process allows the study of the quartic coupling
- Events selected based on properties of jets, the protons and their correlation
- First search for anomalous high-mass $\gamma\gamma \rightarrow WW$ and $\gamma\gamma \rightarrow ZZ$ using reconstructed forward protons
- Limits 15-20x more stringent than previous results



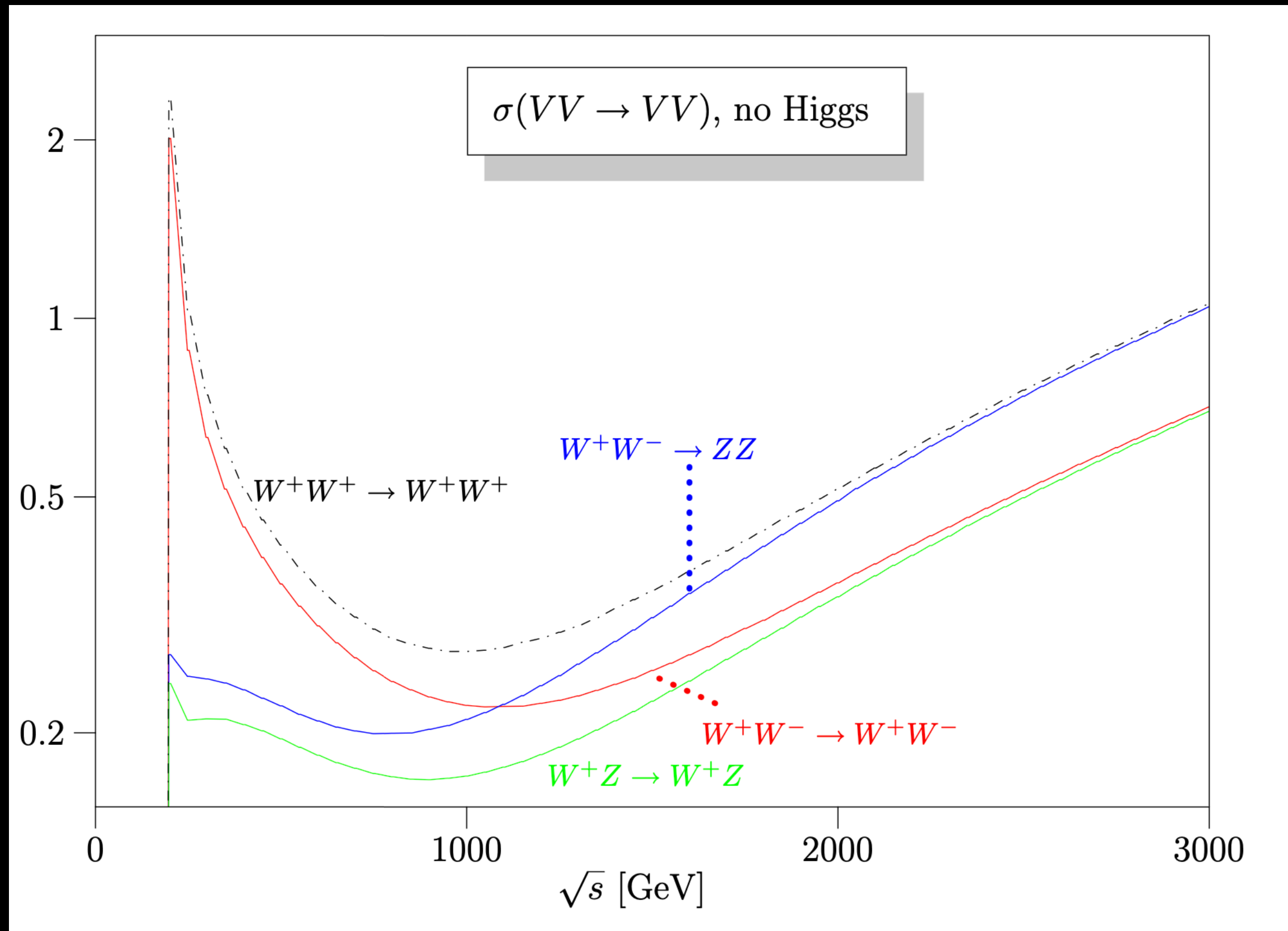
Vector Boson Scattering



- Final state consists of two high transverse momenta (p_T) jets
- Rapidity gap between jets → no color flow
- High mass of the two jets (M_{jj})
- Decay product of the gauge bosons: central with respect to jets
- Pure electro-weak interactions of order at least α_{EW}^4

Why Vector Boson Scattering?

Studying the Higgs
mechanism *Higgslessly*!



arXiv:0806.4145

ChatGPT

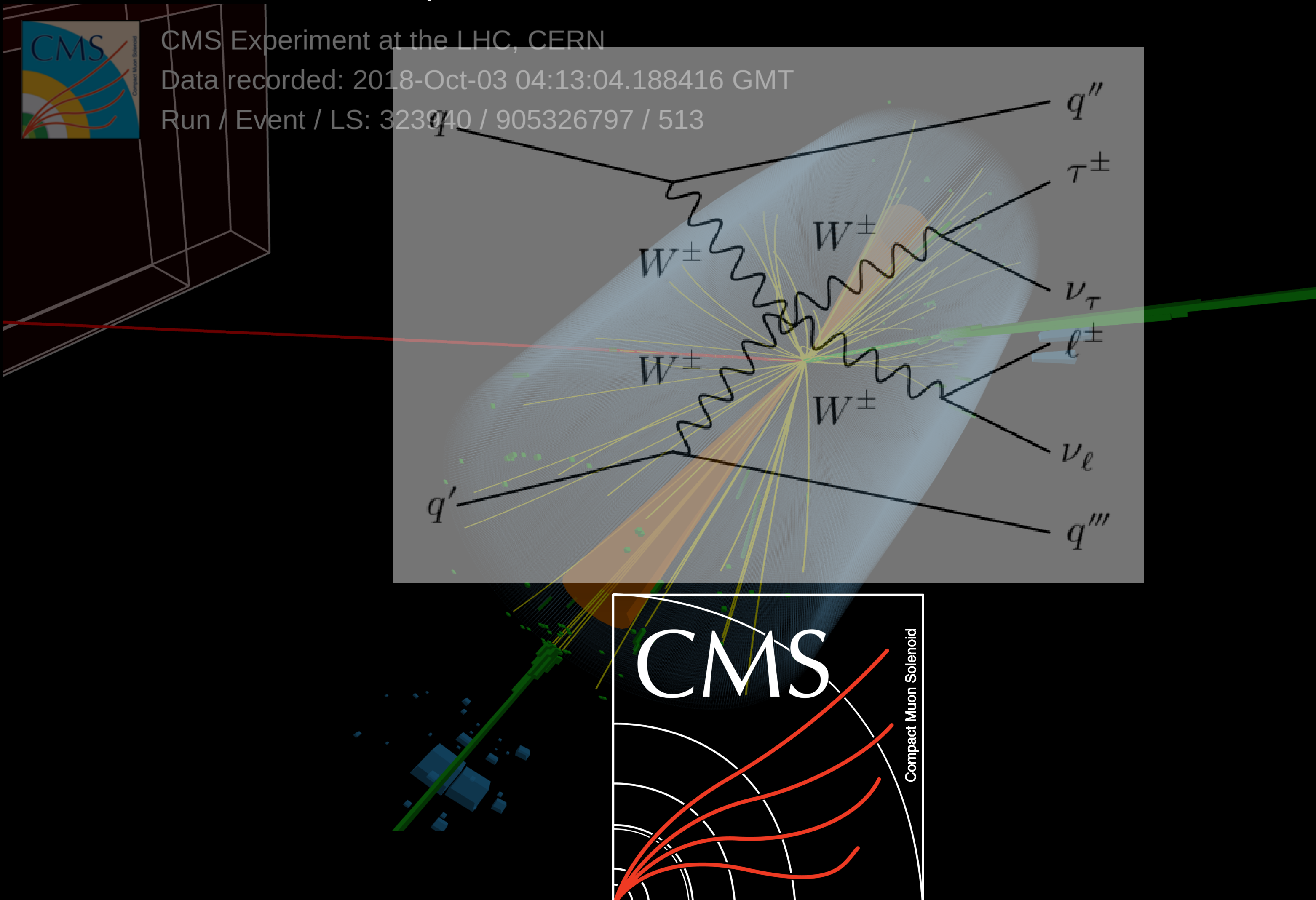
“However, it is important to note that the precise role of the Higgs boson in unitarizing WW scattering, in particular, is still an active area of research and there are ongoing studies to refine our understanding of this process.”

Vector Boson Scattering – evolution of knowledge

\sqrt{s}	Process	Reference	Significance/Status
8 TeV	EW $W^\pm W^\pm jj$ ($2\ell 2\nu jj$)	PhysRevLett.114.051801	2σ
	EW $Z\gamma jj$ ($\nu\nu/\ell\ell\gamma jj$)	PhysLettB770(2017)380-402	3σ
	EW $W^\pm\gamma jj$ ($\ell\nu\gamma jj$)	JHEP06(2017)106	2.7σ
	EW $W^\pm Zjj$ ($3\ell\nu jj$)	PhysRevLett.114.051801	2σ
13 TeV	EW $W^\pm W^\pm jj$ ($2\ell 2\nu jj$)	PhysLettB809(2020)	2016: 5.5σ , Run II $\gg 5.0\sigma$
	EW $ZZjj$ ($4\ell jj$)	PhysLettB812(2021)135992	2016: 2.7σ , Run II: 4.0σ
	EW $W^\pm Zjj$ ($3\ell jj$)	PhysLettB809(2020)135710	6.8σ
	EW $Z\gamma jj$ ($\ell\ell\gamma jj$)	PhysRevD.104.072001	4.7σ , Run II $\gg 5.0\sigma$
	EW $W^\pm\gamma jj$ ($\ell\nu\gamma jj$)	PhysLettB811(2020)135988	2016: 5.3σ
	EW $W^\pm Vjj$ ($\ell\nu jjjj$)	arXiv:2112.05259	4.4σ
	EW $W^\pm W^\mp jj$ ($2\ell 2\nu jj$)	arXiv:2205.05711	5.6σ
	EW $VVpp$ ($4jpp$)	arXiv:2211.16320	CMS with TOTEM
	EW $W^\pm\gamma jj$ ($\ell\nu\gamma jj$)	arXiv:2212.12592	Cross section measurement with full Run II
	$W^\pm W^\pm jj$ ($\ell\tau_{\text{had}} 2\nu jj$)	SMP-22-008	2.9σ

VBS Same Sign WW with hadronic τ

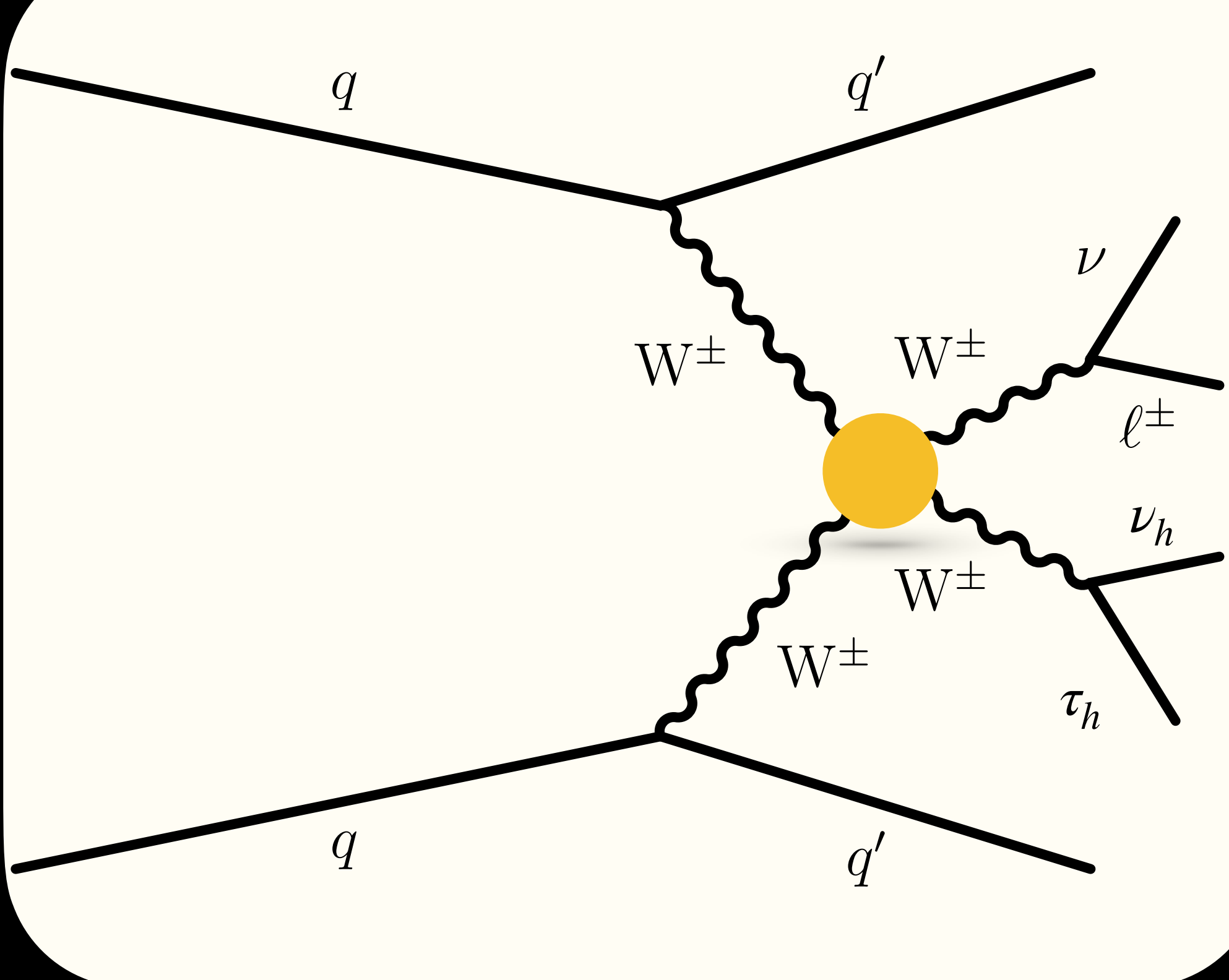
<http://cds.cern.ch/record/2867989?ln=en>



Vector Boson Scattering (VBS)

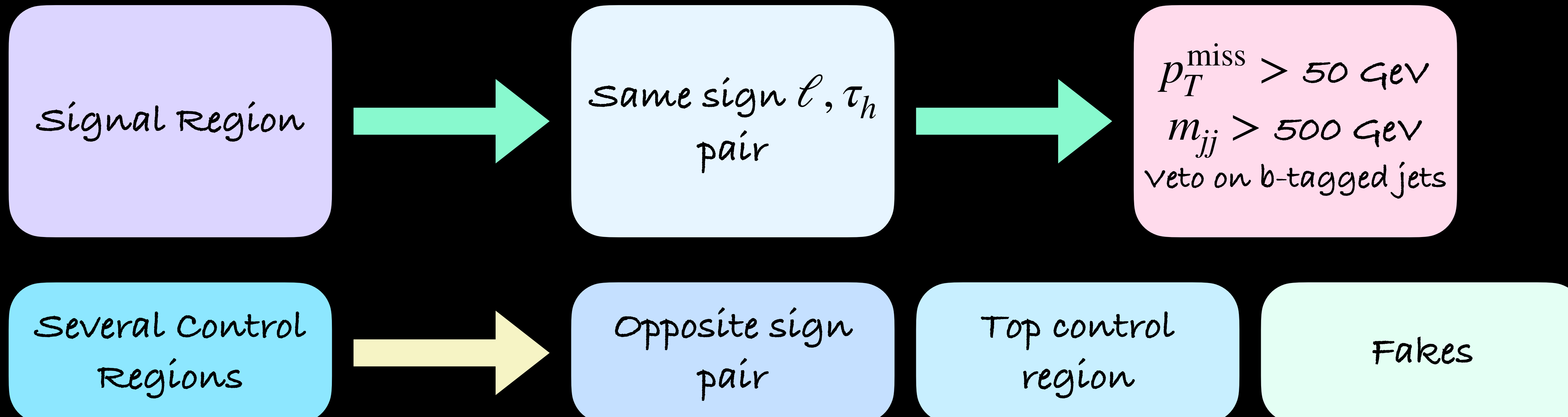
- Study of vector boson scattering processes
→ essential to probe nature of **electroweak symmetry breaking**
- Constraints on various **effective field theory operators** evaluated
- Several kinematic observables sensitive to the effect of new physics

Pure electro-weak interactions of order α_{EW}^6



VBS Same Sign WW with hadronic τ

- Final state where one of the two same-signed W-bosons decays to a hadronic τ
 - Signature: $\tau_h \nu_\tau \ell \nu_\ell (\ell = e, \mu)$
- Evidence of SM process at 2.7σ , signal strength: $1.44^{+0.63}_{-0.56}$
- Public since August 2023



Exploring the implication of new physics modifying the quartic coupling in the Standard Model

$$\mathcal{L} = \mathcal{L}_{SM} + \boxed{\sum_i \frac{c_i}{\Lambda^2} \mathcal{O}_i} + \boxed{\sum_j \frac{f_j}{\Lambda^4} \mathcal{O}_j}$$

- In the past, diboson analyses used to extract sensitivity to dimension-6 operators and vector boson scattering primarily used to extract sensitivity to dimension-8 operators
- Now explore vector boson scattering for both dimension-6 and dimension-8 exploration

Exploring the implication of new physics modifying the quartic coupling in the Standard Model

$$\mathcal{L} = \mathcal{L}_{SM} + \boxed{\begin{array}{c} f_2 \\ \diagdown \quad \diagup \\ g \quad z \\ \diagup \quad \diagdown \\ f_1 \end{array}} + \boxed{\begin{array}{c} q \quad q' \\ \diagdown \quad \diagup \\ W^\pm \\ \diagup \quad \diagdown \\ W^\pm \end{array}}$$

- In the past, diboson analyses used to extract sensitivity to dimension-6 operators and vector boson scattering primarily used to extract sensitivity to dimension-8 operators

Exploring the implication of new physics modifying the quartic coupling in the Standard Model

$$\mathcal{L} = \mathcal{L}_{SM} + \boxed{\text{Diagram A}} + \boxed{\text{Diagram B}}$$

The equation shows the Lagrangian \mathcal{L} as the sum of the Standard Model Lagrangian \mathcal{L}_{SM} and two additional diagrams. Diagram A, enclosed in a green box, shows a quark q and antiquark q' interacting with a red circle representing a new particle. Two wavy lines labeled W^\pm connect the quark-antiquark pair to the red circle. Diagram B, enclosed in a cyan box, shows a similar interaction but with a different internal loop topology.

- Now explore vector boson scattering for both dimension-6 and dimension-8 exploration

VBS Same Sign WW with hadronic τ

- Deep Neural Network (DNNs) trained with used to gain sensitivity to BSM signals

		Wilson coefficient	68% CL interval(s)		95% CL interval	
			Expected	Observed	Expected	Observed
dim-6		$c_{ll}^{(1)}$	$[-12.9, -8.03] \cup [-2.95, 1.91]$	$[-11.6, 0.045]$	$[-14.6, 3.53]$	$[-13.5, 2.11]$
		$c_{qq}^{(1)}$	$[-0.501, 0.576]$	$[-0.341, 0.416]$	$[-0.742, 0.818]$	$[-0.605, 0.681]$
		c_W	$[-0.681, 0.669]$	$[-0.513, 0.481]$	$[-0.987, 0.974]$	$[-0.842, 0.818]$
		c_{HW}	$[-7.00, 6.09]$	$[-5.48, 4.31]$	$[-9.99, 9.05]$	$[-8.68, 7.60]$
		c_{HWB}	$[-41.7, 69.6]$	$[30.7, 89.2]$	$[-66.6, 96.4]$	$[-49.7, 110]$
		c_H	$[-16.6, 18.1]$	$[-12.0, 14.0]$	$[-24.7, 26.3]$	$[-20.9, 22.7]$
		c_{HD}	$[-24.6, 34.7]$	$[-15.3, 31.5]$	$[-38.2, 48.8]$	$[-31.4, 45.5]$
		$c_{Hl}^{(1)}$	$[-28.8, 29.9]$	$[-38.2, 39.5]$	$[-49.4, 49.7]$	$[-69.3, 68.3]$
		$c_{Hl}^{(3)}$	$[-1.43, 2.23] \cup [5.88, 9.54]$	$[-0.045, 8.58]$	$[-2.64, 10.8]$	$[-1.59, 9.94]$
dim-8		$c_{Hq}^{(1)}$	$[-4.53, 4.42]$	$[-3.27, 3.44]$	$[-6.56, 6.44]$	$[-5.55, 5.60]$
		$c_{Hq}^{(3)}$	$[-2.39, 1.37]$	$[-1.88, 0.705]$	$[-3.24, 2.16]$	$[-2.82, 1.61]$
		f_{T0}	$[-1.02, 1.08]$	$[-0.774, 0.842]$	$[-1.52, 1.58]$	$[-1.32, 1.38]$
		f_{T1}	$[-0.426, 0.480]$	$[-0.319, 0.381]$	$[-0.640, 0.695]$	$[-0.552, 0.613]$
		f_{T2}	$[-1.15, 1.37]$	$[-0.851, 1.12]$	$[-1.75, 1.98]$	$[-1.51, 1.76]$
		f_{M0}	$[-9.89, 9.74]$	$[-8.07, 7.70]$	$[-14.6, 14.5]$	$[-13.1, 12.8]$
		f_{M1}	$[-12.5, 13.3]$	$[-9.54, 11.15]$	$[-18.7, 19.6]$	$[-16.4, 17.7]$
		f_{M7}	$[-20.3, 19.2]$	$[-17.6, 15.3]$	$[-29.9, 28.8]$	$[-27.6, 25.8]$
		f_{S0}	$[-11.6, 12.0]$	$[-9.60, 9.82]$	$[-17.4, 17.9]$	$[-15.9, 16.1]$
		f_{S1}	$[-37.4, 38.8]$	$[-40.9, 41.3]$	$[-57.2, 58.6]$	$[-60.9, 61.8]$
		f_{S2}	$[-37.4, 38.8]$	$[-40.9, 41.3]$	$[-57.2, 58.6]$	$[-60.9, 61.8]$

VBS Same Sign WW with hadronic τ

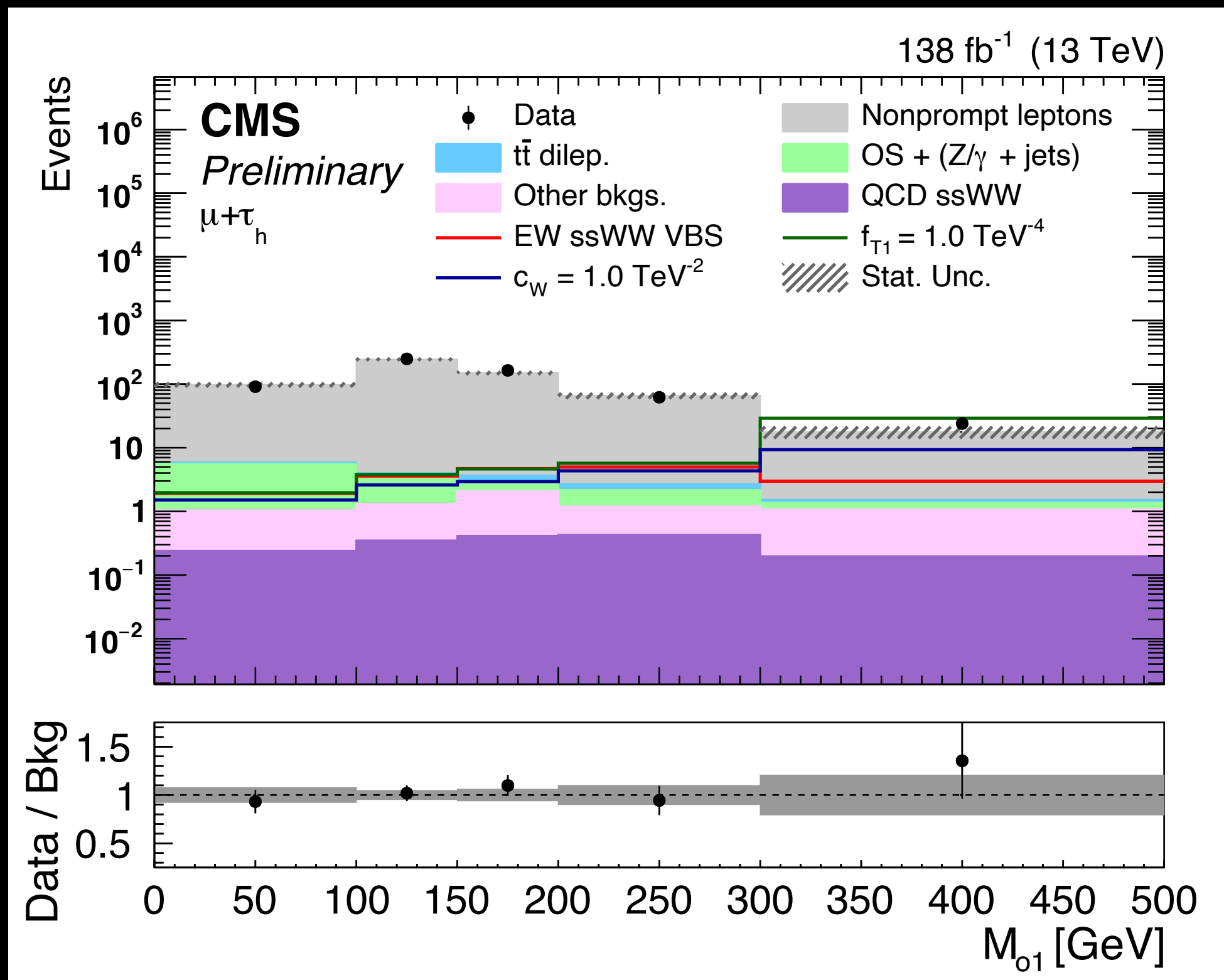
- First simultaneous extraction of dim-6 and dim-8 constraints
- Transverse mass (M_{01}) used as the variable of interest for 2D constraints

$$N \propto |\mathcal{A}|^2 = |\mathcal{A}_{SM}|^2 + \sum_{\alpha} \frac{C_{\alpha}}{\Lambda^2} \cdot 2\Re(\mathcal{A}_{SM} \mathcal{A}_{Q\alpha}^{(6)\dagger}) + \sum_{\alpha, \beta} \frac{C_{\alpha} C_{\beta}}{\Lambda^4} \cdot (\mathcal{A}_{Q\alpha}^{(6)} \mathcal{A}_{Q\beta}^{(6)\dagger}) +$$

Dim6 including linear, BSM and mixed contributions

$$\sum_k \left[\frac{f_k}{\Lambda^4} \cdot 2\Re(\mathcal{A}_{SM} \mathcal{A}_{Qk}^{(8)\dagger}) \right] + \sum_k \frac{f_k^2}{\Lambda^8} \cdot (\mathcal{A}_{Qk}^{(8)} \mathcal{A}_{Qk}^{(8)\dagger})$$

Dim8 including linear and BSM contributions

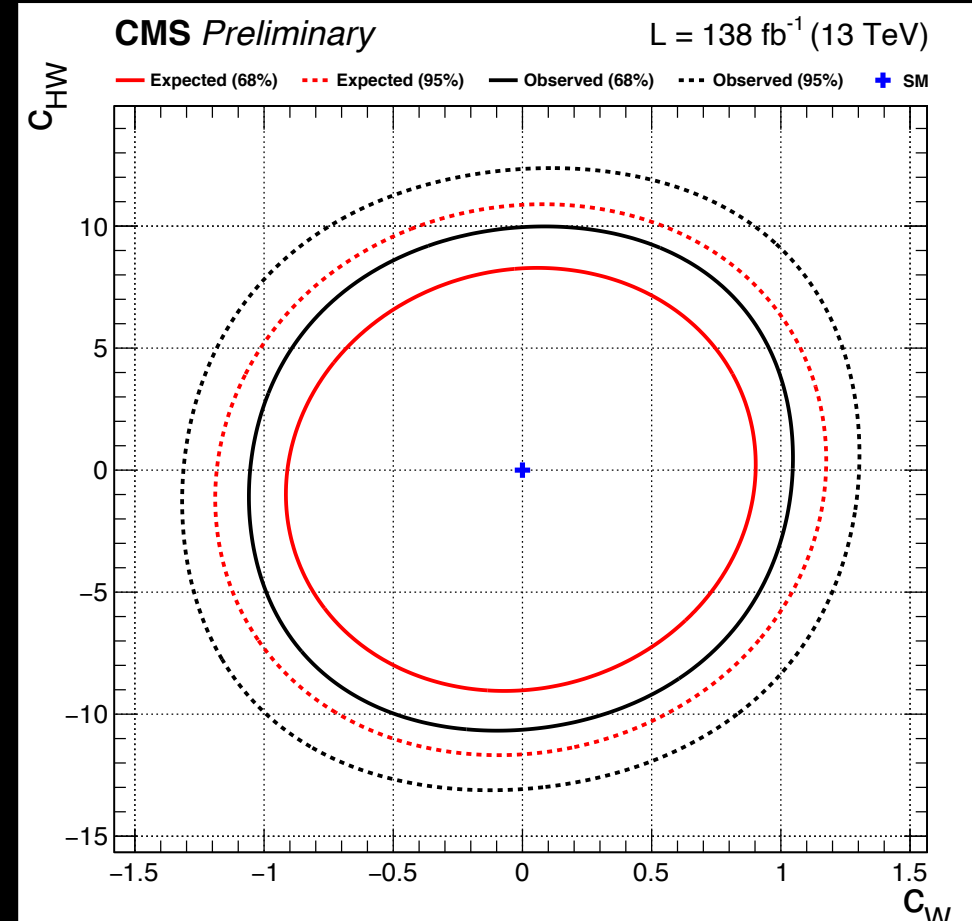
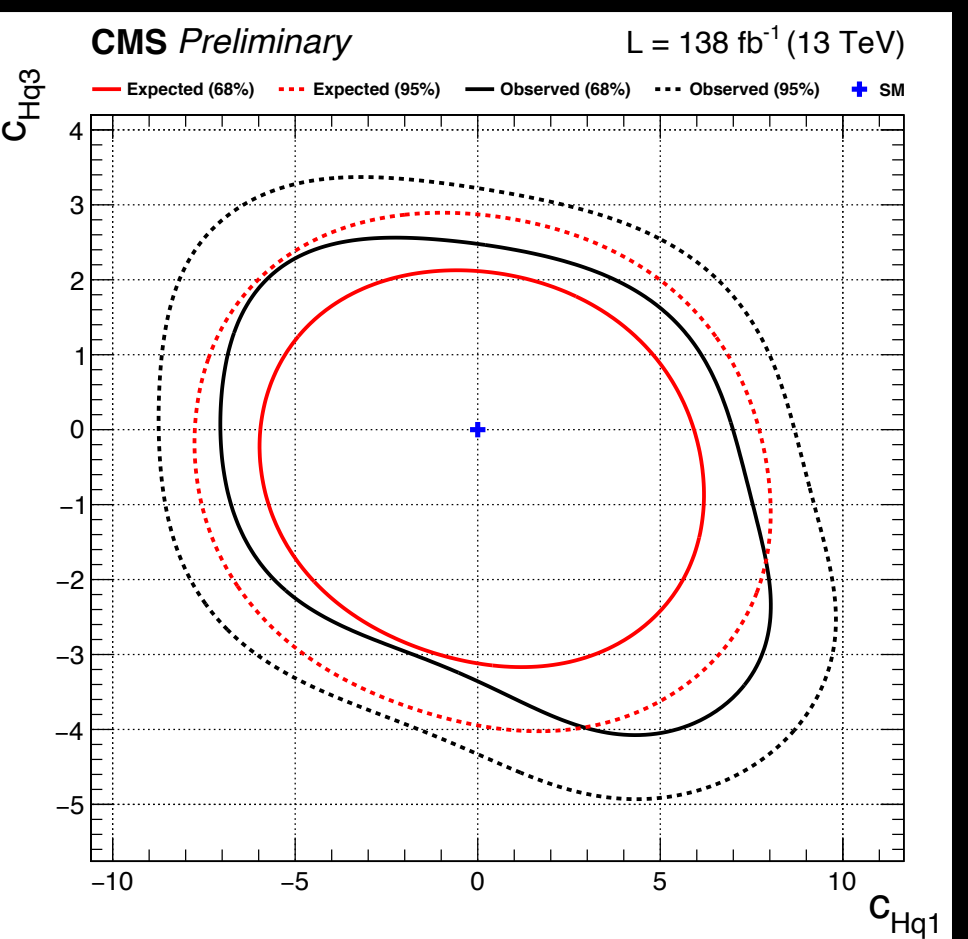
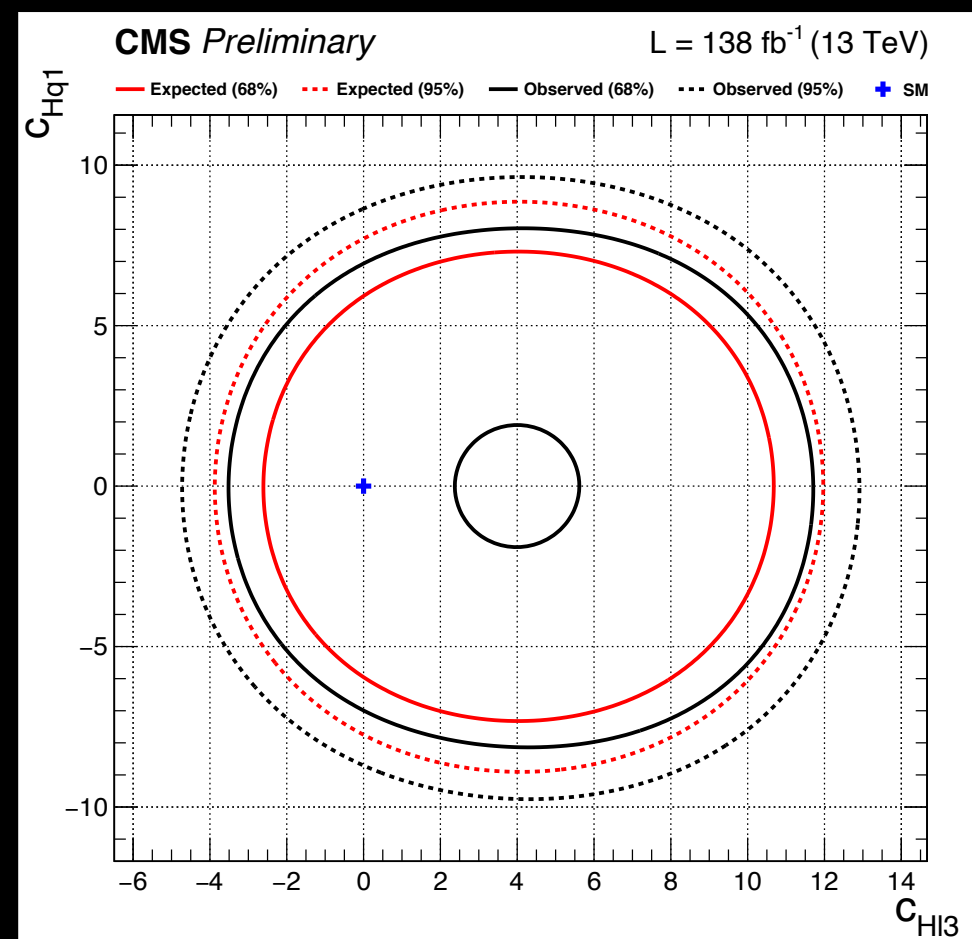


$$M_{01} = (p_{T\tau} + p_l + \vec{p}_T^{miss})^2 + |p_{T\tau} + \vec{p}_T^{miss}|^2$$

VBS Same Sign WW with hadronic τ

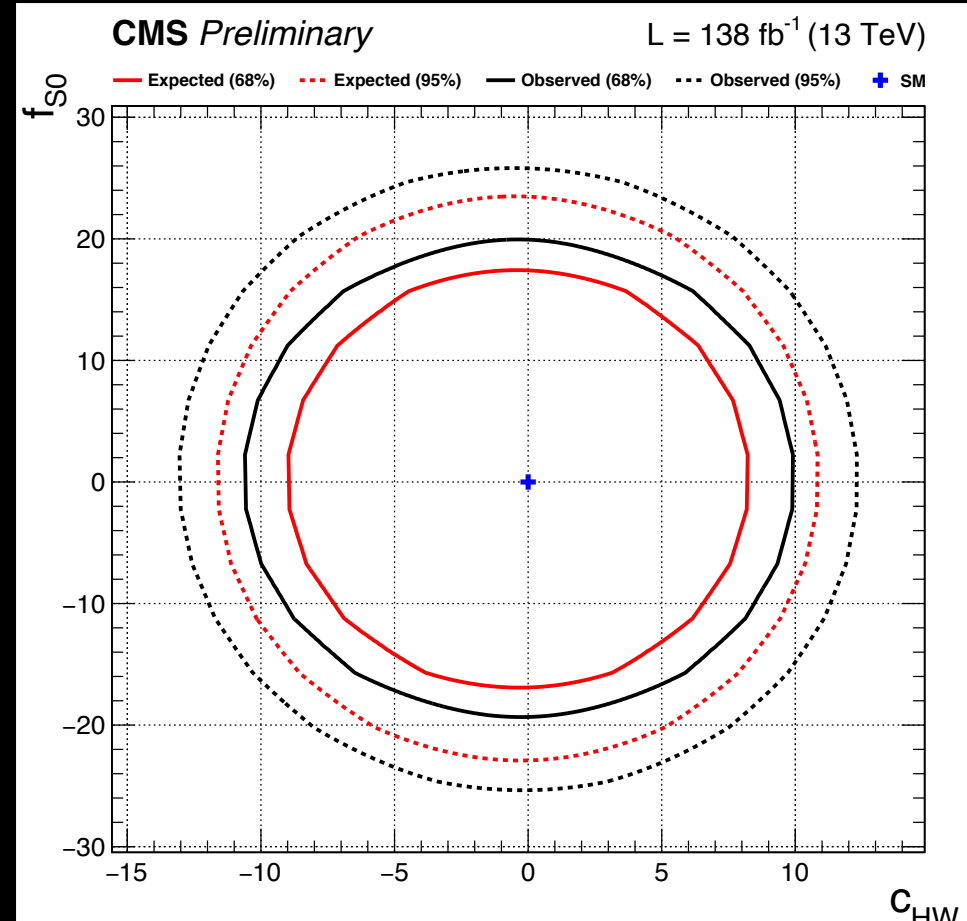
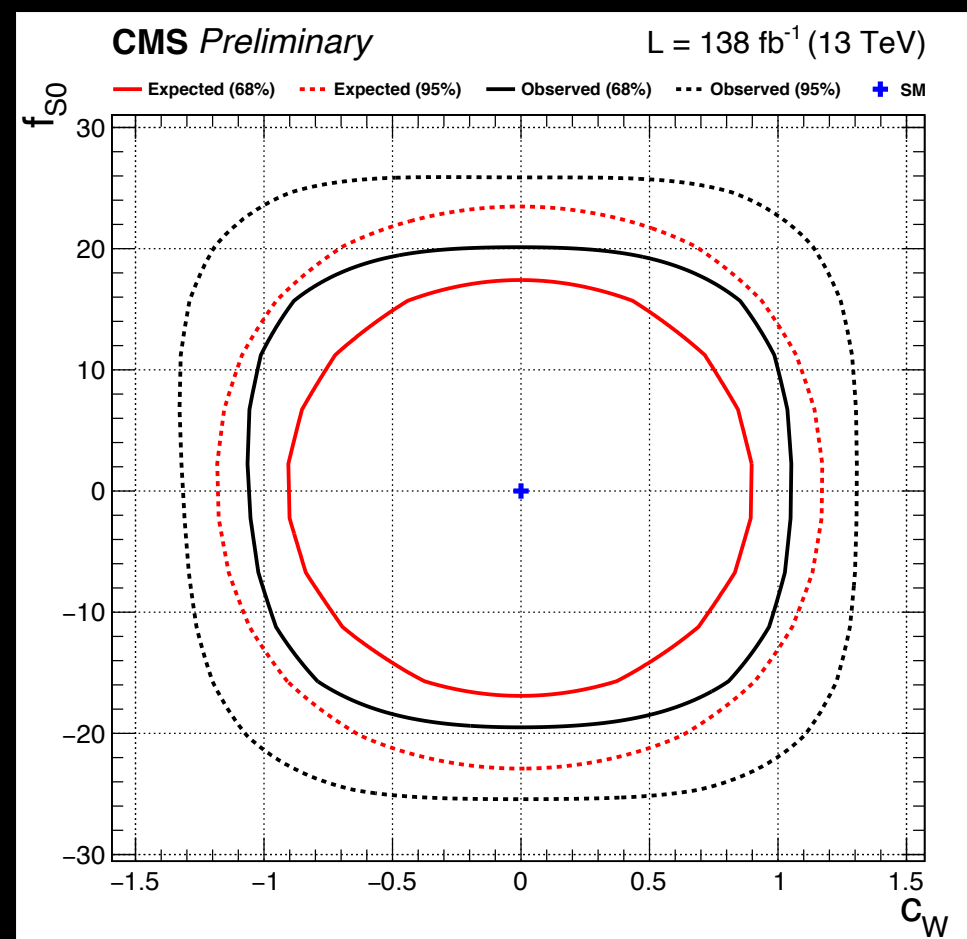
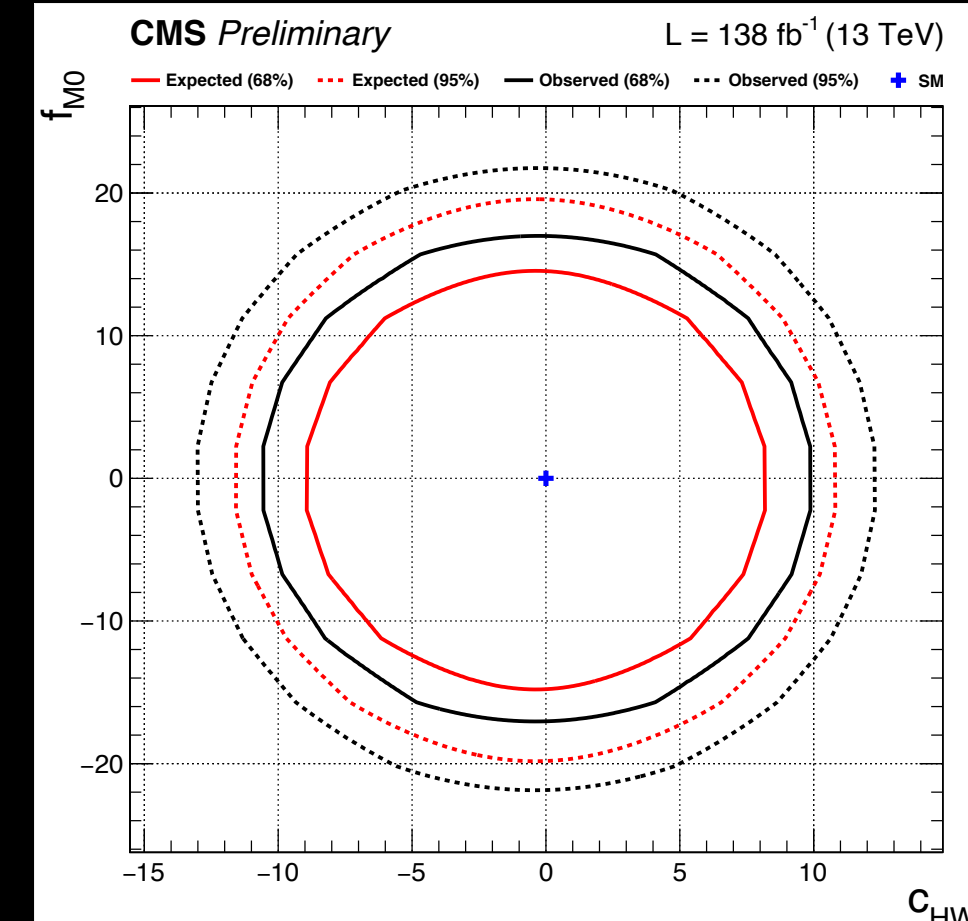
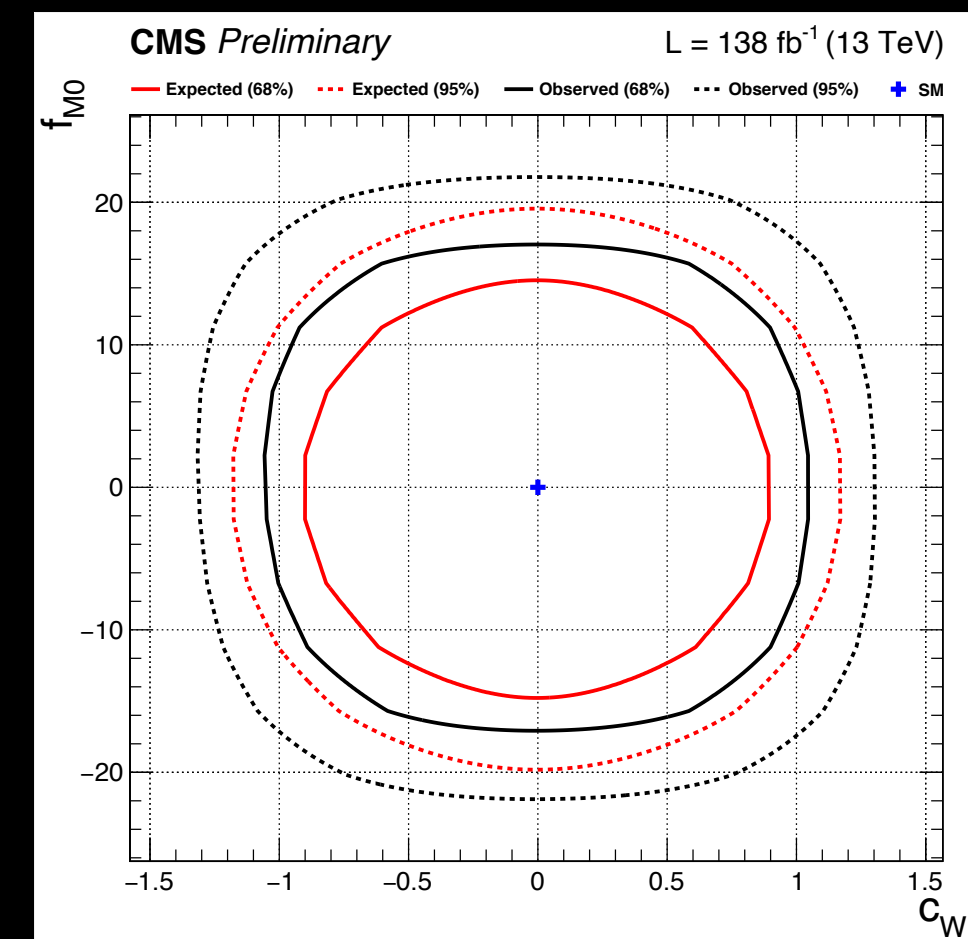
$$M_{01} = (p_{T\tau} + p_l + \vec{p}_T^{miss})^2 + |p_{T\tau} + \vec{p}_T^{miss}|^2$$

- Simultaneous extraction of dim-6 and dim-8 constraints

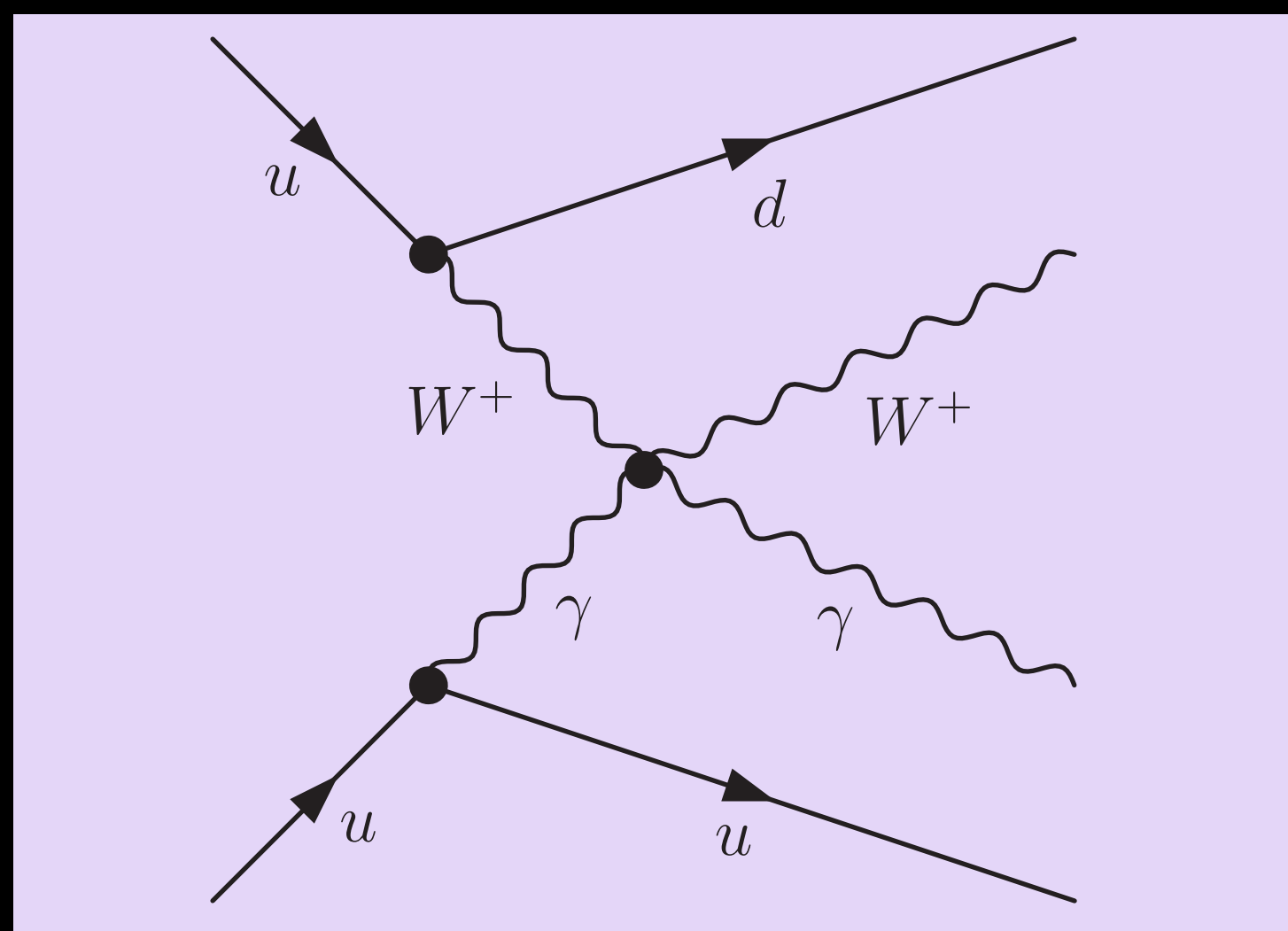


Sensitive to correlation between Higgs-fermion operators

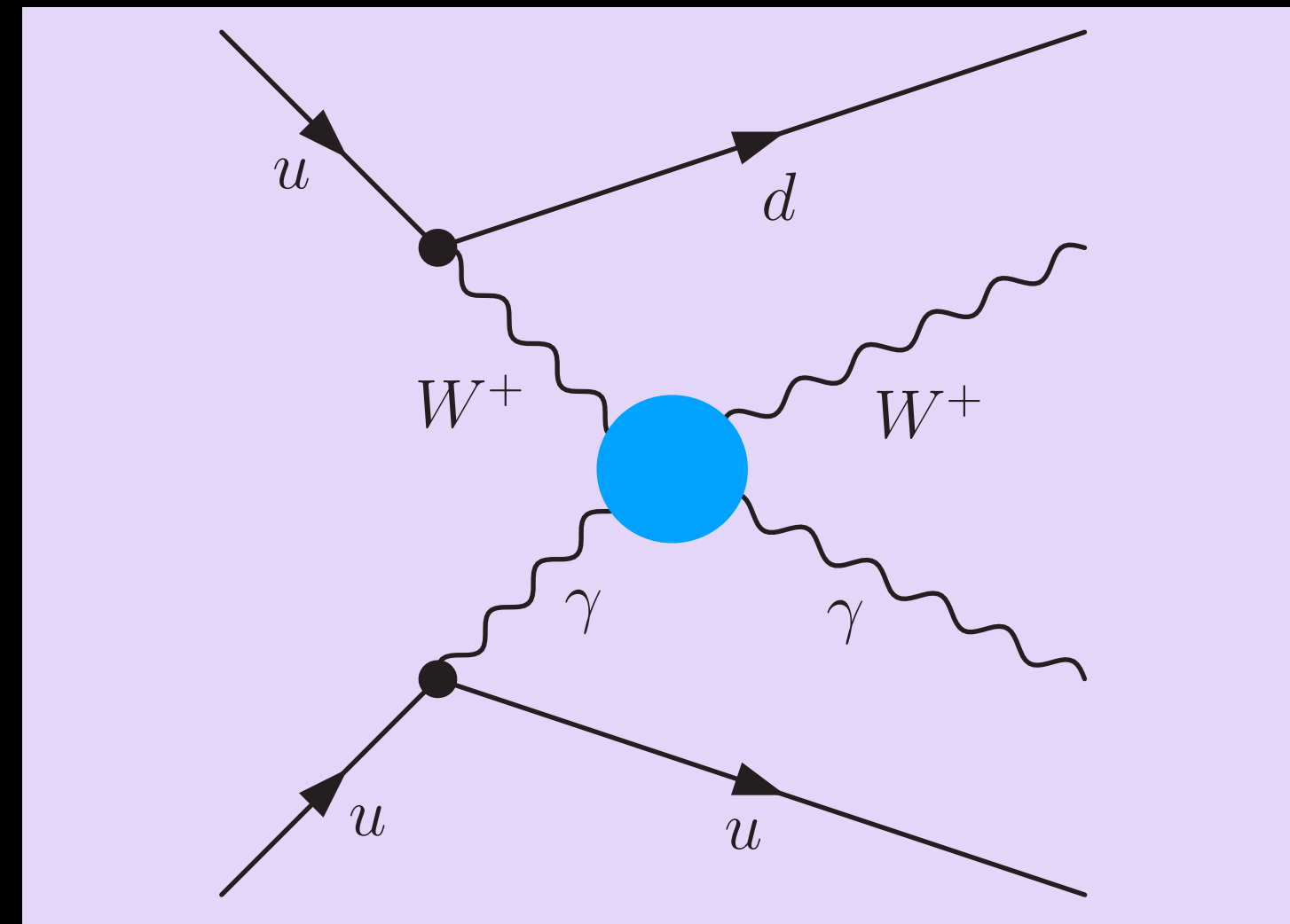
Fits between boson operators of dim-6 and dim-8



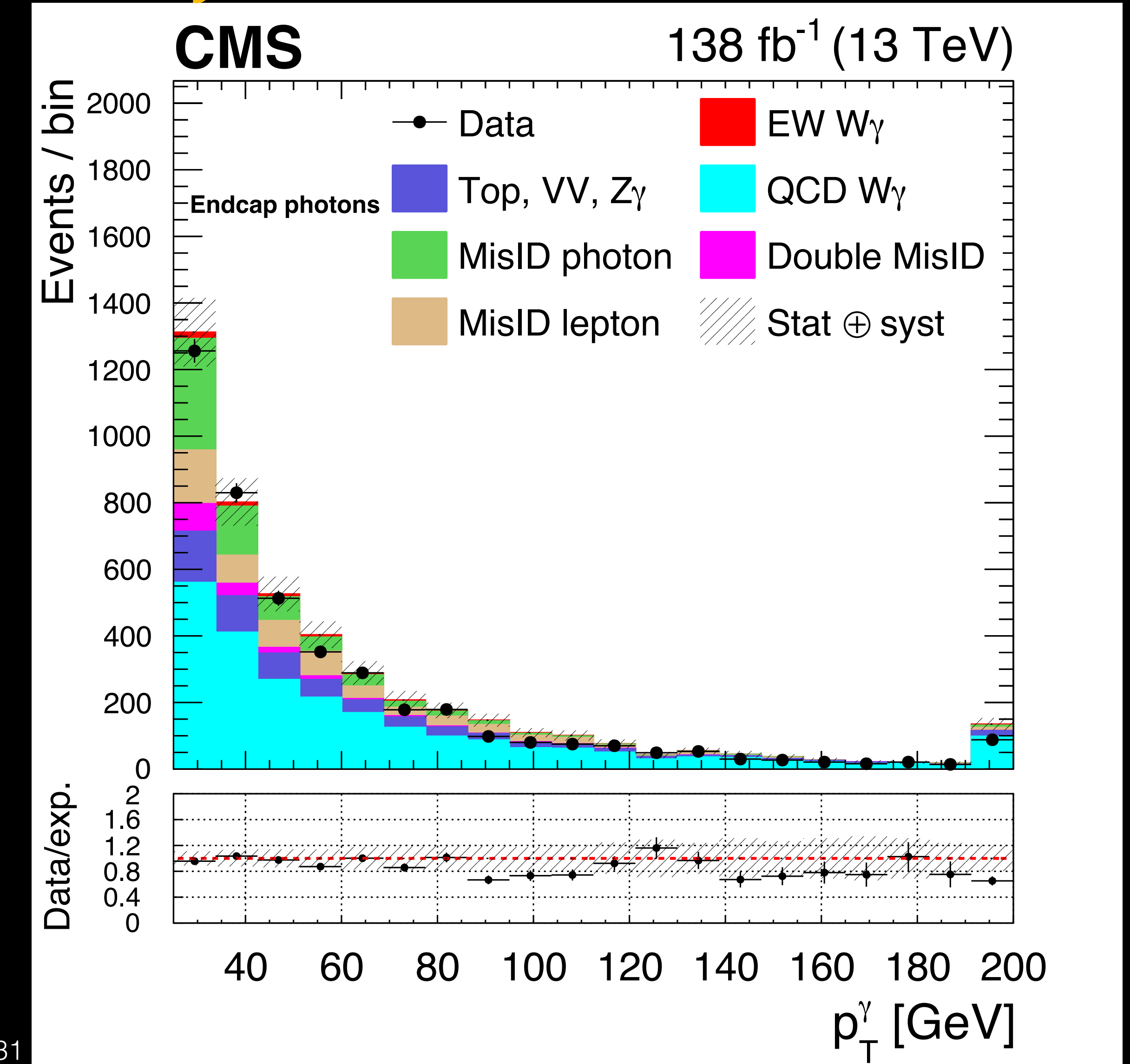
Measurement of the electroweak production of $W\gamma$ with two jets



Measurement of the electroweak production of $W\gamma$ with two jets



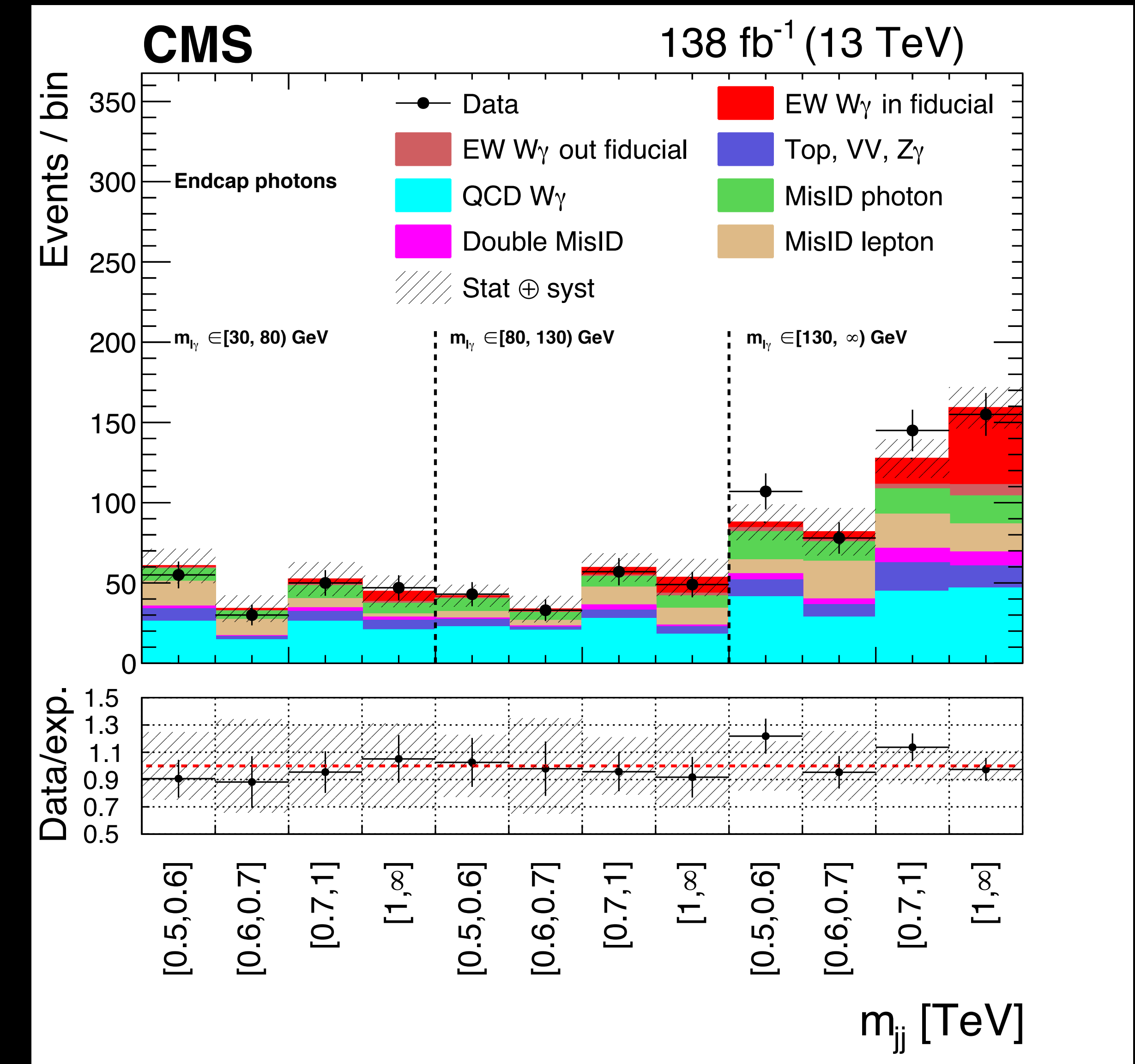
- First observation of the $W\gamma + 2$ jets process with observed (expected) significance of 5.3 (4.8) σ with 35.9 fb^{-1}
- Extensive measurement now possible with full Run II dataset
- Invariant mass of the $W\gamma$ system is sensitive to presence of dim-8 operators



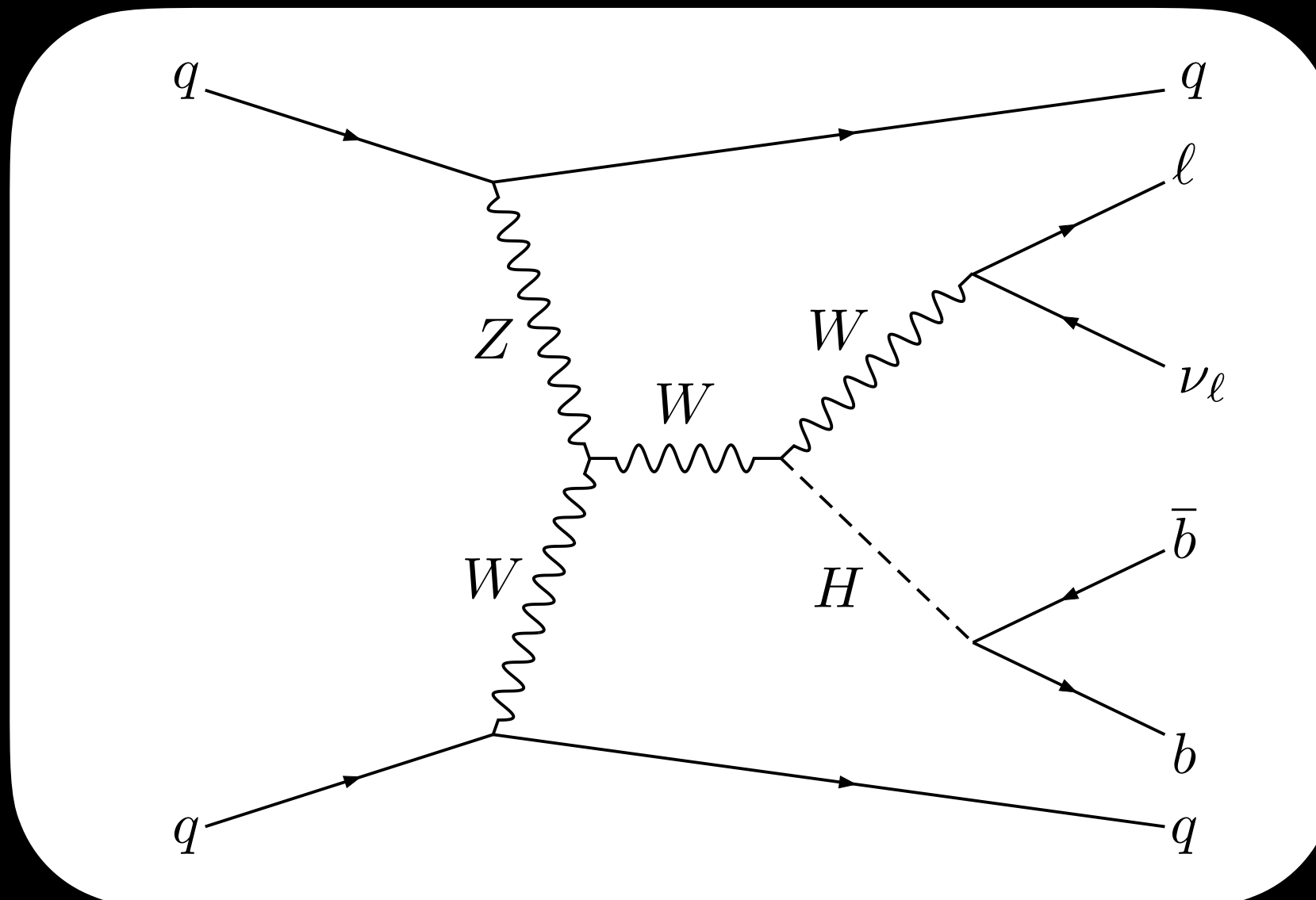
Measurement of the electroweak production of $W\gamma$ with two jets

- Major backgrounds from $W+jets$ and $t\bar{t}$ processes where the jet constituents is misidentified as a photon

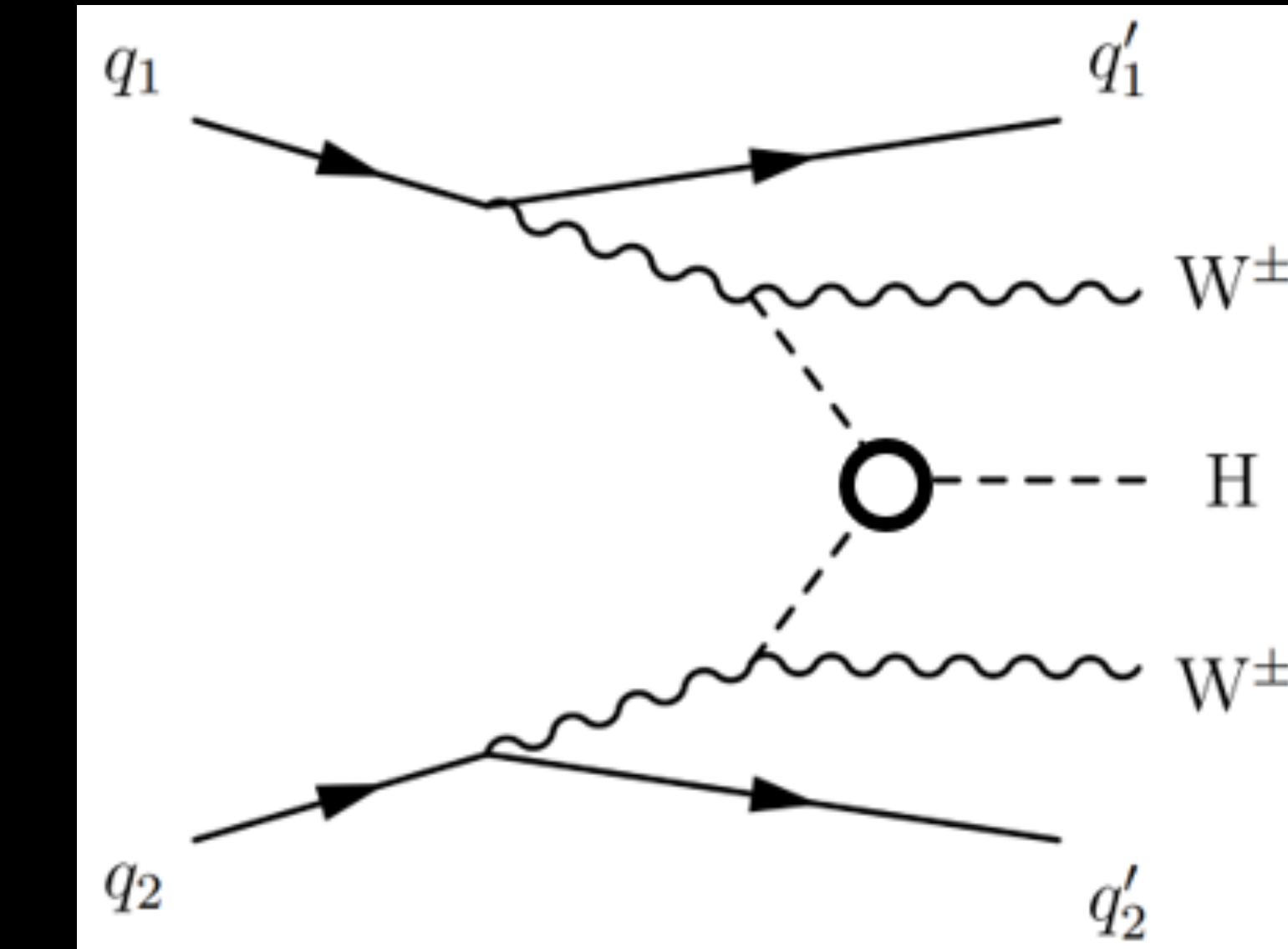
	Barrel	Endcap
EW $W\gamma$ in fiducial region	316 ± 16	90.2 ± 5.5
EW $W\gamma$ out of fiducial region	64.7 ± 2.0	20.4 ± 1.0
QCD $W\gamma$	1301 ± 28	362 ± 13
top, VV, $Z\gamma$	402 ± 14	93.3 ± 7.2
Nonprompt photon	434 ± 13	120.2 ± 5.7
Nonprompt muon	134 ± 27	45 ± 11
Nonprompt electron	189 ± 20	86 ± 13
Nonprompt photon, nonprompt muon	43.0 ± 7.0	14.6 ± 3.4
Nonprompt photon, nonprompt electron	75.5 ± 5.5	25.0 ± 2.0
Total prediction	2960 ± 43	856 ± 21
Data	2959 ± 57	849 ± 32



Search for $HWW/HHWW$ couplings in the VBS production of $W^\pm W^\pm H$ with $H \rightarrow b\bar{b}$ decays



<https://arxiv.org/pdf/2405.16566>



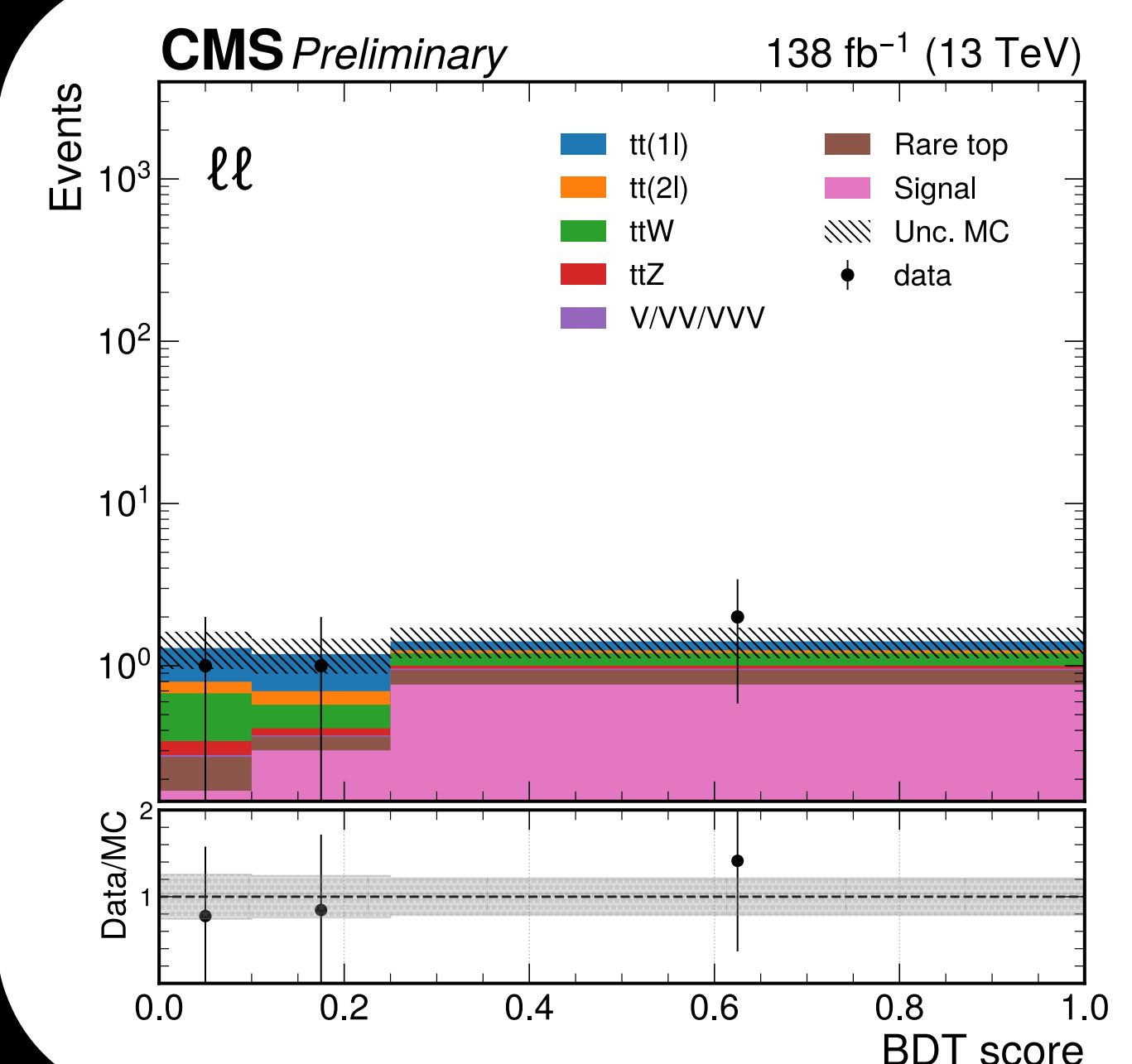
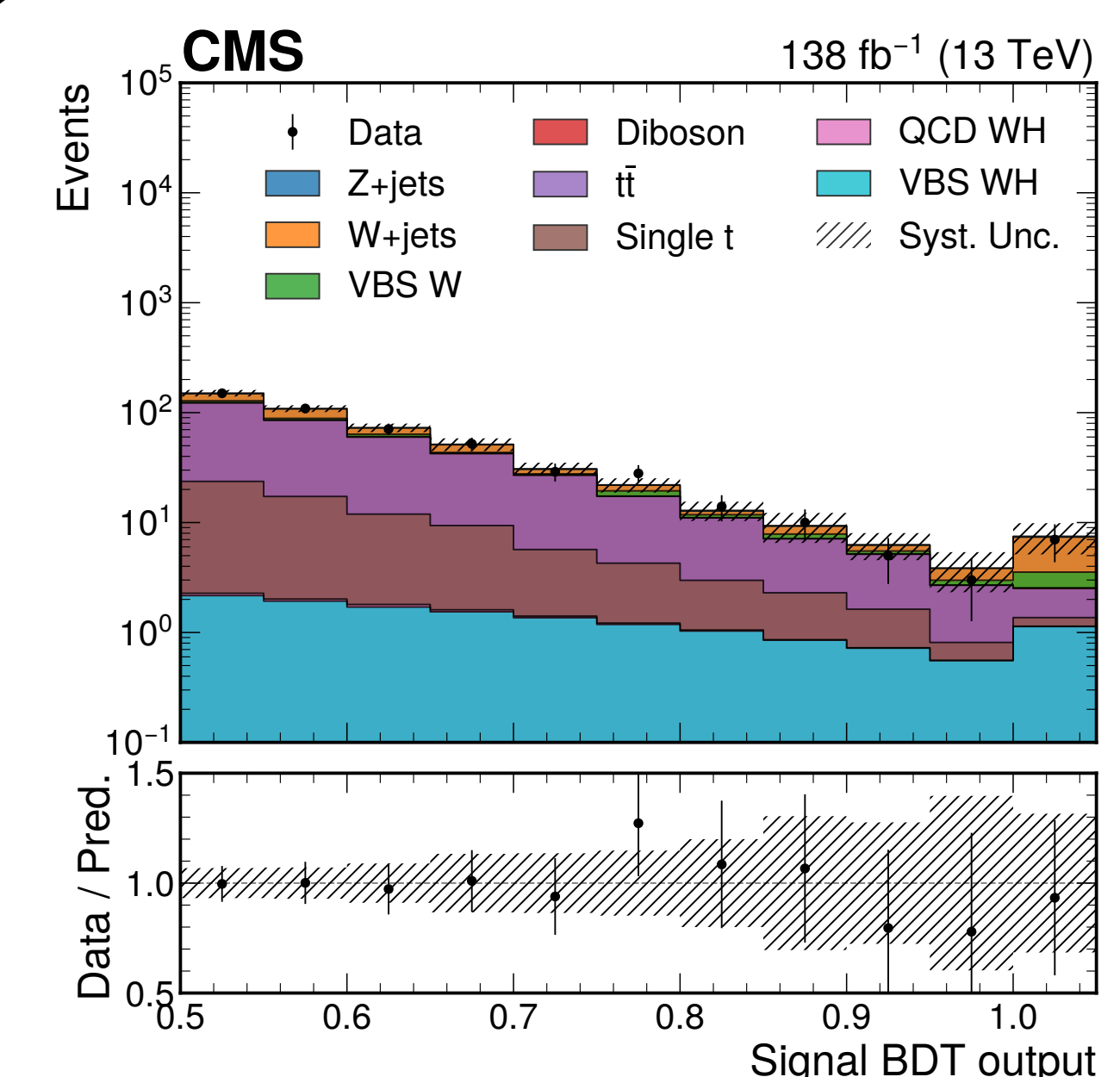
<https://cds.cern.ch/record/2905615>

Search for $HHWW$ couplings in the VBS production of $W^\pm W^\pm H$ with $H \rightarrow b\bar{b}$ decays

- Extraction of sign of W and Z coupling to Higgs performed with W and Higgs in final state
- Boosted decision tree trained against major backgrounds
- All scenarios with $\lambda_{WZ} = \frac{k_W}{k_Z} < 0$ excluded
- For $W^\pm W^\pm H$ low signal yields \rightarrow need more data to set tight constraints on couplings

$W^\pm W^\pm H$

Shorthand	Description
η_J	η of the leading merged jet
$p_{T,J}$	p_T of the leading merged jet
$p_{T,jj}$	p_T of the VBS-jet system
P_{j_0}	magnitude of the three-momentum of the leading VBS jet
P_{j_1}	magnitude of the three-momentum of the subleading VBS jet
$M_{\ell\ell}$	invariant mass of the SS dilepton system
p_{T,ℓ_0}	p_T of the leading lepton
p_{T,ℓ_1}	p_T of the subleading lepton
E_T^{miss}	missing transverse energy
L_T	scalar sum of $p_{T,\ell_0}, p_{T,\ell_1}$, and E_T^{miss}
S_T	scalar sum of $p_{T,J}$ and L_T



Going forward... (practicalities)

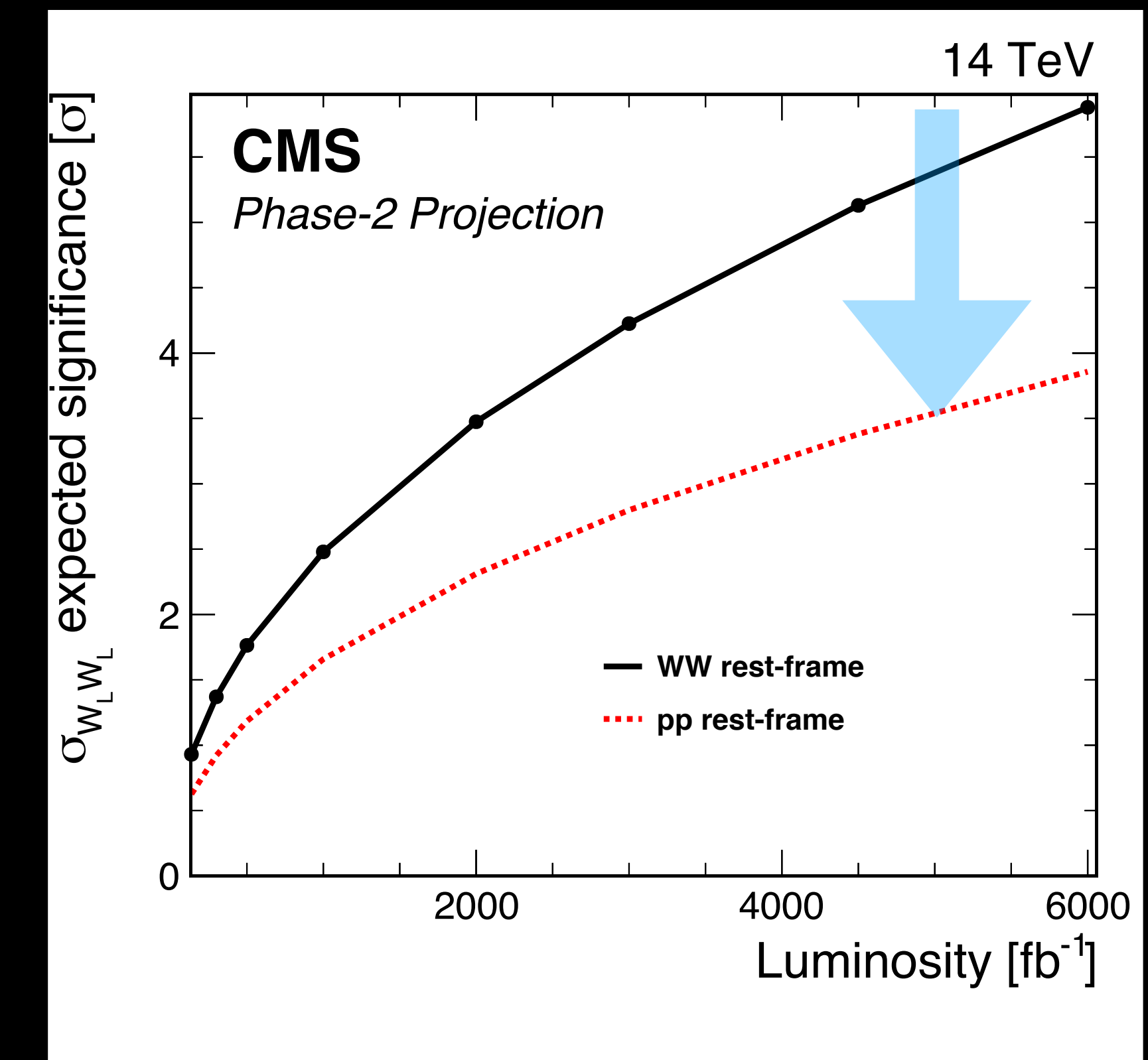
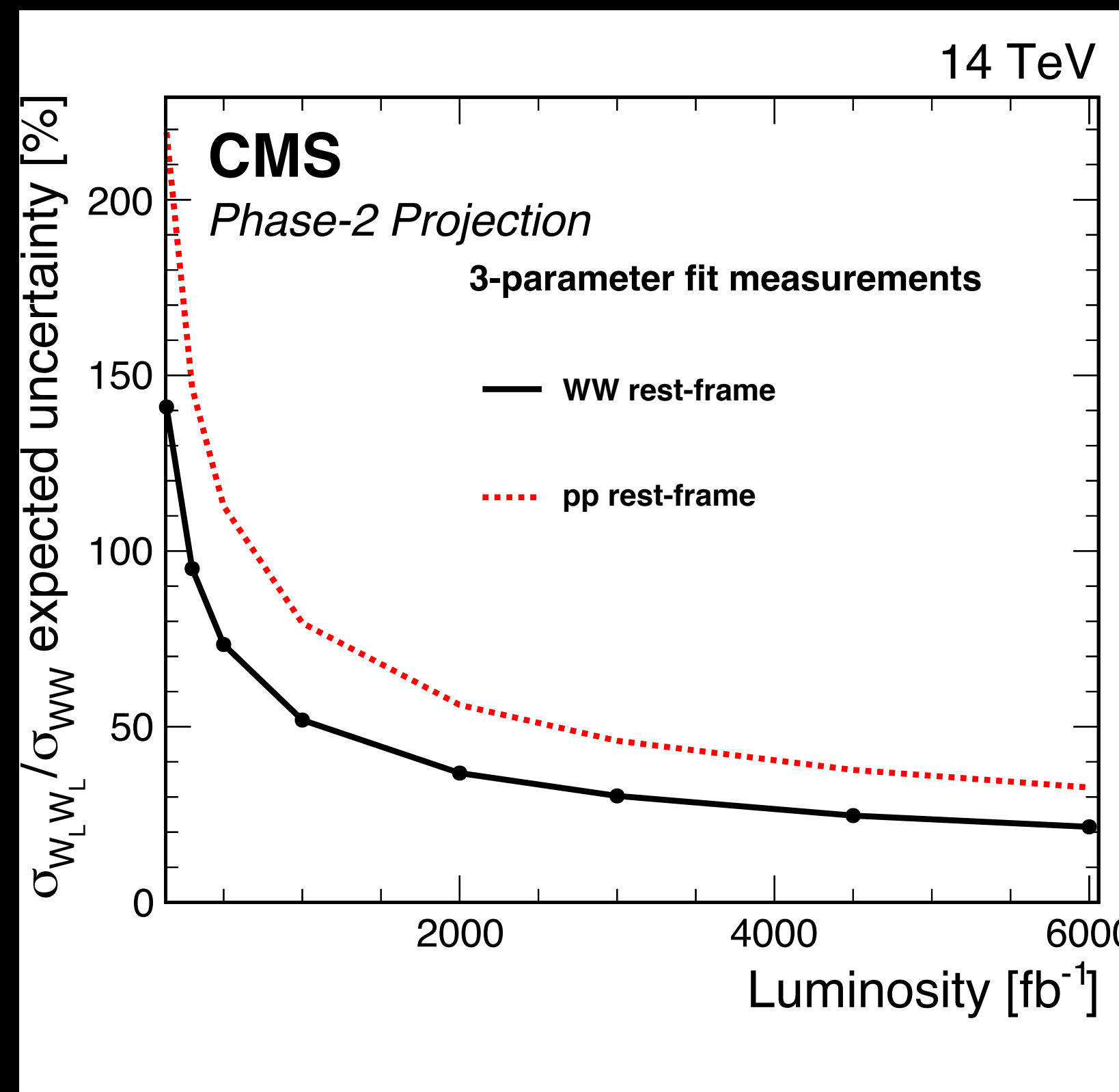
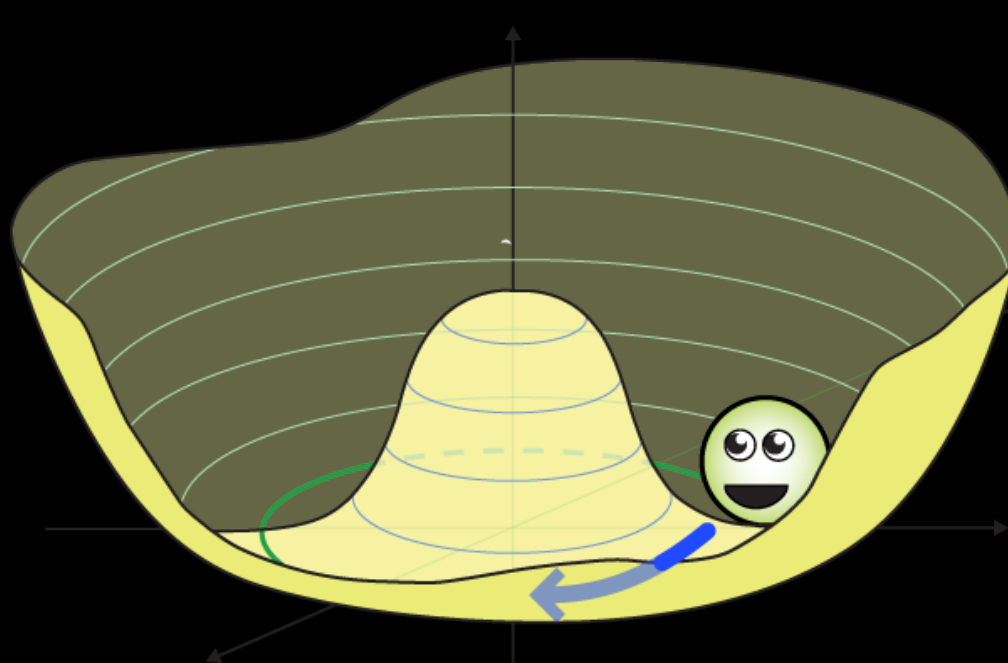
- Study of vector boson scattering processes is an exciting area of research with many new analyses in the last few years
- Run III dataset provides additional opportunities to study these processes in depth
- As the precision program of the LHC is realized, studying generator modeling is crucial
- Many different generators studied with various configurations
 - Features discussion of choice of dipole recoil scheme
 - Synchronize sample production between ATLAS and CMS

Sample name	Generator	μ -scale	Shower	Tune	PDF	further settings
Sherpa (ATLAS)	SHERPA v2.2.2	dynamic scale, m_{WW}	internal	internal	NNPDF3.0-NNLO	multileg-LO, exactly six EW vertices with one additional parton at LO accuracy in QCD
PW+Py8 (ATLAS)	POWHEG v2, VBS approx.	fixed scale, m_W	PYTHIA 8.212	AZNLO	NNPDF3.0-NLO	NLO
PW+Py8 dipole-recoil (ATLAS)	POWHEG v2	fixed scale, m_W	PYTHIA 8.235	AZNLO	NNPDF3.0-NLO	Dipole Recoil [6]
MG5+Py8 dipole-recoil (ATLAS)	MG5_AMCNLO v2.6.2	dynamic scale, $\sqrt{p_T^{\text{jet}1} p_T^{\text{jet}2}}$	PYTHIA 8.235	A14	NNPDF3.0-NLO	LO, Dipole Recoil [6]
MG5+Py8 (CMS)	MG5_AMCNLO v2.3.3	dynamic scale, using a 2→2 topology from the clustered external state	PYTHIA 8.212	CUETP8M1 [7]	NNPDF3.0-LO	LO, exactly six EW vertices
PW+Py8 (VBSscan)	POWHEG v2	dynamic scale, $\sqrt{p_T^{\text{jet}1} p_T^{\text{jet}2}}$	PYTHIA 8.230	Monash	NNPDF3.0-NLO	NLO

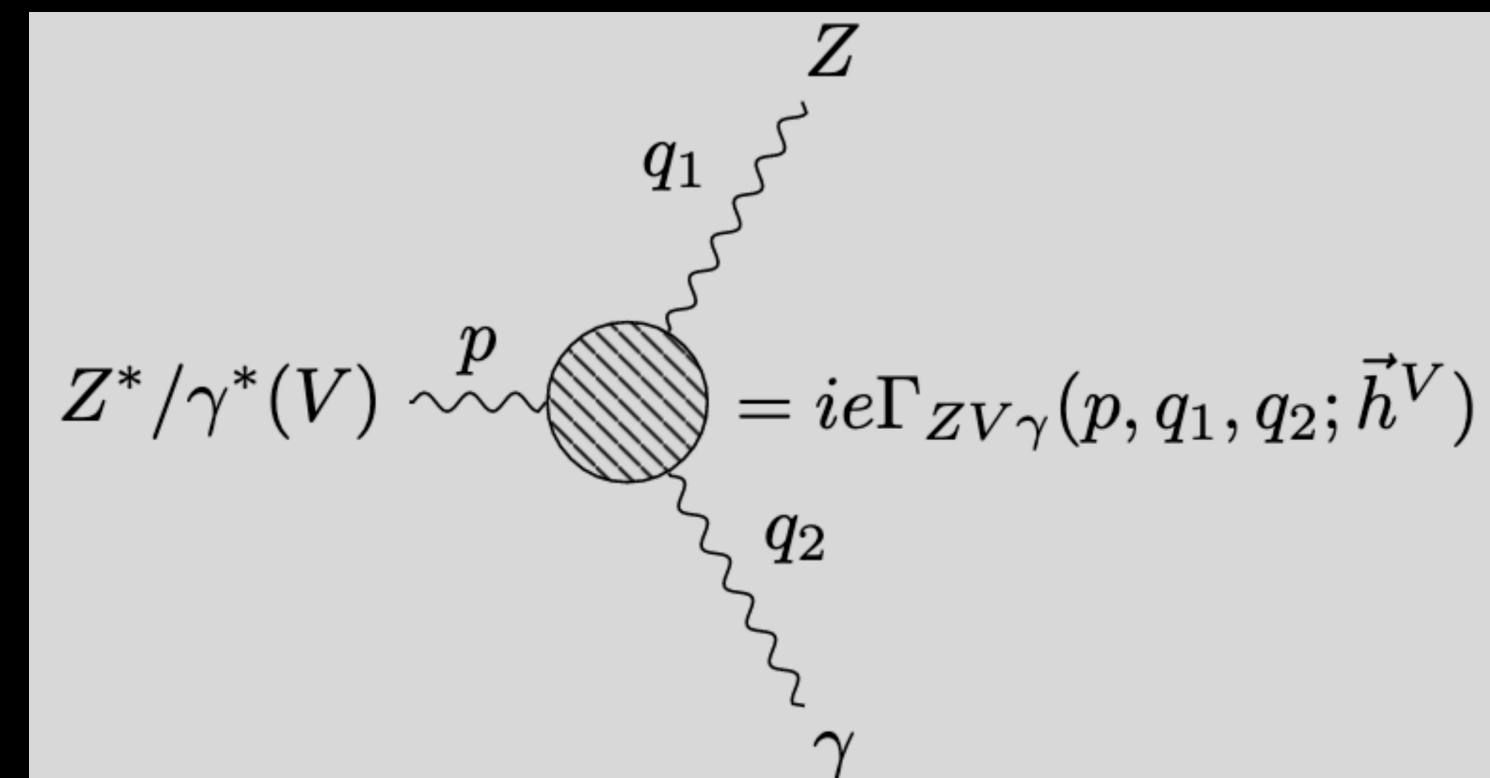
Going forward...

CMS-PAS-FTR-21-001

- Understanding electroweak symmetry breaking → crucial part of LHC physics program
 - Longitudinally polarized scattering of W and Z complementary to direct measurements of the Higgs coupling to gauge bosons
- Analysis projected from Run II to 3000 fb^{-1}



Anomalous neutral gauge couplings in the mono photon channel



Anomalous neutral gauge couplings in the mono photon channel

- Generalized theory of forbidden neutral gauge couplings
 - Parametrized with 8 parameters (h_1 to h_4)
 - Vertex functions describe the most general Lorentz and $U_Y(1)$ invariant interactions of the incoming off-shell Z or γ and outgoing on-shell Z and γ
 - CP violating: h_1^V, h_2^V ; CP conserving: h_3^V, h_4^V

$$\Gamma_{ZZ\gamma}^{\alpha\beta\mu} = \frac{p^2 - q_1^2}{m_Z^2} \left[h_1^Z (q_2^\mu g^{\alpha\beta} - q_2^\alpha g^{\mu\beta}) + \frac{h_2^Z}{m_Z^2} p^\alpha [(p \cdot q_2) g^{\mu\beta} - q_2^\mu p^\beta] + h_3^Z \epsilon^{\mu\alpha\beta\rho} q_{2\rho} + \frac{h_4^Z}{m_Z^2} p^\alpha \epsilon^{\mu\beta\rho\sigma} p_\rho q_{2\sigma} \right]$$

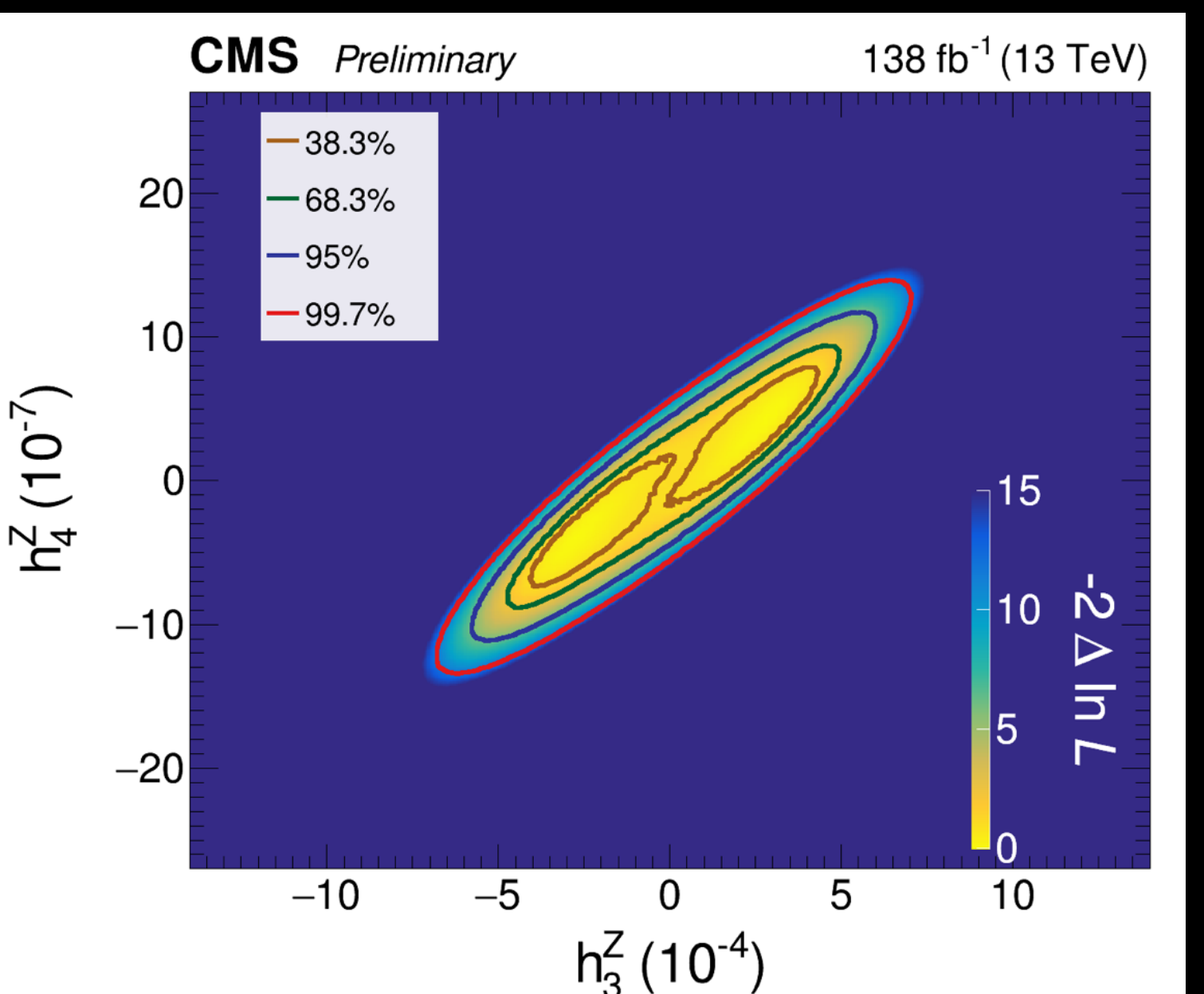
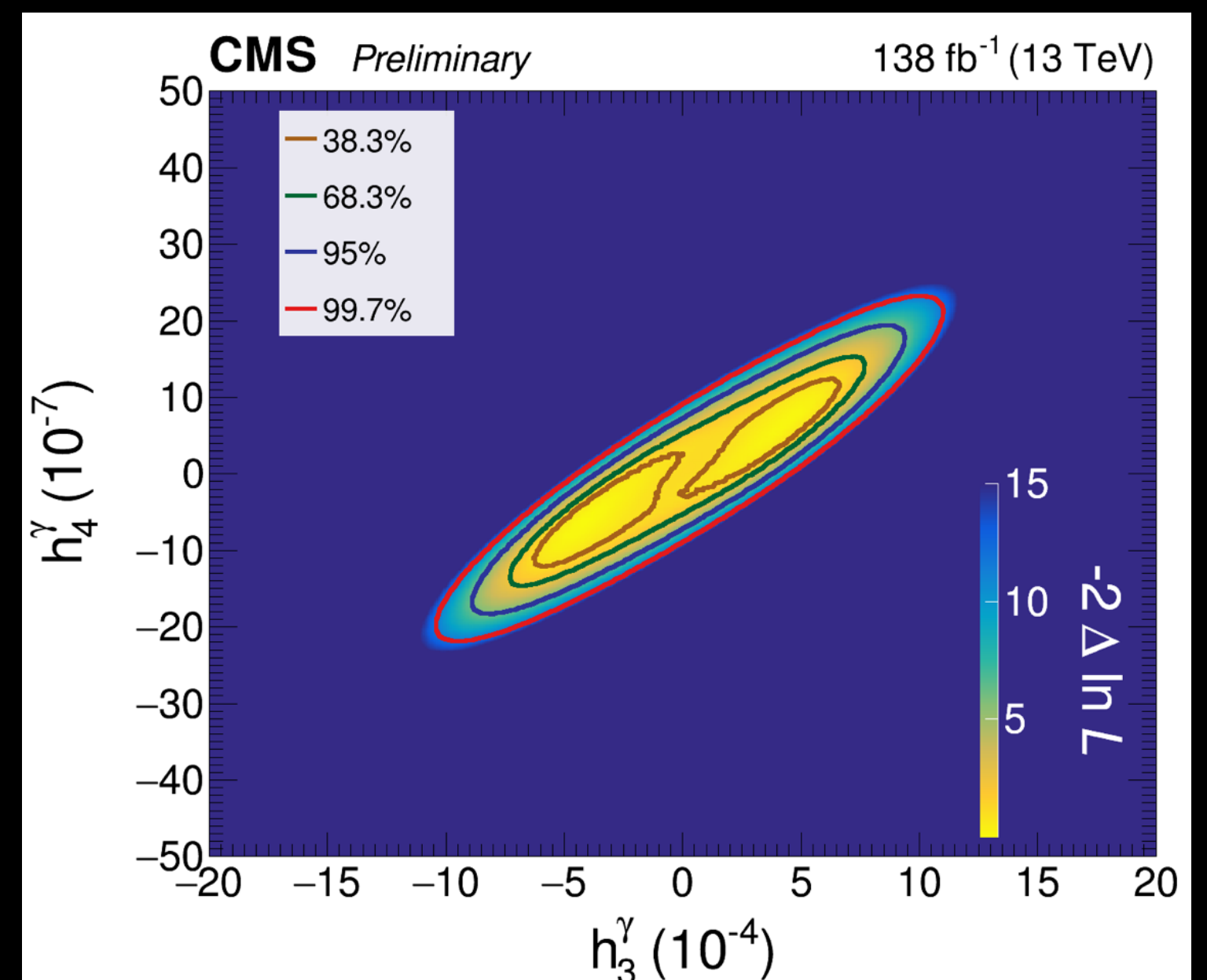
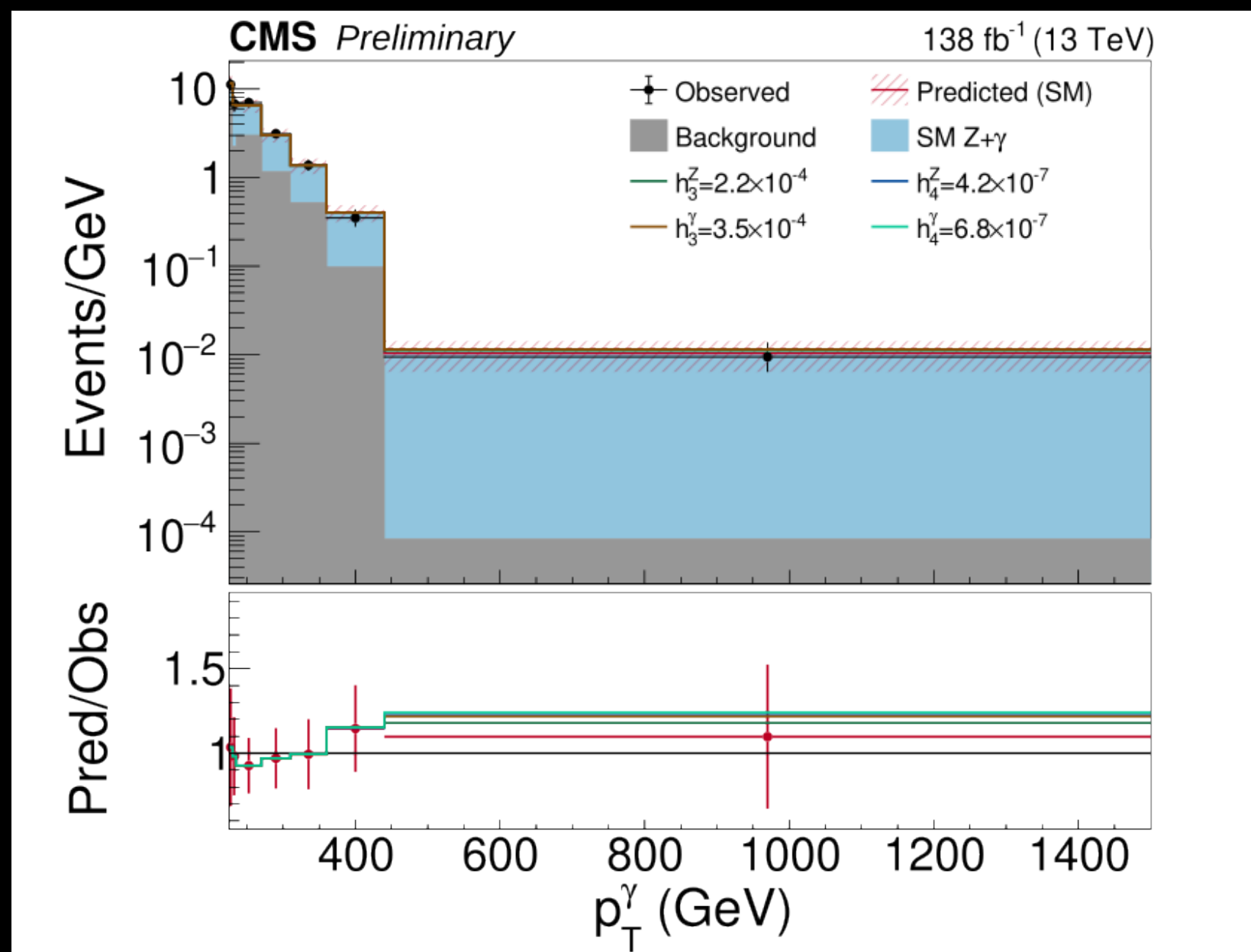
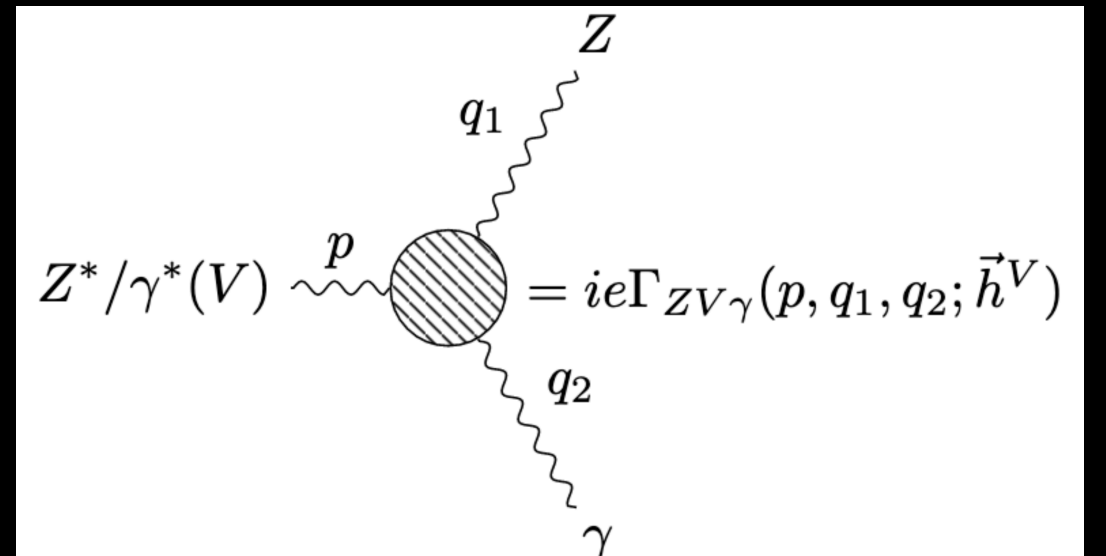
$\Gamma_{Z\gamma\gamma}^{\alpha\beta\mu}$ obtained with some simple substitutions to the above equation

Ellis et al:

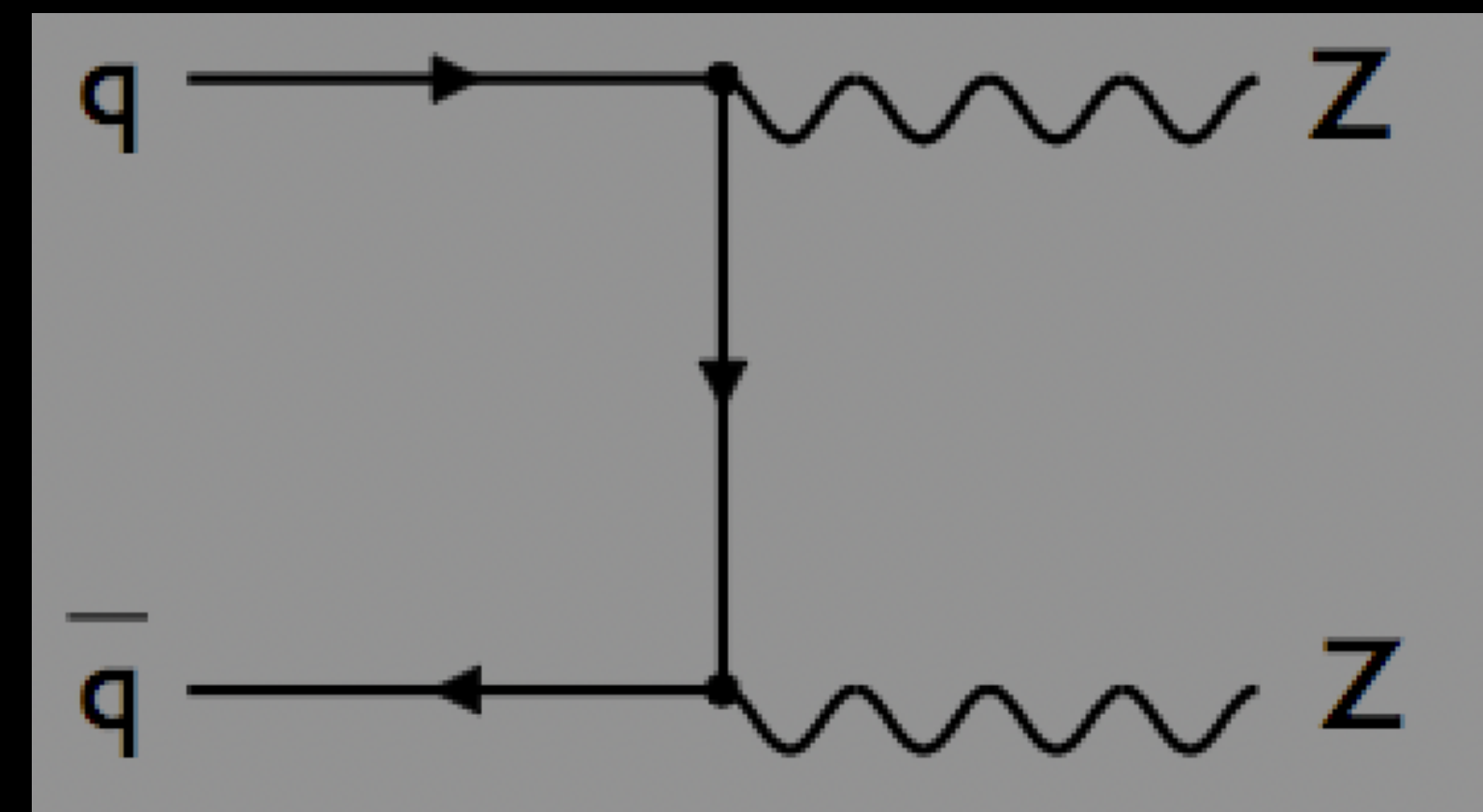
[https://indico.cern.ch/event/1330671/contributions/5601599/
attachments/2735050/4755768/Offshell+CPV_Dimension8.pdf](https://indico.cern.ch/event/1330671/contributions/5601599/attachments/2735050/4755768/Offshell+CPV_Dimension8.pdf)

Anomalous neutral gauge couplings in the mono photon channel

- New physics most likely to show up as deviation at high p_T
 - Photon p_T is the variable of interest
- Backgrounds range from $W + \gamma$, $V + \text{jets}$, $\gamma + \text{jets}$ and **dibosons** estimated using **data-driven methods** and **simulations**



Search for $ZZ \rightarrow b\bar{b}$ and $ZH \rightarrow b\bar{b}$

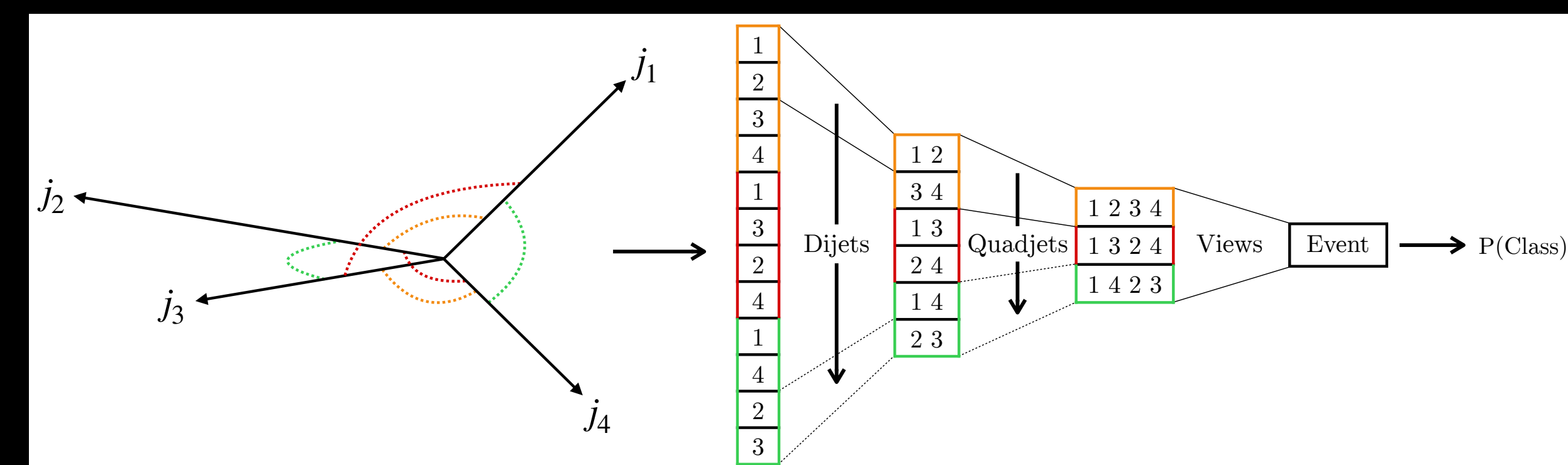
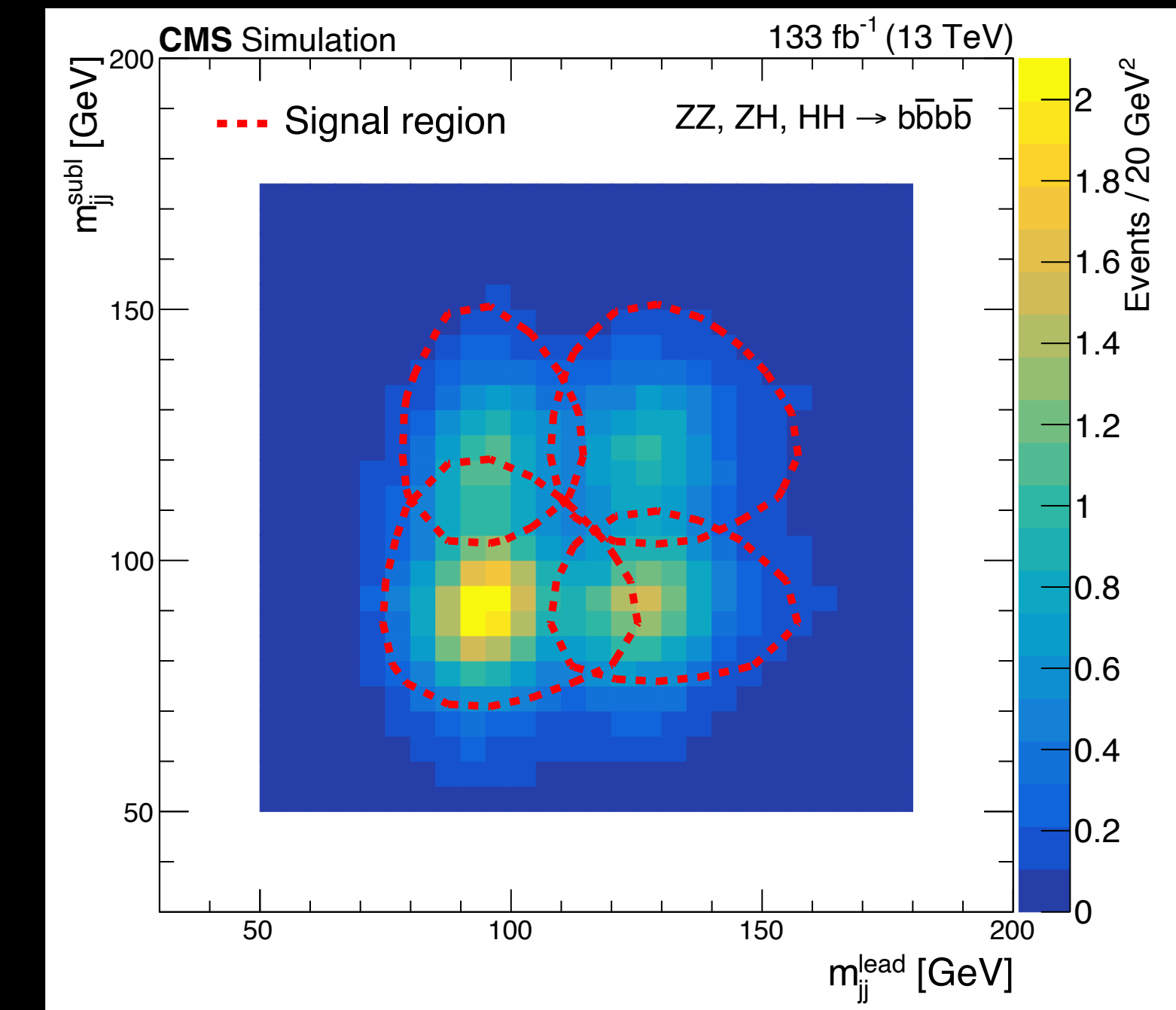


Search for $ZZ \rightarrow b\bar{b}$ and $ZH \rightarrow b\bar{b}$

- Diboson ZZ process is interesting to study in its own right
 - Additionally, major background for DiHiggs measurement
- Define signal regions based on:

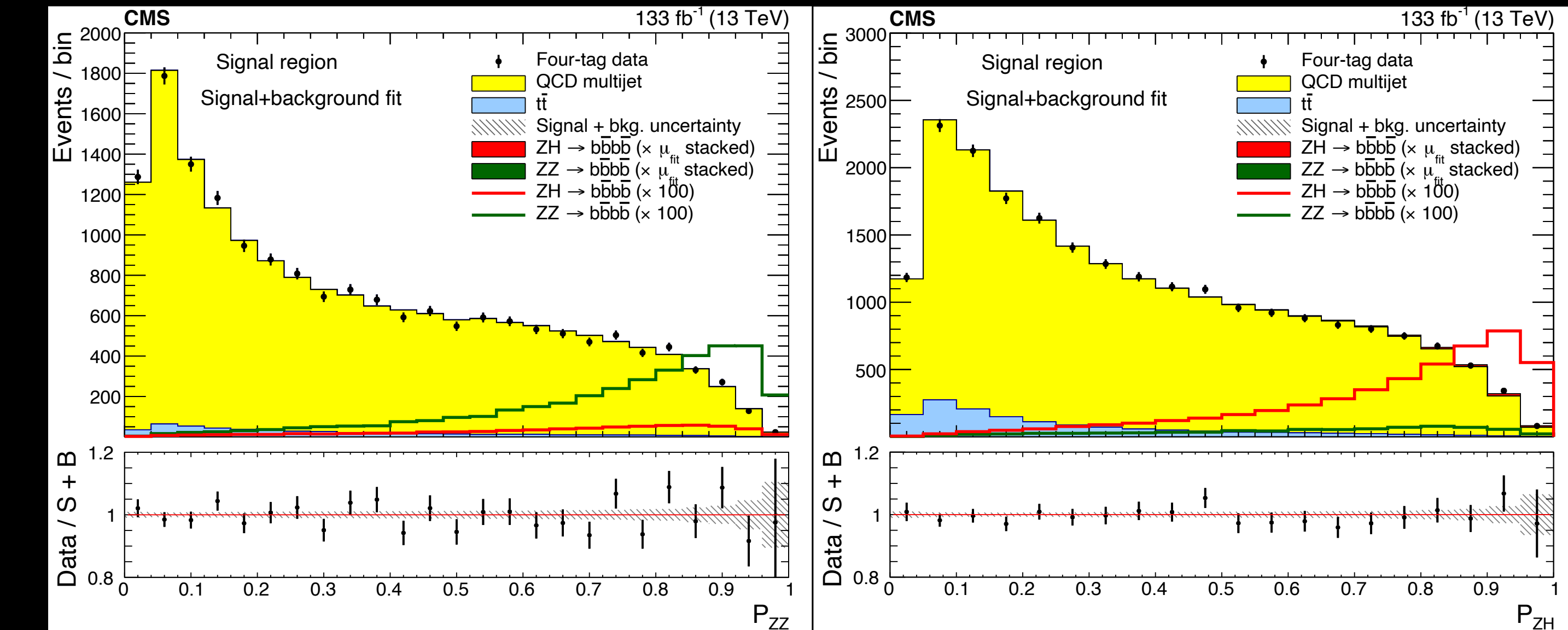
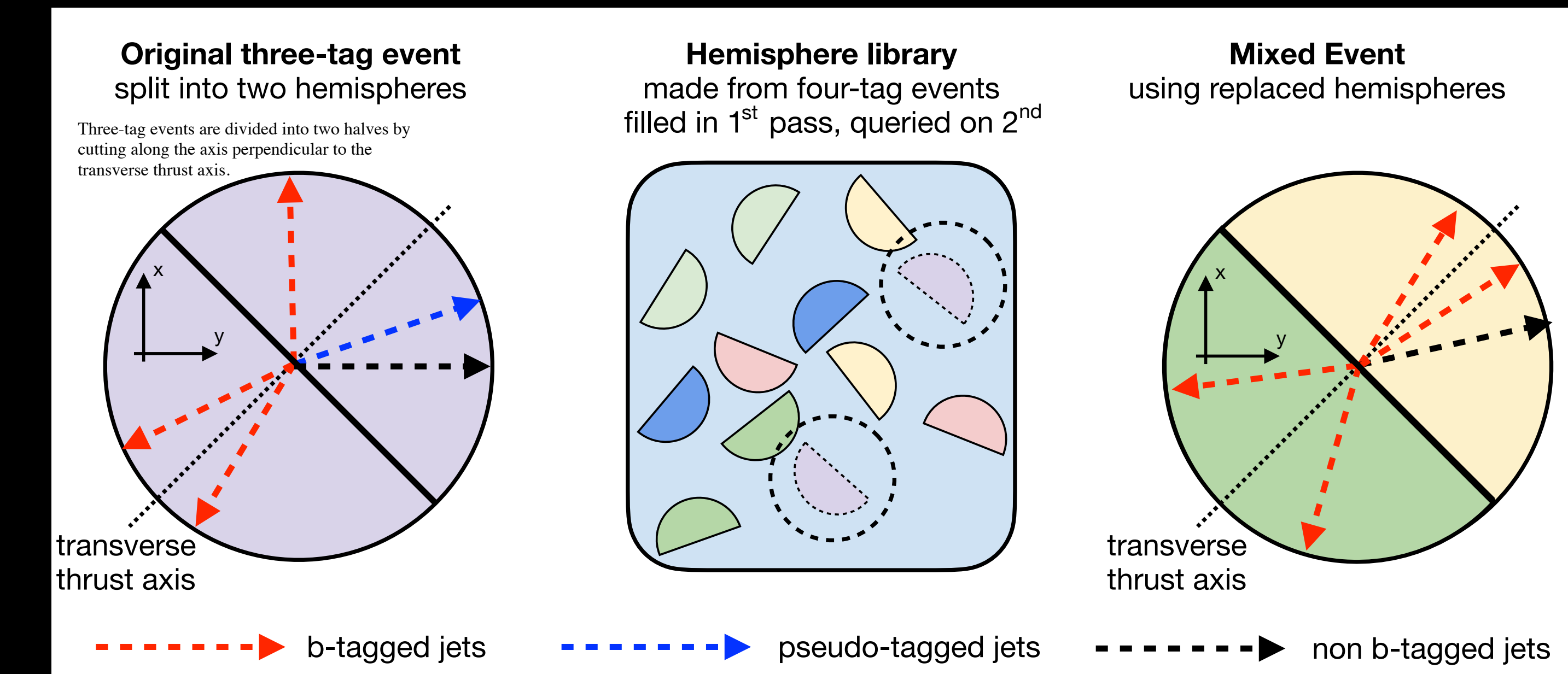
$$X_{B_1 B_2} = \sqrt{\left(\frac{m_{jj}^{\text{lead}} - m_{B_1}}{\sigma_{m_{jj}^{\text{lead}}}} \right)^2 + \left(\frac{m_{jj}^{\text{sublead}} - m_{B_2}}{\sigma_{m_{jj}^{\text{sublead}}}} \right)^2}$$

- Hierarchical combinatorial residual network trained for 4-jet diboson topology
 - Jet image formed from pixels representing jet 4-vector
 - Copies of jet pixels arranged to form 1-D image → pairs of adjacent pixels represent the three possible jet pairings
 - Second layer → six dijet pixels to form a three-pixel quadjet image
 - Final processing leads to event probabilities that determine event class
- Multijet background modeled similarly after reversing b-tagging criteria



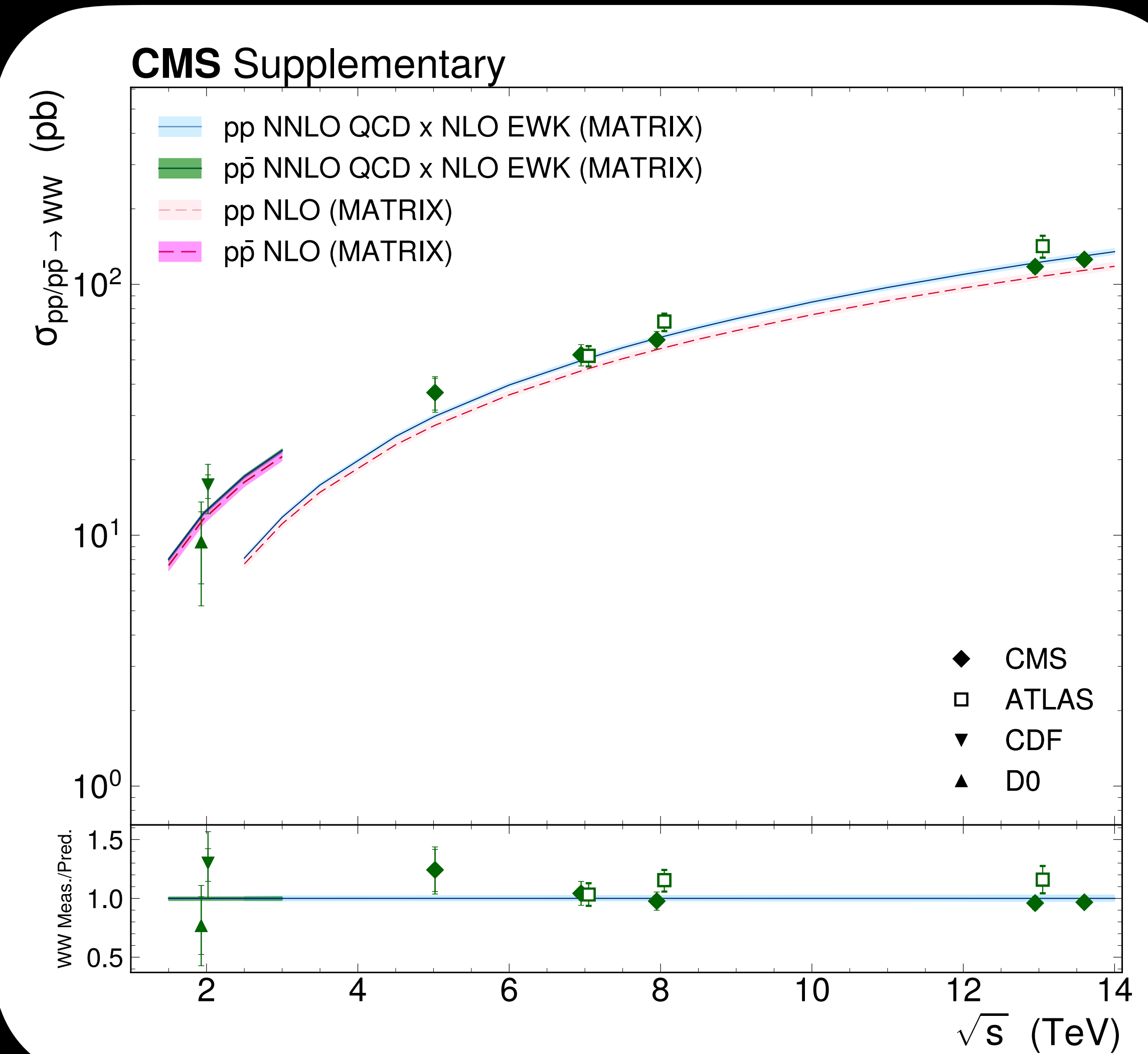
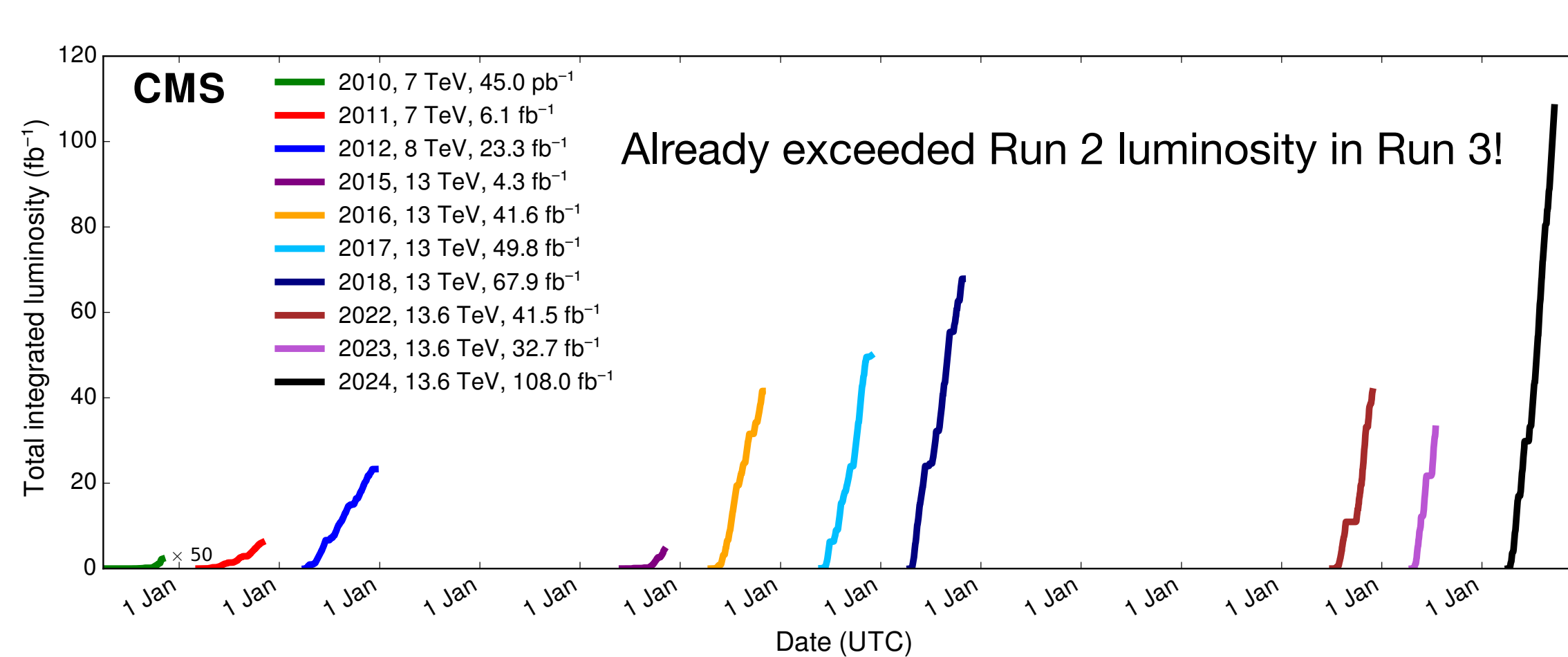
Search for $ZZ \rightarrow b\bar{b}$ and $ZH \rightarrow b\bar{b}$

- Background modeling validated by high-event-count proxy for the four-tag background
- Synthetic data generated by using the hemisphere technique:
 - Event split into hemispheres and library generated
 - Corrections introduced to account for $t\bar{t}$ background contamination
- Mixed models allow testing for biases in the background model that can mimic a signal
 - Check with and without unconstrained signal template
- $ZZ \rightarrow b\bar{b}$ observed with 3.8σ significance
- $ZH \rightarrow b\bar{b}$ observed with 5.0σ significance



Stress testing the Standard Model

- The full Run 2 dataset allowed us to observed rare processes predicted by the SM
- Precision tests of multiboson processes and improving background predictions for Higgs self coupling measurements were possible
- Run 3 luminosity already exceeds Run 2



Additional Material

Introducing the dramatis personae The Standard Model of Particle Physics

Quarks

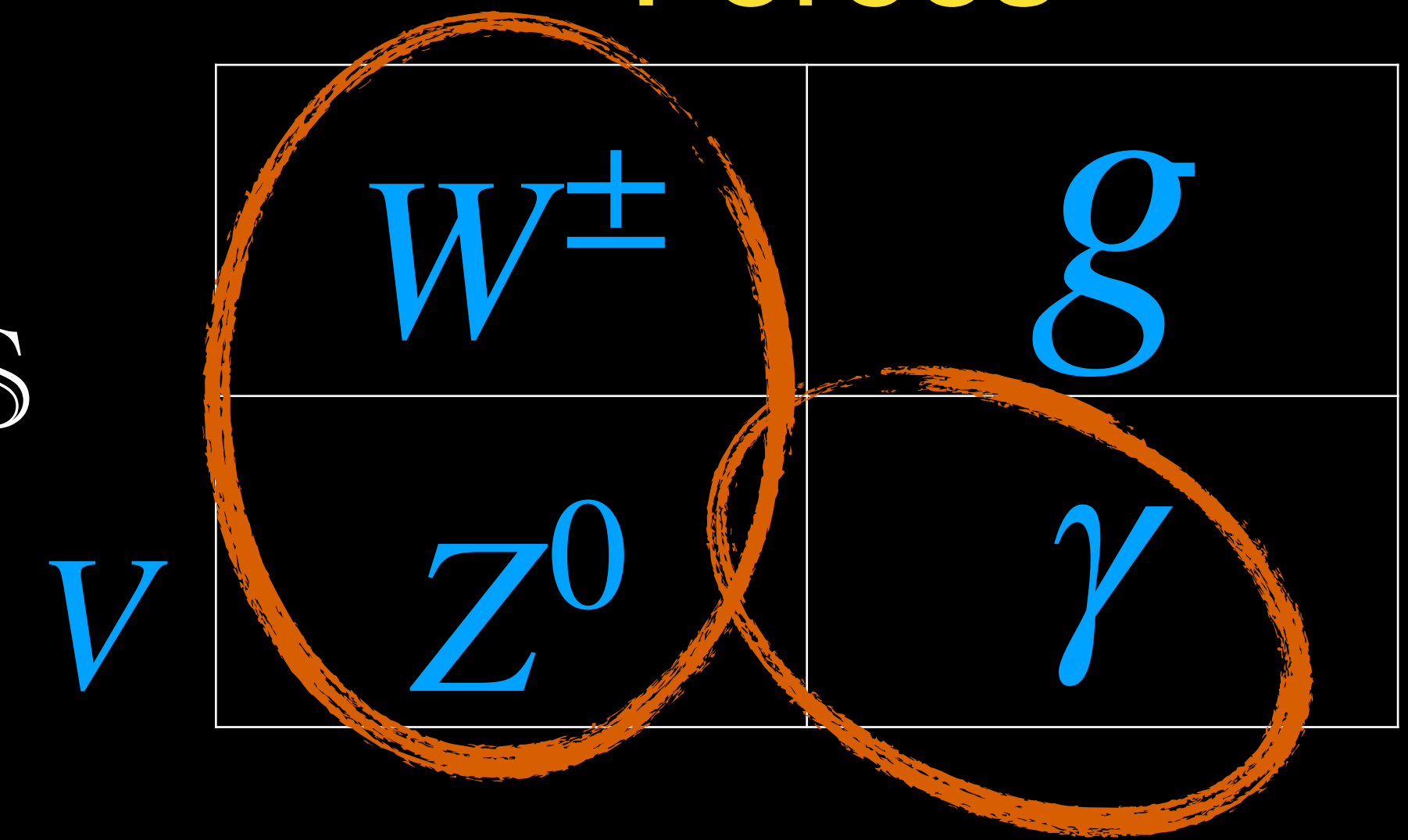
u	c	t
d	s	b

Leptons

e	μ	τ
ν_e	ν_μ	ν_τ

Forces

HIGGS



Focus of my talk:

- Explore the gauge boson sector → interplay between W , Z , and γ
- Enables fundamental tests of the Standard Model

Observation of $WW\gamma$ production at $\sqrt{s} = 13$ TeV

Control region	Same sign $WW\gamma$ control region	$\text{Top}\gamma$ control region
Definition	Require charged leptons of identical charge	Flip b-veto and remove cut on transverse mass of the WW-system
Target processes	Validate non-prompt lepton background modeling	Validate top-quark and non-prompt photon background modeling

Observation of $WW\gamma$ production at $\sqrt{s} = 13$ TeV

Process	SR (0 jet)	SR (≥ 1 jet)	SR (total)	SSWW γ CR	Top γ CR
WW γ	122 ± 23	132 ± 27	254 ± 47	1.0 ± 0.2	12.8 ± 2.7
QCD V γ	72.0 ± 6.4	94.7 ± 9.3	167 ± 14	12.2 ± 2.2	12.6 ± 1.2
VV	15.1 ± 1.4	21.6 ± 2.4	36.7 ± 3.5	24.9 ± 1.7	2.0 ± 0.3
Top	56.6 ± 6.5	271 ± 26	328 ± 32	2.4 ± 0.6	2434 ± 85
Nonprompt ℓ	45.7 ± 4.0	77.2 ± 6.5	122.9 ± 9.7	197 ± 14	40 ± 11
Nonprompt γ	109.1 ± 9.0	301 ± 24	410 ± 32	19.9 ± 1.6	793 ± 62
Total	420 ± 20	898 ± 29	1318 ± 43	257 ± 14	3294 ± 57
Data	414	916	1330	259	3287

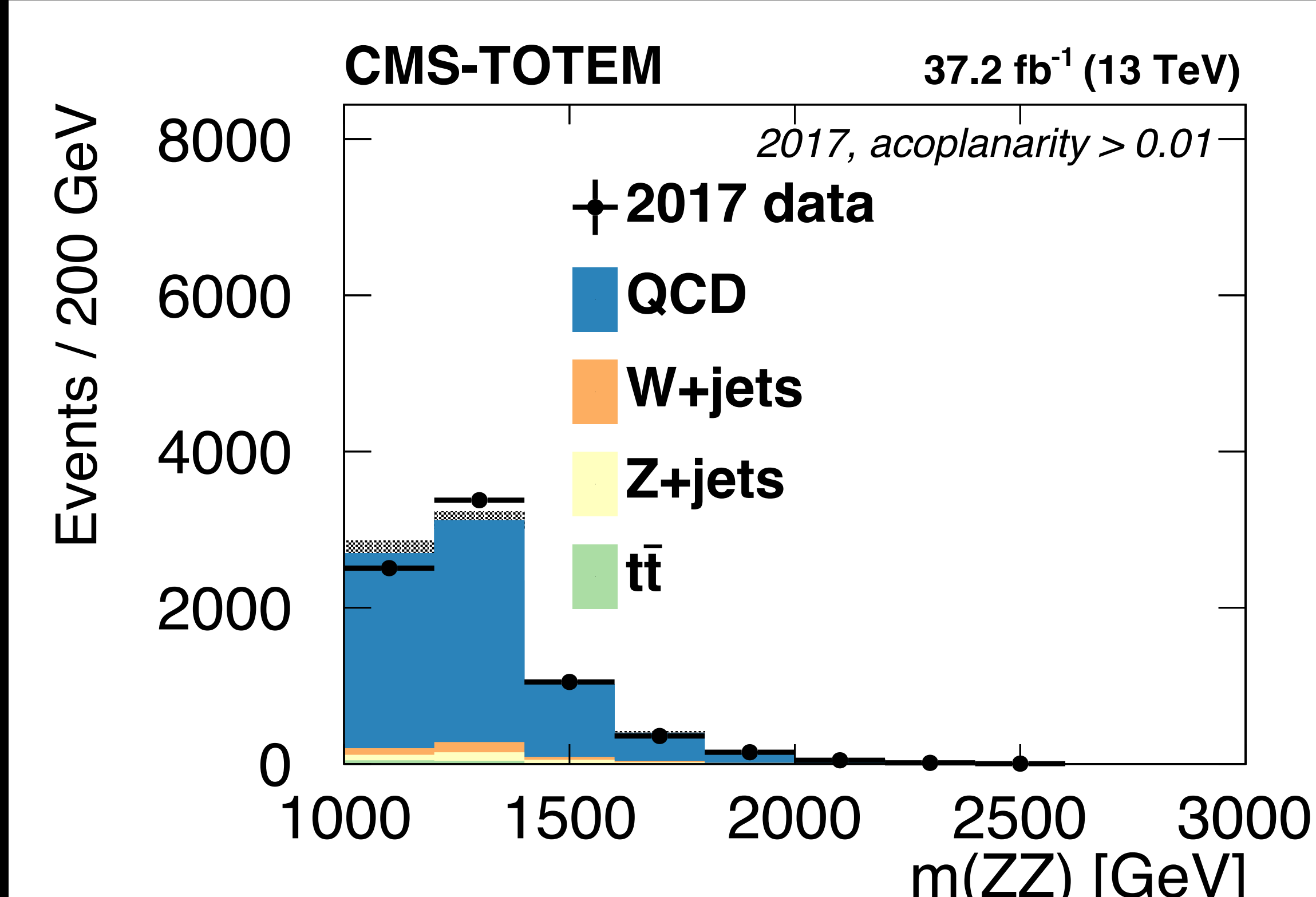
Background
dominated

- Simultaneous extraction of signal and control regions



Search for exclusive $\gamma\gamma \rightarrow WW$ and $\gamma\gamma \rightarrow ZZ$ production in final states with jets and forward protons

Number of events	region	N_{evt} (2016)	N_{evt} (2017)	N_{evt} (2018)
Anti-acoplanarity sideband	δ	1.5 ± 1.1	1.6 ± 0.8	14.2 ± 3.0
Anti-pruned mass sideband	δ	0.4 ± 0.2	0.9 ± 0.2	9.9 ± 0.9
Event mixing	δ	$0.5 (< 2.1)$	$1.5 (< 3.6)$	11.6 ± 9.4
Expected signal $(a_0^Z / \Lambda^2 = 1 \times 10^{-5} \text{ GeV}^{-2})$	δ	1.3	1.4	9.0
Anti-acoplanarity sideband	σ	1.5 ± 1.1	3.7 ± 1.5	37.4 ± 5.6
Anti-pruned mass sideband	σ	2.1 ± 0.8	5.4 ± 1.3	41.7 ± 3.1
Event mixing	σ	2.0 ± 1.8	6.3 ± 5.1	42 ± 16
Expected signal $(a_0^Z / \Lambda^2 = 1 \times 10^{-5} \text{ GeV}^{-2})$	σ	1.0	1.6	12.8



Effective Field Theory interpretation in $\gamma\gamma \rightarrow \tau\tau$

$$\mathcal{L}_{BSM} = \frac{C_{\tau B}}{\Lambda^2} \bar{L}_L \sigma^{\mu\nu} \tau_R H B_{\mu\nu} + \frac{C_{\tau W}}{\Lambda^2} \bar{L}_L \sigma^{\mu\nu} \tau_R \sigma^i H W_{\mu\nu}^i + h.c.$$

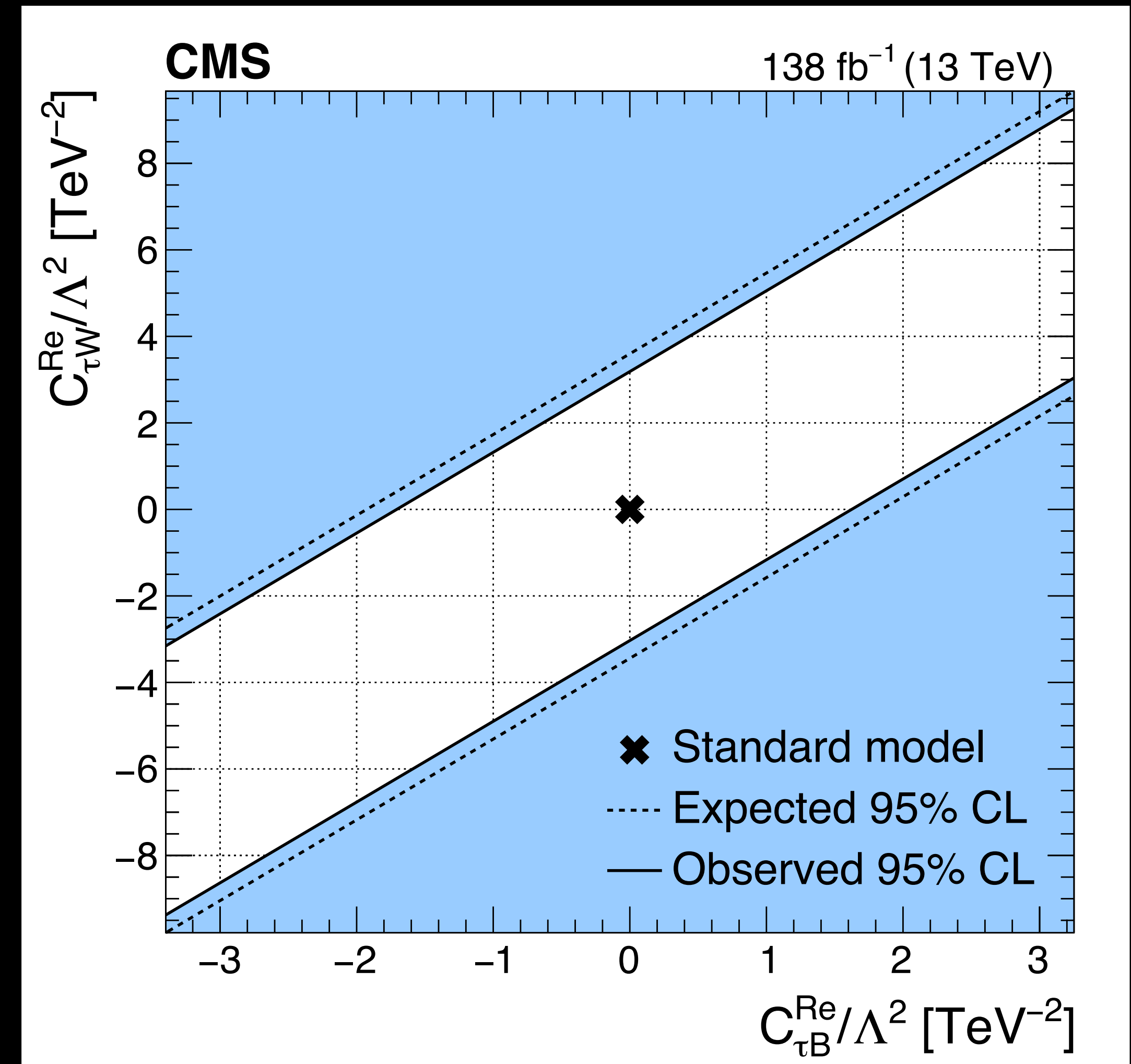
$\tau\tau\gamma$ vertex parametrized as:

$$V_{\tau\tau\gamma} = ie\gamma^\mu = \frac{\nu\sqrt{2}}{\Lambda^2} [\text{Re}[C_{\tau\gamma}] + \text{Im}[C_{\tau\gamma}]i\gamma_5] \sigma^{\mu\nu} q_\nu$$

$$C_{\tau\gamma} = (\cos\theta_W C_{\tau B} - \sin\theta_W C_{\tau W})$$

BSM contribution to a_τ :

$$\delta a_\tau = \frac{2m_\tau}{e} \frac{\sqrt{2}\nu}{\Lambda^2} \text{Re}[C_{\tau\gamma}]$$



Measurement of the electroweak production of $W\gamma$ with two jets

This paper presents a measurement of the EW $W\gamma jj$ production at $\sqrt{s} = 13$ TeV based on the complete Run 2 data collected during 2016–2018, superseding the previous CMS result [4]. A complete set of tabulated results of this analysis is available in the HEPData database [5]. In addition to increased integrated luminosity, our new results include: (i) an updated fiducial region requiring jets with $p_T > 50$ GeV; (ii) the removal of the missing transverse momentum requirement from the fiducial region definition; (iii) the treatment of the interference term between the EW- and quantum chromodynamics (QCD) induced processes as a background component; (iv) and the treatment of the out-of-fiducial signal contribution as a background component.

9 Fiducial cross section measurement

The fiducial cross section measurement for the EW $W\gamma$ production at 13 TeV is extracted with the same 2D m_{jj} – $m_{\ell\gamma}$ binning used for the signal significance. The fiducial region is defined based on the particle-level (for leptons, photons, jets) quantities: one lepton $p_T^\ell > 35$ GeV and

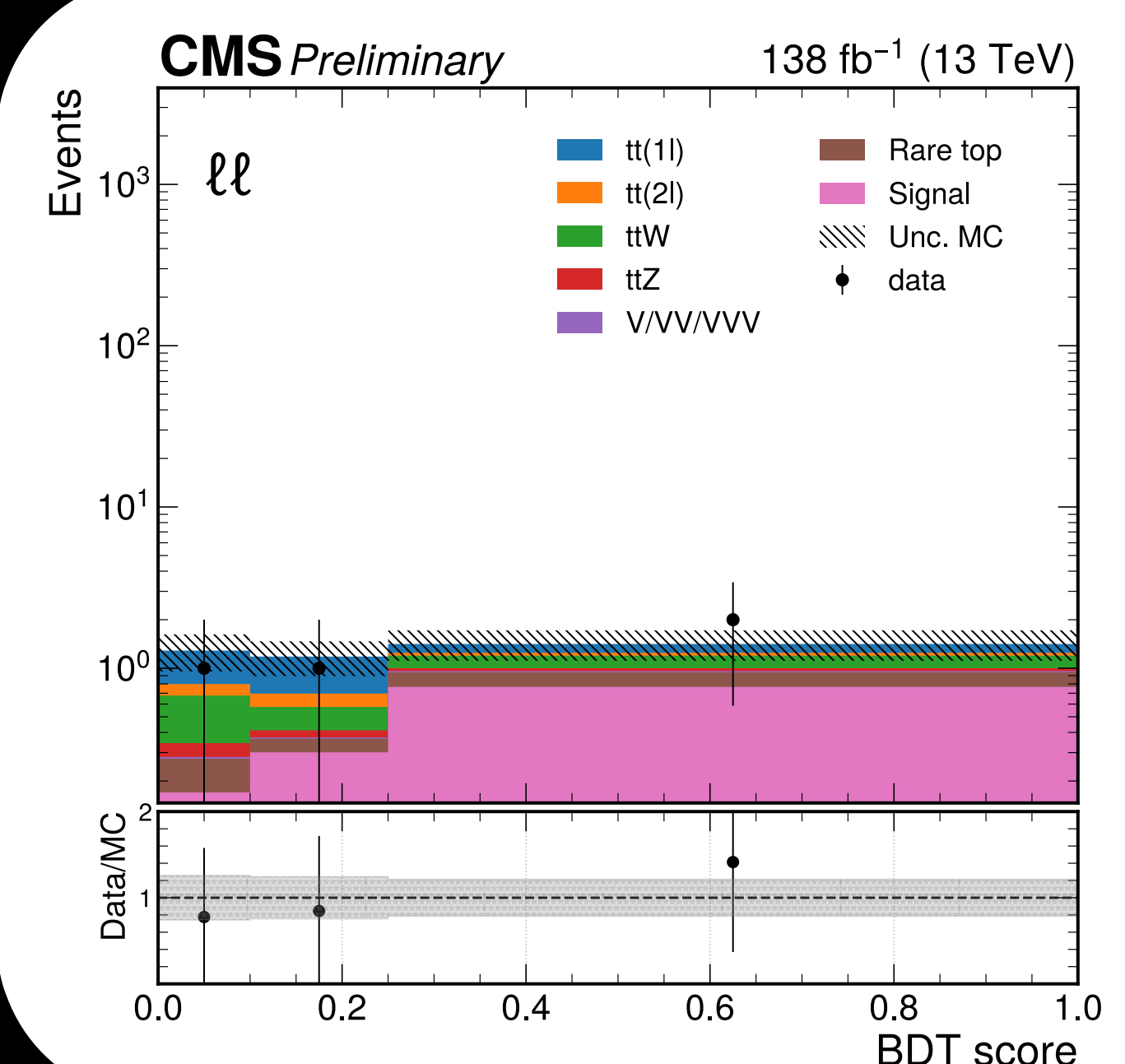
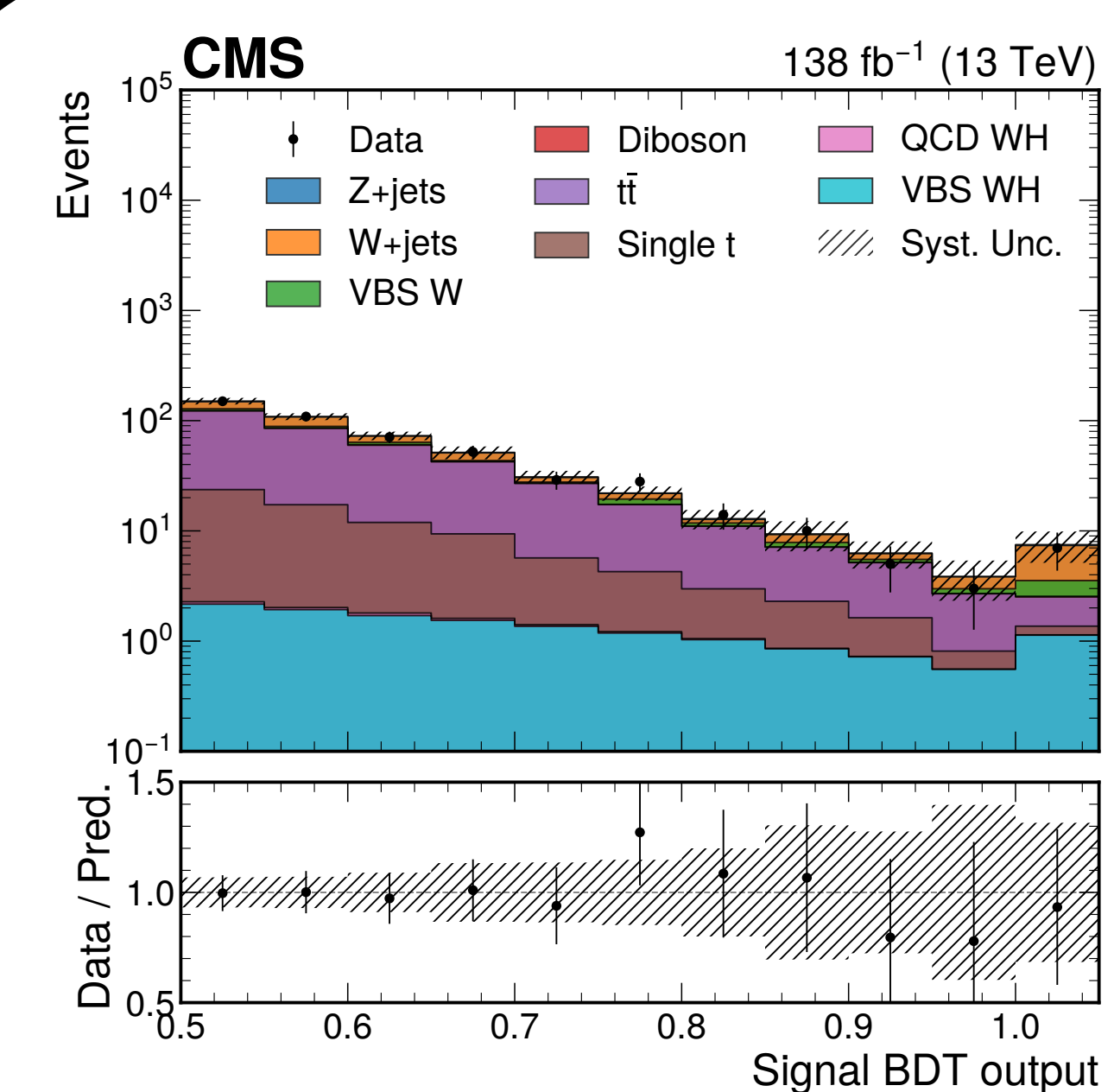
$|\eta_\ell| < 2.4$, $p_T^{\text{miss}} > 30$ GeV, $p_T^\gamma > 25$ GeV, $|\eta_\gamma| < 1.444$ or $1.566 < |\eta_\gamma| < 2.5$, $\Delta R_{\ell\gamma} > 0.5$, $m_T^W > 30$ GeV, and two jets with $p_T^{j1(2)} > 50$ GeV, $|\eta_j| < 4.7$, $m_{jj} > 500$ GeV, $\Delta R_{jj} > 0.5$, $\Delta R_{j\ell} > 0.5$, $\Delta R_{j\gamma} > 0.5$, and $|\Delta\eta_{jj}| > 2.5$. The leptons are reconstructed at the particle level with fully recovered final-state radiation. The acceptance is defined as the fraction of the signal events passing the fiducial region selection, and is estimated using MG5. The theoretical uncertainty in the extrapolation between the fiducial and SR is negligible (< 1%). We define the cross section as $\sigma^{\text{fid}} = \sigma_g \hat{\mu} \alpha_{\text{gf}}$, where the cross section for the signal events is $\sigma_g = 0.776$ pb calculated with MG5 at LO in QCD [12], the observed signal strength parameter $\hat{\mu} = 0.88^{+0.19}_{-0.18}$, and the

Search for $HHWW$ couplings in the VBS production of $W^\pm W^\pm H$ with $H \rightarrow b\bar{b}$ decays

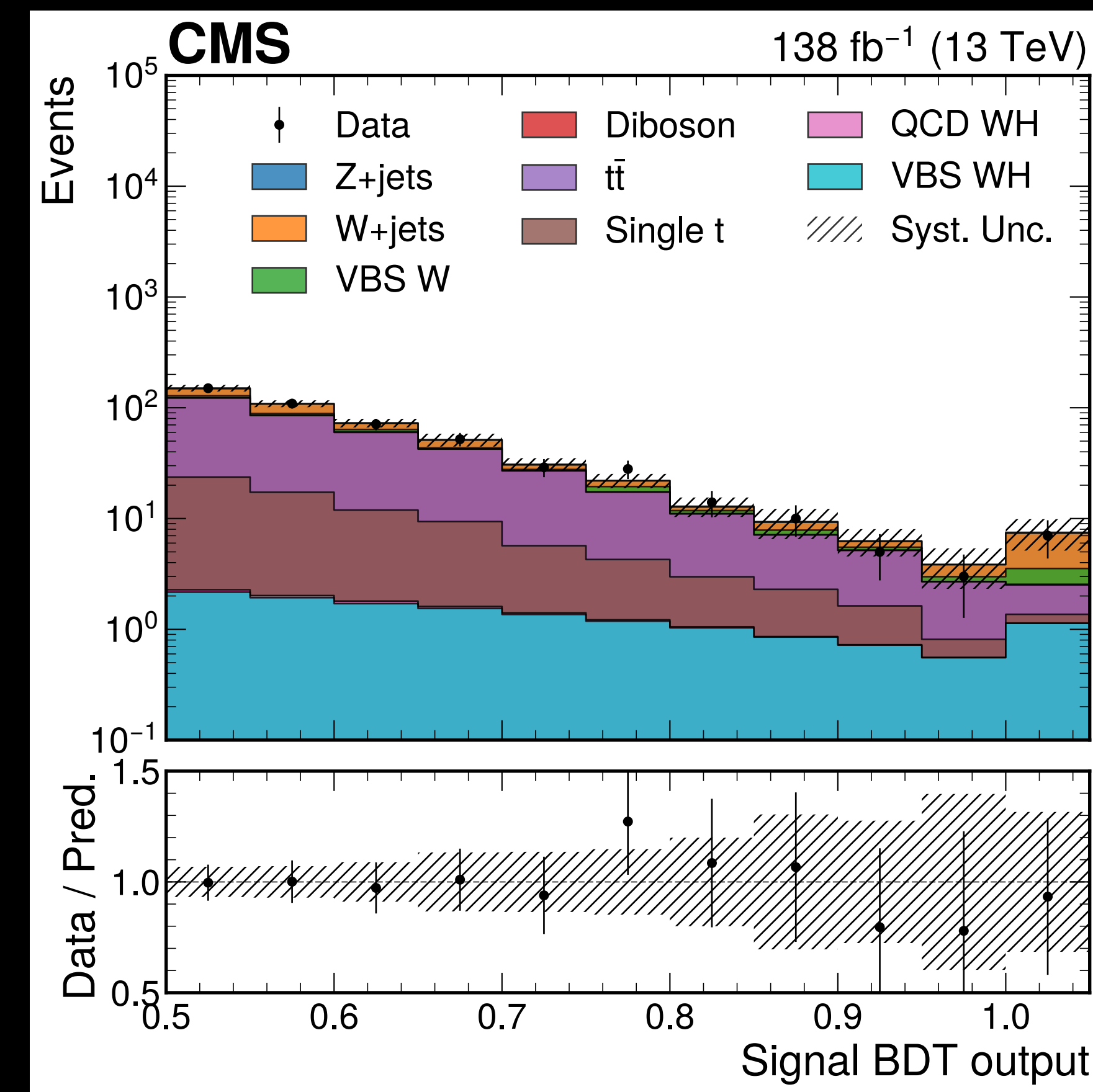
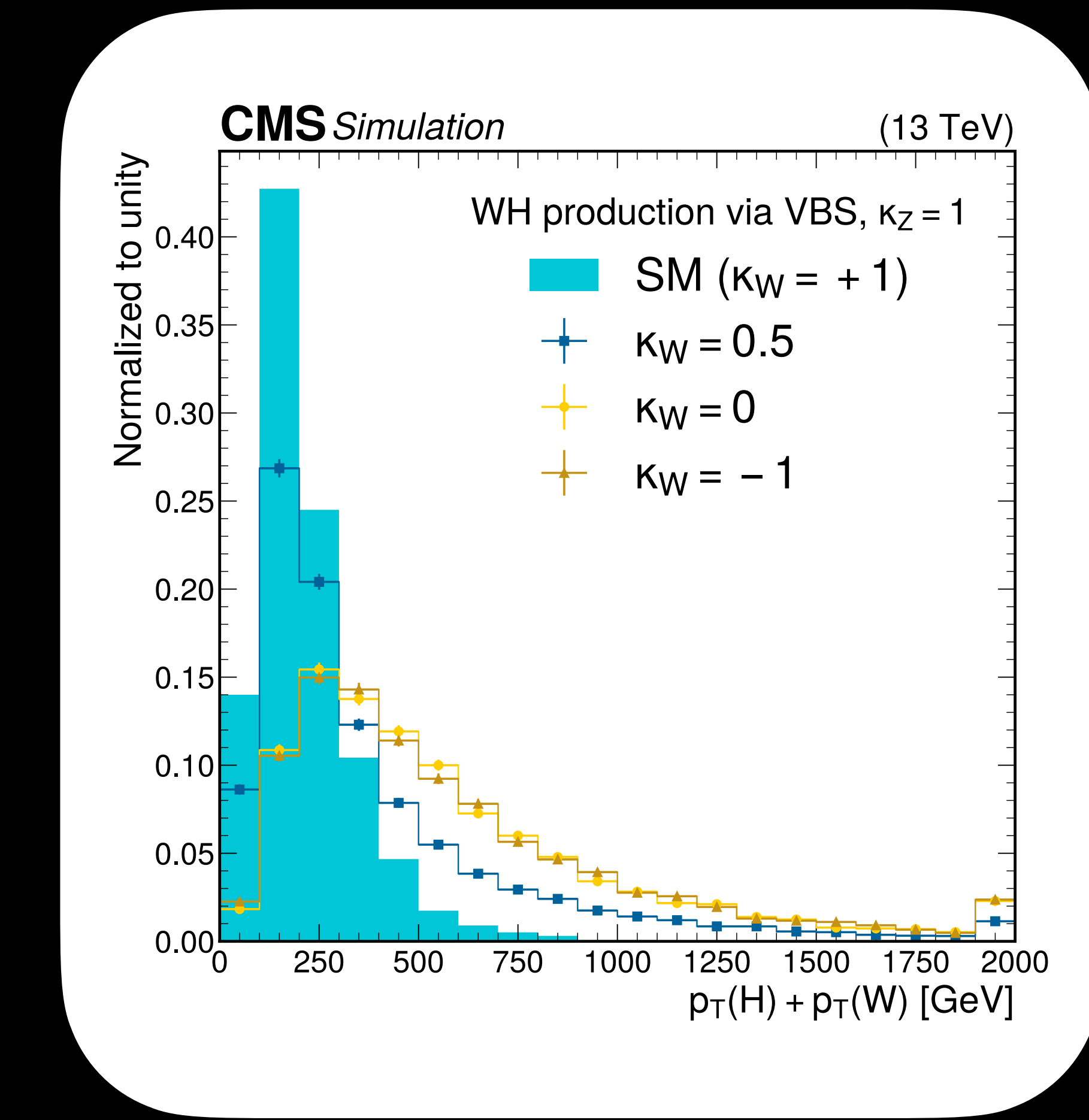
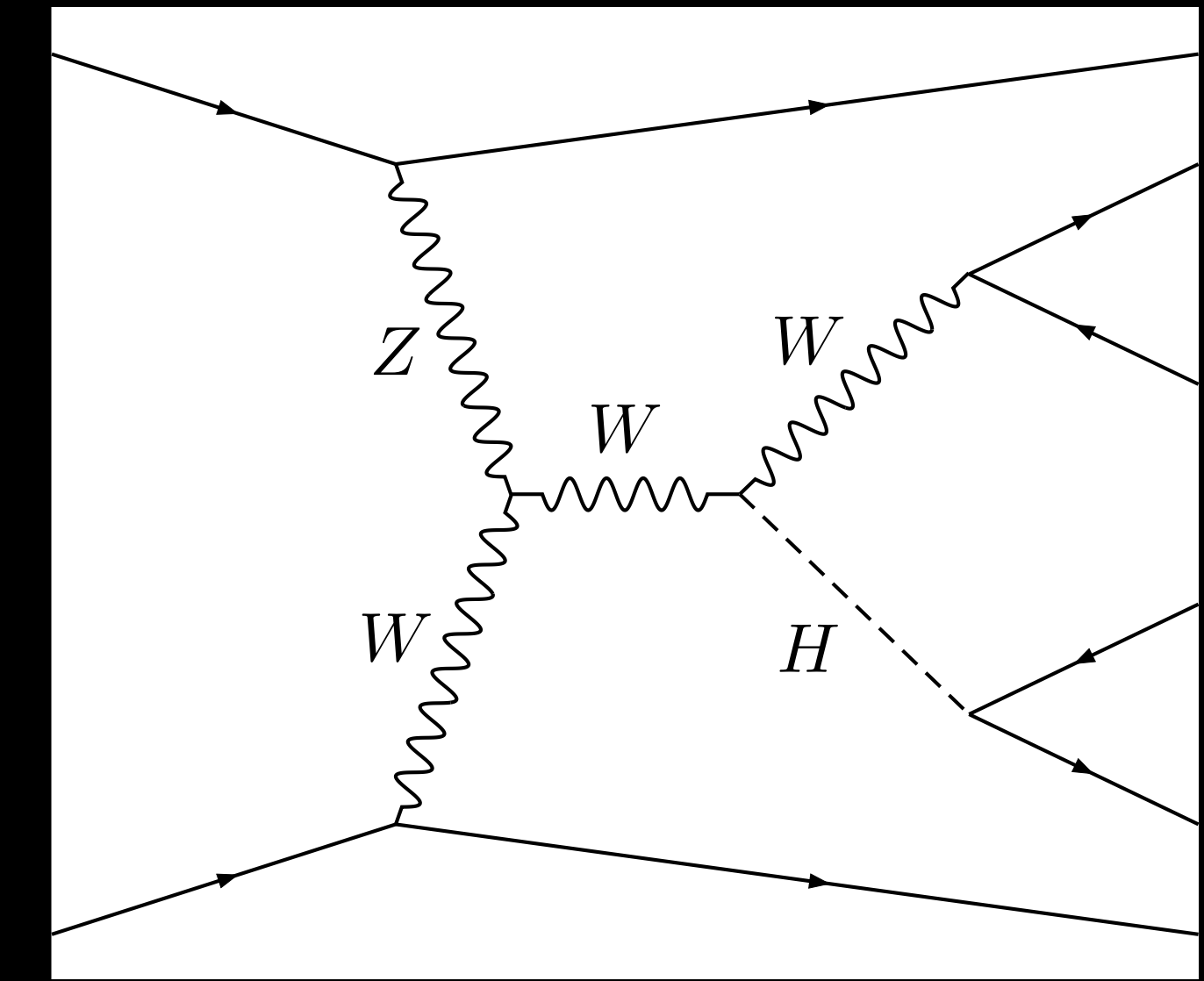
- Extraction of sign of W and Z coupling to Higgs performed with single W and Higgs in final state
- Final state: 2 same-signed leptons (one τ lepton permitted), a boosted jet, non-VBS contribution removed by requiring $m_{jj} > 100$ GeV
- Boosted decision tree trained against major backgrounds
- Low signal yields \rightarrow need more data to set tight constraints on couplings

$W^\pm W^\pm H$

Shorthand	Description
η_J	η of the leading merged jet
$p_{T,J}$	p_T of the leading merged jet
$p_{T,jj}$	p_T of the VBS-jet system
P_{j_0}	magnitude of the three-momentum of the leading VBS jet
P_{j_1}	magnitude of the three-momentum of the subleading VBS jet
$M_{\ell\ell}$	invariant mass of the SS dilepton system
p_{T,ℓ_0}	p_T of the leading lepton
p_{T,ℓ_1}	p_T of the subleading lepton
E_T^{miss}	missing transverse energy
L_T	scalar sum of $p_{T,\ell_0}, p_{T,\ell_1}$, and E_T^{miss}
S_T	scalar sum of $p_{T,J}$ and L_T



Study of WH production and extraction of relative sign of the W and Z couplings



Search for $ZZ \rightarrow b\bar{b}$ and $ZH \rightarrow b\bar{b}$

Source	ZZ	ZH
Statistical uncertainty	75	77
Total systematic uncertainty	67	64
Background model	61	56
(Variance)	(46)	(46)
(Extrapolation)	(40)	(33)
b tagging	9	17
Jet energy scale and resolution	9	5
Others	24	24

	ZZ	ZH
Signal strength expected (stat. only)	$1.0^{+1.9}_{-1.7}$ ($1.0^{+1.4}_{-1.3}$)	$1.0^{+1.5}_{-1.4}$ ($1.0^{+1.1}_{-1.1}$)
Signal strength observed	$0.0^{+2.0}_{-1.7}$	$2.2^{+0.9}_{-0.8}$
Expected upper limit at 95% CL (stat. only)	3.8 (2.8)	2.9 (2.3)
Observed upper limit at 95% CL	3.8	5.0

Search for $ZZ \rightarrow b\bar{b}$ and $ZH \rightarrow b\bar{b}$

The mixing algorithm is based on the technique developed in a previous CMS $HH \rightarrow 4b$ analysis [20]. The first step involves creating a collection of hemispheres (hemisphere library) from events in the four-tag data set. Each event is split into two hemispheres using the plane orthogonal to the transverse thrust axis [20], which is chosen based on the assumption that it is a good proxy for the initial gluon directions in the underlying scattering process. Jets on one side of the plane are assigned to one hemisphere, those on the other side are assigned to the other hemisphere. Four variables are computed using the sum of the four-vectors of all the jets in that hemisphere: the invariant mass, the longitudinal momentum, and the transverse momentum perpendicular and parallel to the transverse thrust axis. The jet and b jet multiplicities are also computed for each hemisphere. The library is created with events that pass the jet kinematic requirements but before the dijet invariant mass requirement given in Eq. (1) is applied.